Doctoral Dissertation
Doctoral Program in Architecture and Landscape Heritage (37th Cycle)

Semantic classification of airborne LiDAR data. Built and landscape heritage analysis in 2D/3D GIS environment.

Marco Cappellazzo

******

Supervisors:
Prof. Antonia Spanò Ph.D, Supervisor
Prof. Donatella Rita Fiorino Ph.D, Co-Supervisor
Dr. Giacomo Patrucco Ph.D, Co-Supervisor

Doctoral Examination Committee:
Prof. Mattia Previtali Ph.D, Politecnico di Milano, *Referee*
Prof. Giuseppina Vacca Ph.D, Università degli Studi di Cagliari, *Referee*
Prof. Elisa Farella Ph.D, Fondazione Bruno Kessler Trento
Prof. Mauro Lo Brutto Ph.D, Università degli Studi di Palermo
Prof. Giulia Sammartano Ph.D, Politecnico di Torino

Politecnico di Torino
2025

This thesis is licensed under a Creative Commons License, Attribution - Noncommercial - NoDerivative Works 4.0 International: see www.creativecommons.org. The text may be reproduced for non-commercial purposes, provided that credit is given to the original author.

I hereby declare that, the contents and organisation of this dissertation constitute my own original work and does not compromise in any way the rights of third parties, including those relating to the security of personal data.

…….....

Marco Cappellazzo

Turin, February 10, 2025

Summary

Abstract

The framework of landscape heritage conservation is extremely complex due to the historical stratification, territorial extension, and heterogeneity of such context. In fact, it is not possible to study and preserve landscapes without a thorough knowledge of the geographic relationships that landscapes, as cultural and environmental heritage, establish with the territory they occupy and the people who inhabit them.

Considering this complex context, remote sensing methodologies are nowadays increasingly crucial for acquiring accurate spatial data for heritage documentation processes. In fact, the technological development of surveying sensors and operating platforms over the last decades has been directed toward the enhancement of consistency, richness, expeditiousness, and resolution of the acquired dataset. However, although the Cultural Heritage (CH) domain could benefit from recent advancements, issues arise while managing such extensive and high-resolution datasets. Specifically, automating the semantic structuring of raw spatial data is a well-known challenge when dealing with extended data, where machine learning (ML) techniques provide several methodologies that are studied to overcome manual labeling activities. In this regard, the Geographic Information Science (GIS) environment adequately supports multi-dimensional and interdisciplinary 2D/3D data interpretation and analysis. Yet, these methodologies are not fully addressed and consolidated, especially considering the landscape and built heritage contexts. Thus, finding an automated, efficient approach for analyzing, mapping, and preserving landscape heritage becomes crucial.

Given the aforementioned issues and challenges, the present doctoral thesis focuses on the integration of airborne Light Detection and Ranging (LiDAR) data with ML methods for the semantic classification of both landscape and built heritage. Namely, this work proposes a systematic approach of identification and mapping at the base of conservation processes by using high and low-scale airborne LiDAR data and tailored ML models toward CH sites analysis, with particular interest in terrains difficult to access or presenting complicated geographical conditions. The research is based on the application of a methodological framework in two different case studies in Italy: Spina Verde Park in Como and the defensive landscapes of Sardinia. Each of these case studies is characterized by challenges ranging from highly vegetated areas, hiding archaeological structures in the Como Park, to extended and poorly documented defensive systems across both coastal and rural surface areas in Sardinia. The scheme of this research in Spina Verde Park involves high-density airborne LiDAR data for detecting and mapping anthropogenic features, such as trails related to ancient settlements. In this regard, the leverage of a high-resolution dataset has been useful to test specific deep learning (DL) pipelines that have been studied more by exploiting similar-scale datasets. The Sardinian case study concerns historical defensive landscapes characterized by several fortification systems, such as Spanish coastal towers and bunkers from the Mediterranean Wall, which demand advanced data structuring pipelines considering the widespread distribution of artifacts and chrono-typological heterogeneity. Moreover, the second case study addresses the specific challenges of automating the semantic classification of low-resolution airborne point clouds.

In this regard, key methodologies include supervised ML and DL, supported by unsupervised techniques, such as point cloud semantic segmentation and object

class identification methods. These approaches develop a semi-automated, repeatable process for data structuring and generating Digital Terrain Models (DTMs). This thesis demonstrates how the application of neural network models to airborne LiDAR data can accomplish highly accurate landscape classification with a high level of automation. Nevertheless, the results presented in the thesis also highlighted the efficiency of such ML workflows by reducing the time required for data processing while ensuring standards in data accuracy towards heritage conservation.

Specifically, during this research experience, different automated methods have been proposed for the semantic classification of raw 3D data and the mapping of anthropogenic features related to landscape microtopography characteristics. The contribution also addresses accessibility gaps in geospatial analysis by exploring software and coding solutions that enhance the usability of AI-powered tools for heritage professionals, therefore developing flexible workflows for the application of data structuring and analysis strategies for CH.

Finally, the originality impact of the thesis is linked to knowledge enhancement in the field of landscape heritage conservation through the development of a transferable and scalable methodology that exploits machine learning methodologies for multi-sensor remote sensing applications.

Thank you.

To Oscar, Lorenza, and Matteo

To my beloved *Paradis* Island

To my friends and colleagues

"I see...

That's it.

I've been here too long for my own good.

It's been three long years...

I was just a kid... I didn't know anything.

If only I had not remembered having loved ones...

I...Would have become... A coward who leaves things unfinished.

It's too late now... I don't know what's right anymore.

But the only choice for me now...

...is to face the consequences of my actions...

...and as a warrior...

...fulfill my duty to the bitter end!"

RB

Acknowledgment

Firstly, I would like to thank my parents, Lorenza and Oscar, and my brother Matteo, for their constant support. Despite the sea and several kilometers separating us, you have never made me feel alone. I know you're not really used to hearing these words coming from me, but well, exceptionally, it can be said: I love you. Thank you for everything, even though I will probably never be able to thank you enough for all you have given me.

The DCC: Edoardo Giuseppe Giorgio 'Dodi' Sechi and Roberto 'Bob' Deligios, my acquired brothers. We share sweet and bitter memories, and I really can't tell you how important you are to me. On every occasion, you have demonstrated your support, never missing providing words of encouragement and moments of great fun. Thank you.

My supervisors, Nannina Spanò, Giacomo Patrucco, and Donatella Rita Fiorino, thank you for your guidance and support. Nannina, you have made me know and have made me fall in love with this "thing" called geomatics. You have always given the best and most correct advice, never failing to critically and punctually analyze my ideas and limitations despite my silences, pushing me to the proper path. Thank you for these and more. Giacomo, the researcher, you have truly been a 'sensei' and 'senpai' to me. You have pushed me to overcome my shortcomings, always providing words of support. You have taught me the meaning of being a researcher, the importance of scientific rigor, and the room for maneuver and flexibility needed to navigate the challenges of a PhD. Professor Donatella, thank you for your valuable time, your constant commitment to listening to the updates of my work, and for providing those insightful questions and meaningful observations that helped me view my research beyond the 'bastions' of the 'geomatics fortress'.

Marco Avena, we have come to you. We have shared this path, almost like one person, given that no one has ever seen us in the same room at the same time, nah, I'm joking... Thank you for the continuous moments of discussion in our secluded corner of the lab and thank you for every moment that helped drown the tough moments in laughter. In the end, despite everything, we made it.

The happy three friends of the Lab, you are probably the only ones who have seen Marco and me in the same place, oops joking again... Jack, the friend, thank you for every post-work beer and fun moment, talking about memes, mangas, cinema, and more. Oh, well, I guess this is The One Piece. Vittorio and Stefano, I'm finishing the things to say, and it is not possible to mention everything we have said and we have shared during our coffees, beers, and so on. I guess that the same thanks that have been given to Jack are also valid for you. Thank you, outcasts.

Giulia, you were my first co-worker here, a great friend, and an exemplary researcher. I'm grateful for all your advice in starting and addressing the PhD and all the moments outside the work hours, also working (oh yes, working outside lab hours does count).

To Professor Fulvio Rinaudo, who kindly agreed to serve as the internal reviewer. Thank you for dedicating your time to reading my work and for providing valuable feedback and advice that has helped strengthen this thesis. To Professor Fabio Giulio Tonolo, thank you for your support over these years, for listening to me and providing valuable advice on my work, as well as for the moments of laughter outside of work.

To all my friends and loved ones from Sardinia and Turin. I can't mention you all due to space constraints, but thank you for supporting me, even if only with a conversation or a word of encouragement.

To the referees. Thank you very much for your contribution and the time you dedicated to reviewing my thesis.

List of Tables

List of Figures

Chapter 1 – Introduction

Introduction

Nowadays, the semantic classification of unstructured data is a crucial issue for geomatic disciplines, specifically in remote sensing (RS) techniques for 3D metric surveys. In fact, the sensors' technological advancements in recent decades have allowed the enrichment and expeditiousness of acquired spatial data, leading the geomatics community to question the impact of data processing, especially where the analysis, the semantic and relational structuring of spatial data is particularly relevant. From this premise, the significance of the resulting challenges also varies according to the specific application context. The landscape and built heritage documentation and mapping framework have benefited from RS techniques despite data analysis and semantic content enrichment being especially crucial issues in such a complex and fragile context. Landscapes, which are defined by the harmonic concurrence of anthropic activities and the natural environment (Petzet, 2008), are a well-known example that demonstrates the sensitivity of the application context, which will be further discussed in Section 1.2. Therefore, it is not possible to study, analyze, and preserve landscapes without a thorough and continuous knowledge of the geographic relationships that landscapes, as cultural and environmental heritage, establish with the territories they occupy and the people who inhabit them. For example, archaeology research studies highlighted the importance of spatial

analyses of the interactions of widespread historical construction with the environment in specific territories, leading to the archaeological landscape definition (Knapp & Ashmore, 2000). In this context, built heritage spread systems can also be considered a fundamental part of cultural landscapes. In fact, according to (ICOMOS Guidelines on Fortifications and Military Heritage, 2021), the global diffuse historical fortifications are a well-known example of the integral relationship between military and defensive structures with cultural landscapes those are placed in.

In this framework, the global topic of the conservation of cultural landscapes is directly connected with the strategies to document and analyze the environmental and anthropic relationships that characterize cultural heritage (CH) (Stubbs, 2009). Here, knowledge enrichment is thus a foundation for continuous heritage conservation strategies (Della Torre, 2003), where the regular input of data requires the research to focus on developing consolidated and accurate methodologies for the automation of analysis, validation, and semantic classification of the collected datasets.

The Ph.D. research is therefore focused on the development of semi-automatic strategies and methods that guarantee human control in the semantic structuring of spatial data in support of studies and analyses for the conservation of built and landscape heritage. Starting from this brief introduction, in the following sections, the thesis framework will be further developed by clarifying the literature gaps, research questions, and objectives (Section 1.1) and describing the heritage application contexts (Section 1.2).

1.1 Research framework

Since the strategies that can be implemented towards the conservation of landscape and built heritage are considered a crucial topic (Jokilehto, 2018; Stubbs, 2009), the frameworks for CH documenting and digitizing, even though it has been

extensively discussed, remain crucial and actual (Eppich et al., 2007; Moullou et al., 2024). In fact, the topic of data acquisition, modeling, and interdisciplinary cooperation remains relevant, particularly due to technological advancements, which lead to both the accumulation and obsolescence of data. In this context, the geomatic field integrates surveying technologies, data management, and processing about the earth and environment (Gomarasca, 2009). Nevertheless, geomatic science, which has long been applied to heritage preservation strategies, offers significant contributions to the management of conservation processes. This is possible through the constant acquisition, processing, and visualization of data, which can then also be developed in three-dimensional modeling processes (Bitelli et al., 2007). In this context, it is also important to underline that the research development in heritage parametric information modeling (Logothetis et al., 2015) forwards interesting perspectives in the field of documentation and 3D data management. In fact, the most actual themes in geomatics applied to CH focus on improving technologies and methodologies for mapping and structuring the acquired data. Specifically, the 3D metric survey methods provided by Remote Sensing (RS) and the spatial analyses and effective data management capabilities offered by Geographic Information Sciences (GIS) are well-established and reliable tools for supporting heritage preservation efforts (Forte & Campana, 2016; Luo et al., 2019).

In particular, in this research framework, the semantic structuring of acquired data is a crucial topic in order to address the demands set by planned conservation strategies (Della Torre, 2022; Nishanbaev et al., 2019). In this sense, it is crucial to underline that the continuous update of information is obtainable through the data harmonization of acquisitions from various sensors and at different scales (Adamopoulos & Rinaudo, 2019; Kioussi et al., 2013).

1.1.1 Methodological framework

Starting from this introduction, the geomatic methodological framework of this research emphasizes airborne RS technologies for defining microtopographic characteristics of heritage objects and ground features on highly accurate elevation data across relatively large areas. These data can be produced using both Light Detection and Ranging (LiDAR) and digital photogrammetric methods, exploiting various platforms such as airplanes, helicopters, and drones. Furthermore, consequent products, such as Digital Height Models (DHMs), are considered extremely valuable for the 3D reconstruction of territory and, thus, landscapes. The DHM terminology in the present dissertation is used to indicate generally a digital elevation model, with a Digital Terrain Model (DTM) and Digital Surface Model (DSM) as particular cases that respectively filter or not surface features (e.g., trees, buildings) (Granshaw, 2020).

In this sense, the study of microtopography is also complex, as it considers terrain parameters such as slope, aspect, flow path, ruggedness index, wetness index, and curvature that characterize the surface. Yet, the state-of-the-art topography studies converge on evaluating elevation models of the ground surface for environmental monitoring applications that range between 1 cm and 1 m, as well demonstrated by (Shukla et al., 2023). Therefore, DHMs are considered in the literature as the characteristic 3D reconstruction of the earth's surface, derived from aerial acquisition by sensors equipping vehicles (planes, helicopters, drones, etc.) and can be derived from LiDAR and photogrammetric methods. Their use is traditionally related to the most varied application sectors, reducing time acquisition and ensuring high and accurate productivity, especially for urban 3D modeling or terrain morphology analysis (Remondino, 2011; Sammartano et al., 2021) and heritage landforms mapping (Spanò et al., 2018). Starting from these considerations, this doctoral research evaluates the use of both active (LiDAR) and passive (digital photogrammetry) RS technologies for the basic definition of

microtopographic characteristics, starting from highly accurate elevation data over extended heritage contexts.

Various studies can be cited among the environmental sectors most influenced by adopting automatic remote sensing techniques. In this framework, multispectral and hyperspectral imagery also represents a significant contribution to earth and hazard monitoring (Bendea et al., 2008; Boccardo & Giulio Tonolo, 2012a). Since the start of the millennium, the interest in this topic has been underlined by a continuous flow of research examining its applications and underlying principles. In fact, several works relate to hydrographic networks and morphological variations of watercourses concerning floods (Turitto et al., 2010), forest management applications for forestry censuses, canopy height, and biomass estimation (Hemingway & Opalach, 2024; Kerr & Ostrovsky, 2003), coastal protection (Mancini et al., 2013), glacier monitoring (Corte et al., 2023), and recognition and monitoring of avalanches and landslides (Petschko et al., 2016; Scaioni et al., 2014).

Moreover, even CH domain disciplines related to archaeological and landscape studies have benefited from RS technology applications, specifically for airborne DHM data classification (Forte & Campana, 2016). In this sense, in recent decades, LiDAR airborne, also identified as Airborne Laser Scanner (ALS), data processing and applications have been widely studied (Z. Chen et al., 2017). Moreover, it is important to underline the potential of RS and Machine Learning (ML) techniques in CH site prospection (Argyrou & Agapiou, 2022). However, it should be mentioned that the interest in artificial intelligence for remote sensing processing has been long applied to different application domains, such as cartography automation (Hsu, 1979) and multispectral image processing (Estes et al., 1986). Yet, the literature also reported the shared interest in recent decades in the importance of considering multiple data sources for identifying historical artifact features (Chane et al., 2013; Freeland et al., 2016; Guyot et al., 2018; Niculiță, 2020). In this framework, the cited works inquiries about the use of DHM in order to acquire and analyze data concerning extended heritage sites. While

several research studies adopted the processing of converted raster from 2.5D to 2D, the most recent trend is moving towards directly analyzing the original data from 3D point clouds acquired through LiDAR sensors equipped on aerial vectors. In particular, in the framework of heritage application, the aim is to investigate new methodologies that are largely adaptable for the detection of archaeological features by employing ML techniques. In fact, 3D point cloud data structuring through semantic segmentation techniques is increasingly studied nowadays (Argyrou & Agapiou, 2022; Grilli et al., 2017) in order to reduce human involvement in the data processing stage. Deep Learning (DL) techniques, where artificial Neural Networks (NNs) are trained on labeled datasets (Varney et al., 2020; Ye et al., 2020), have shown great promise in accurately classifying and segmenting point clouds or mesh (Hu et al., 2021; Sarker et al., 2024; Zeng et al., 2024; X. Zhang et al., 2022). While DL semantic segmentation methodologies have been extensively studied, also for the CH domain, specific NN detector methodologies for point clouds mostly pertain to autonomous driving and robotics application fields (X. Chen et al., 2016; Mattausch et al., 2014).

However, despite ongoing research, these methodologies are not yet fully established, particularly in the heritage study domain, where the focus is more on building-scale applications rather than landscape-scale contexts. Moreover, the last decade's studies have been directed toward the employment of high-scale point cloud and mesh data acquired from UAS LiDAR platforms (Kölle et al., 2021).

In this framework, this doctoral research investigates the application of the presented methodologies on two different case studies, aiming to integrate RS and ML techniques for data analysis and structuring in landscape heritage contexts. The following section further explains and discusses the specific aims and expected outcomes of the thesis.

1.1.2 Research questions and aims

Given the analysis of the current state of the art of geomatics techniques related to the CH framework, it is important to present the principal research questions and the answering aims that this research thesis proposes to address.

- Since the preservation of built and landscape CH strictly depends on efficient and continuative documentation actions (Eppich et al., 2007; Moullou et al., 2024), also the cataloging of such documentation is consistent with conservation objectives, as stated in the (ICOMOS Ethical Principles, 2020). In this framework, remotely sensed dataset collection should also be addressed toward a standardized and accessible semantic data structuring. Is it thus possible to enhance the automation of these processes leveraging GeoAI methodologies?

- In the framework of RS and ML integration, the technological advancement of remote sensing techniques has allowed the possibility of acquiring dense and consistent 3D datasets from manned and unmanned airborne platforms (Bundzel et al., 2020; Kölle et al., 2021). In this sense, very high-resolution datasets nowadays represent the state of the art for applying point cloud semantic segmentation methodologies. Moreover, ML techniques have not been fully explored and consolidated for CH domain applications. Is it thus possible to provide efficient and automatic data structuring pipelines for existing regional low-scale datasets even though they have not been acquired for heritage documentation and detection purposes?

- In the framework of CH mapping, it is worth underlining that using airborne laser scanning (ALS) technique to investigate archeological landscapes in highly forested areas is considered particularly valuable

(Albrecht et al., 2020). Still, the automation of LiDAR data semantic segmentation is also a key point for the generation of accurate DHMs. Moreover, it is important to specify that historical ground artifacts such as trails, standing stones, walls, roads, canals, earthworks, and similar features are represented and observable from the interpolated DTM. Is it then possible to automate the detection of non-mapped anthropogenic shapes?

- ICOFORT guidelines stated that there is a higher lack of knowledge concerning historical defensive and military systems and artifacts, and there is a necessity for conservative plans that should be supported by adequate documentation (ICOMOS Guidelines on Fortifications and Military Heritage, 2021). Furthermore, the spread of coastal defense systems and the numerosity of artifacts are challenging issues in the accomplishment of well-conducted documentation. In this sense, the detection of non-mapped widespread heritage from existent datasets could represent a valuable perspective for the preservation of defensive systems. Is it thus possible to apply LiDAR deep learning object detection methodologies for the mapping of such artifacts and systems?

- Finally, the accessibility to technical coding environments and specific machine learning methodologies and scripts could represent a gap for Heritage conservation experts. In this framework, graphical interface software and coding environments (e.g., ArcGIS Pro, Anaconda) could represent a solution to overcome a lack of technical, but not theoretical, knowledge. However, exploiting such a platform could also generate issues related to low levels of control and algorithm personalization and, thus, performances.

To answer these questions, the present doctoral research studied integrated automatic methodologies to evaluate, process, manage, and structure remotely sensed 3D and 2D geospatial data in extended and significant landscape and archaeological contexts. In fact, considering the fragility of the application context and the increasing amount of required data, the aim is to study machine learning and deep learning techniques for automating the classification of remote sensing data. In addition, current ML methodologies are often applied separately, while the present doctoral research aims toward a holistic integration of the various approaches. Still, another goal was to analyze this approach from a multi-scale perspective. On the one hand, the studied cultural landscapes are linked to territorial spatial analyses and thus coherent with mid and low-scale data. On the other hand, the objects and features that define landscapes often require to be observed through the collection and management of higher resolution datasets. To address this, the methodologies examined—semantic classification, semantic segmentation, and detection—are combined to develop an original method.

1.1.3 Original contribution of the thesis

In order to develop an original methodologic approach, two different case studies have been selected, in order to test the replicability of the method and guarantee the aimed multi-scale approach. Specifically, multi-sensor and multi-scale acquisition techniques are crucial for archaeological and defensive landscape mapping and analysis to provide information on the artifact at the architectural scale and investigate the object starting from the system that embeds it at the landscape and territorial scale (Figure 1).

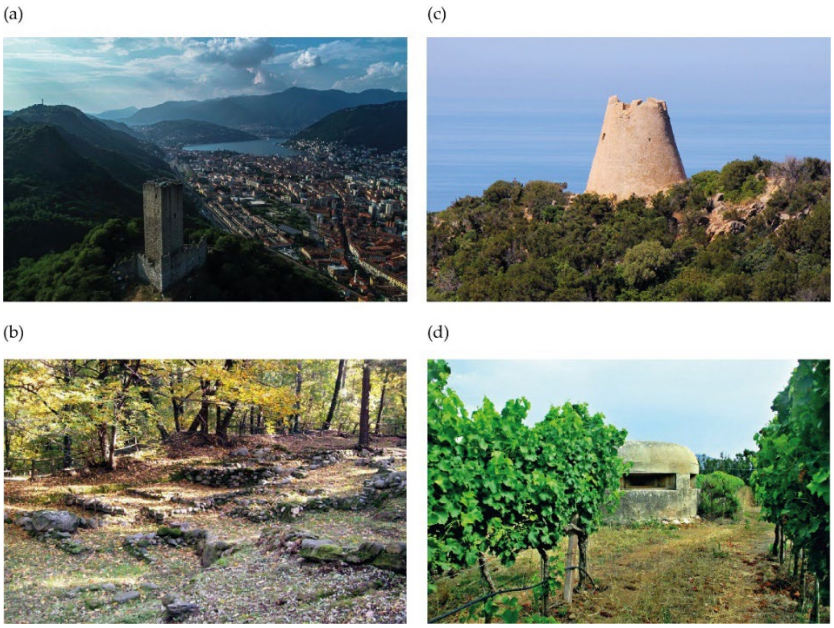

Figure 1. Studied areas and Heritage contexts from Case Studies 1 and 2. Spina Verde Park in Como (Italy), where inside the hilly protected area (a) embeds several archaeological sites, such as the protohistoric Pianvalle settlement ruins (b). Sardinian defensive and military Heritage artifacts: Capo Boi tower, Sinnai – Cagliari (Sardinia), Italy (c). Position no. 5 of Stronghold V, Porto Ferro – Alghero (Sardinia), Italy (d) – credits LabG4CH (a) author (d), University La Sapienza (b), Sardinia region (c).

The case studies of Spina Verde Park in Como (Figure 1a-b) and Sardinia Defensive Landscapes (Figure 1c-d) will be presented and further discussed in Section 1.2.1, focusing on the heritage framework topics, starting from the analysis of the territorial extension, anthropic settlement morphology, and consistency of present artifacts and sites.

In this dissertation, the aim is to develop an automatic and transferrable macro-class semantic segmentation model for airborne LiDAR point clouds in order to adequately and rapidly structure the primary 3D data yet also to generate accurate DSMs and DTMs. In fact, since remote sensing and machine learning integrations have been widely studied on high-resolution datasets (Kölle et al., 2021; Varney et al., 2020), a first case study has been selected and exploited to test and evaluate unsupervised and supervised DL point cloud methodologies leveraging high-scale point clouds through a tailored airborne LiDAR survey acquired from helicopter (Section 3.1.1). In addition, it is also important to underline that the literature lacks research studies that develop methodological pipelines leveraging existing low-scale

ALS point clouds. In this sense, bridging the gap in the lack of automated methodologies applied to existent ALS datasets could also be considered a significant advancement for CH domain data structuring. In fact, one of the aims is also to investigate GeoAI semantic structuring pipelines leveraging existing open-source ALS datasets that have not been acquired for this specific purpose. Specifically, public administration available point cloud datasets are usually acquired for cartographic production and territorial and hazard monitoring through digital orthoimages and elevation model generation (Brovelli et al., 2009). Subsequently, the second case study has been exploited to test the supervised semantic segmentation methodologies, leveraging an existent low-scale regional dataset (Section 3.1.2). At the same time, the second case study is also useful for testing the implementation of unsupervised segmentation techniques by integrating multispectral satellite open access and the 3D existing low-scale data.

Starting from the segmented point clouds, the research also aimed to study a workflow aiming also the integration with traditional ML methodologies for the detection of non-mapped anthropogenic earthworks by automatically classifying DTM visualizations and geomorphological raster analyses. In this sense, the originality of the contribution consists in the process of adopting and evaluating machine learning and deep learning techniques, both individually and as part of the overall proposed workflow.

Furthermore, in the second case study, the doctoral research also aimed at preliminary investigations regarding the application of object-detection techniques for specific defensive and military heritage artifacts mapping (Figure 1 c-d).

Finally, it should be underlined that aiming at automation for data structuring and artifact mapping represents a valuable support tool for Heritage conservation professionals and academics. In this sense, the research also aims to improve Heritage domain users accessibility to data and classification models by exploiting Graphical User Interface (GUI) software and coding solutions, such as ESRI ArcGIS Pro and Anaconda.

1.2 Heritage framework

In order to deepen the knowledge of the heritage application framework towards the specific methodologic approaches that will be adopted in this research, it is crucial to question the main reasons for the preservation of CH and the answering strategies to address heritage conservation challenges.

Since the necessity is to address technical methodological challenges related to landscape analysis and preservation, it is useful to briefly introduce the study of heritage conservation within European society, starting in the 20th century. During the previous century, a fundamental idea for the evaluation of cultural heritage emerged: the value of history, preferred over aesthetic value. A historical object, building, or site becomes a monument not because of its aesthetic qualities but because it is recognized as a repository of historical memory, which is considered essential for the identity of a nation (Riegl, 1903). Starting from the end of the world conflict, the value of CH conservation and protection has been widely shared at a more global level. In fact, contemporary society, through the protection actions carried out by UNESCO, considers the preservation of CH fundamental. Furthermore, it is specified that monuments, sites, and objects that represent an exceptional interest for the community should be protected and preserved from anthropogenic destruction and natural decay actions (Convention Concerning the Protection of the World Cultural and Natural Heritage, 1972). After the ratification of the Convention, everything concerning cultural heritage has had to confront the epochal changes brought by growing globalization. However, even assuming the importance of multiculturalism addressed by globalization, it should be clear that the foundational character of each culture's values cannot exist without considering the centrality of each territory, constituted by space and collective memory (Choay, 2012). In fact, in the second part of the 20th century, the homogenizing of cultural identity and CH assets management caused by the accelerating process of globalization led to a reduction of cultural diversity (Stubbs,

2009). Despite the spread of Western culture and globalization, which has created several threats, the perception and awareness of local, regional, and national identity has recently led to increasing international efforts for CH preservation.

In this framework, the International Council of Monument and Sites (ICOMOS) work for the protection of tangible and intangible heritage has represented a turning point. In fact, as stated in previous paragraphs, as far as tangible heritage is, to some extent, a repository of memories and values, it can also be said that it is linked to intangible heritage. In this regard, cultural landscapes are a perfect example of the integration of human work and nature, where tangible and intangible heritage are "two sides of one coin" (Bouhenaki, 2003). It is, in fact, appropriate to refer to Genius Loci (Petzet, 2008) to describe the complex and continuous evolution of anthropic relational phenomena occurring in the territory. The fresco from Ambrogio Lorenzetti (Figure 2) efficiently depicted the stratification and the relationships that the territory has with human activity. In fact, moving far from the ordered and rational urban and agricultural landscape, there is a transition to an unordered and wild landscape (Romano & Trisciuoglio, 2008).

Figure 2. Picture of the fresco "Effetti del Buon Governo in Città e in Campagna" (1338-1339) painted by Ambrogio Lorenzetti in Palazzo Pubblico in Siena (Tuscany, Italy) – credits Google Arts.

Therefore, the sequence of human activities and different cultures over time has resulted in territories often exhibiting layers of natural and artificial objects, creating heterogeneously complex and stratified landscapes. In this sense, the definition of cultural landscape embodies the environmental and human characteristics of a defined area. Natural environment features are considered to include the combination of hydrology, geology and landforms, vegetation, and fauna, while anthropic imprints are the records of the additional and continuous cultural process occurring throughout time (Petzet, 2008). Consequently, these areas are subject to continuous developments aimed at exploiting their beauty and addressing what humans perceive as limitations (e.g., accessibility), which are sometimes the greatest potential of a territory unaffected by anthropogenic degradation phenomena. Therefore, this specific characteristic represents, at the same time, a risk of anthropic degradation and an opportunity to avoid immobilism and aestheticization (Settis, 2010). Moreover, it also should be clear that a long absence of anthropogenic phenomena that define and characterize the landscapes significantly contributes to generating marginal landscapes and territories (Tosco, 2014), which are instead exposed to obliteration, as from the example of the alpine military road in Figure 3.

Figure 3. 13th kilometer totem of the military road from Traversiera Valley in Cuneo (Piedmont, Italy) – credits Pietro Tarozzo.

The correlation between the natural environment and anthropic activities is especially important, as environmental protection regulations are also present and are related to heritage conservation and valorization necessities. In fact, the regulation frameworks for heritage and the natural environment are characterized by an extended stratification. Concerning the specific Italian context, it has been established that the protection of landscape and national historical and artistic heritage is indispensable, primarily through Article 9 of the Republican Constitution. The existence of this article within the fundamental principles of the nation is unique globally, but it is also important because it assigns a central role to landscape in cultural development and heritage protection. Although this provision expresses a preliminary and incomplete definition of landscape as a mere object of legal protection, the incorporation, even at that time, with cultural heritage is considered interesting. Only with the arrival of the European Landscape Convention, which superimposes every other national law (Council of Europe Landscape Convention, 2000) the factor of human perception is introduced as an essential condition for the existence of landscape:

<<"Landscape" means an area, as perceived by people,
whose character is the result of the action and interaction of
natural and/or human factors>>

Art. 1 c. a, Florence, (Council of Europe Landscape Convention, 2000)

The Italian national regulation (Codice Dei Beni Culturali e Del Paesaggio, 2004) is then responsible for the regulation and the protection of built and landscape cultural heritage assets. This decree was developed to replace the two previous laws regarding cultural heritage: the Bottai 1939 law and the Galasso law of 1985. Specifically, in addition to establishing regulations for landscape protection, compared to the previous laws, the 2004 Cultural Heritage and Landscape Code outlines the methodological and procedural guidelines for regional

landscape plans, marking a significant innovation in the evolution of planning models. However, not all regional administration bodies have accomplished the drafting of landscape plans or delegating regulatory responsibilities to the urban planning tools of individual municipalities, thus creating a complex situation (Settis, 2010). Furthermore, the regulations for landscape protection are added to the rules for natural environment protection, which introduces additional complexity to the regulatory labyrinth. In this framework, Natura 2000 is one of the most important initiatives of the European Union since its aim is to preserve natural biodiversity. The network involves about 26,000 natural sites, land, and sea, so far pointed as a goal for conserving or restoring the natural habitats and wild species of community interest. The Habitats Directive-92/43/EEC and Birds Directive-2009/147/EC are the respective legislature in control of the Natura 2000 network, which jointly establishes the basic measures essential to ensure protection and management for natural systems, species of wildlife, and their habitats in a sustainable manner.

In this extremely complicated context, the focus topics pertain to archaeological and historical defensive landscapes, whose, as mentioned in the introduction, are well-known examples of the strong connection between anthropic activities and the natural environment. In fact, the importance of territorial relationships between human activities and the environment is a relevant topic both for archaeological and historical defensive landscapes. In this sense, archaeological knowledge and management is widely recognized as a crucial issue for understanding the origins and development of human society and identifying cultural and social roots. Still, in order to better define the archaeological landscape context, it is worth mentioning Article 1 of the (Charter for the Protection and Management of the Archaeological Heritage, 1990) by the International Committee for the Management of Archaeological Heritage (ICAHM). According to ICAHM, archaeological heritage is that part of the material heritage that comprises all significance of human existence and consists of places relating to all manifestations

of human activity, abandoned structures, or linked movable artifacts. Given this definition, and specifically the vast historical evolution of the Italian context, it is crucial to underline that the stratification and territorial distribution of archaeological heritage are its principal characteristics, forming complex archaeological landscapes. This, therefore, requires careful consideration of methods and methodologies for the conservation of such an extended heritage context. The same considerations can also be issued to landscape contexts related to defensive and fortified historical heritage. In fact, military heritage is strictly linked to the history of human settlements and territories, since from prehistory to modern times, military structures have been a major concern for human communities to defend themselves (Marotta, 2018). In modern times, forts and defensive structures have become integrated into territories and settlements, generating thus cultural landscapes that are often referred to as "defensive landscapes" or, alternatively, "military landscapes" (Fiorino, 2017). Starting from this definition, the Italian military and defensive architectural landscape is characterized by a widespread, extended, and heterogeneous collection of sites that are irregularly distributed, featuring buildings and areas of significant architectural and landscape value (Fiorino et al., 2017a). Moreover, as mentioned in the previous section, (ICOMOS Guidelines on Fortifications and Military Heritage, 2021) stated that it is possible to assume that there is a higher lack of knowledge concerning defensive heritage rather than other types of heritage due to the painful projection of memories that are associated with these monuments. Moreover, since the first aim of the defensive structure was to grant inviolability, military heritage is often completely inaccessible or difficultly accessible nowadays (ICOMOS, 2021). Given this, there is an urgent necessity for shared and consolidated conservation plans that should be supported by adequate and rapid documentation.

In this complicated framework, geomatics techniques for CH mapping and analysis lead to efficient and shared documentation practices among researchers and professionals (Eppich et al., 2007). The consolidation and protection of landscape

heritage for the future, thus, increasingly depend on the strategies in place for mapping, managing, and analyzing data to foresee potential economic development opportunities, which consequently leads to efficient and continuative conservation (Holtorf & Högberg, 2020).

Furthermore, it is necessary to consider the methods of investigation introduced by the various disciplinary sectors involved in the conservation processes, as well as the methods of cataloging the available information (Della Torre, 2003). In the specific case of defensive heritage, the lack of updated and standardized data from administrations makes it necessary to study and establish a unified method for data structuring and management. Still, in this context, the main aim is to provide a critical analysis of these artifacts, understanding the functions, their morphological conformation, and their location and relationships within the territory.

Despite this extremely difficult context, the complexity and dynamism of the territory and the desire to study and preserve landscapes are the factors that motivated the choice of the topic. In this sense, it should be underlined that the dissertation investigated the presented automated data structuring methodologies for the study of such widespread cultural landscapes that pertain to heterogeneous contexts, such as forested areas or adjacent to urbanized areas. The following section thus deepens the description of the selected case studies that pertain to archaeological and defensive cultural landscape contexts.

1.2.1 Case studies and domain knowledge-based datasets

Since the heritage and research framework and aims have been presented, this section describes the chosen case studies and the extensive analysis of the landscape heritage contexts and artifacts through the exploration of GIS mapping solutions and representation techniques. As mentioned in the previous paragraphs, since the thesis aims to structure and analyze remote sensing data for extended landscape contexts, two case studies have been selected to conduct the investigation from a multi-scale perspective. Moreover, it is worth underlining that the application of the presented techniques in two different case studies is also useful in analyzing the robustness, replication, and suitability of the methodologies for heterogeneous Heritage contexts. In fact, the two case studies are characterized by a different scale and extensions, as well as by the different consistency and typology of the artifacts that define the analyzed landscapes.

As shown in Figure 4, Case Study 1 is in north Italy (Lombardy region), specifically in Como municipality. Case Study 2 is instead characterized by two different areas, both located on Sardinia Island.

The following sub-sections will further develop and discuss the two case studies.

Figure 4. Map of the Case studies. The first case study pertains to the landscape and archaeological site of the Parco Spina Verde, Como–Lombardy. The second case study relates to Sardinian military and defensive landscapes and consists of two separate research areas: Cagliari (Area 1) and Alghero (Area 2). Datum WGS 1984 (EPSG: 4326) – credits ESRI, ISTAT (data), author (elaboration).

Case Study 1: Spina Verde Park in Como, Italy

The first case study of this research, as shown in Figure 4, is related to the area of Spina Verde Park in Como (Lombardy, Italy).

The Spina Verde Park lies in a hilly, high-forested area in the southern part of Como Municipality, surrounded by the city's urban edges (Figure 5). Throughout the park's territory, numerous sites and archaeological traces belong to a series of widespread proto-historic urban settlements active during the first millennium BC (De Marinis et al., 2001). Specifically, a proto-urban settlement is considered to be the process of formation of a proto-urban society that takes place at different times. These processes that occurred from the Bronze Age to the Iron Age developed urban forms according to the various European areas but with similar synoecism, cultural aspects, and central places (De Marinis, 1986). The archaeological sites in the Como area pertain to one of the major settlements of the Golasecca culture, which occurred from the final Bronze Age to the early Iron Age when its maximum expansion covered almost 2 km^2. Several archaeological evidences are present in the area (Catacchio et al., 2019; Merlo & Frigerio, 1986):

- Quarries – sandstone and marl extraction sites used for building materials until the Roman Age.
- Rock engravings – rock art is present in many sites, manifesting as isolated engravings and articulated decorative motifs (Figure 5a-b).
- Metal working areas –these areas present evidence, such as furnaces and casting molds (Figure 5c-d).
- Rock "Cameras" – the so-called "Camera" is a building technique characterized by a rock dug structure, complex or sub-rectangular in plan, varying in size, from 11x10x3 m to 3x2x1 m (Figure 5e-f).
- Huts – these types of constructions are characterized by a dry-stone basement with wooden walls, either square or rectangular in plan, varying in size from 11x8 m to 8x7 m.

- "Recinto" – the so-called "Recinto" is a building technique characterized by a partial dug in the ground, covered with a stone basement, obtaining thus a lower semi-basement compartment and an elevated upper compartment (Figure 5g-h).

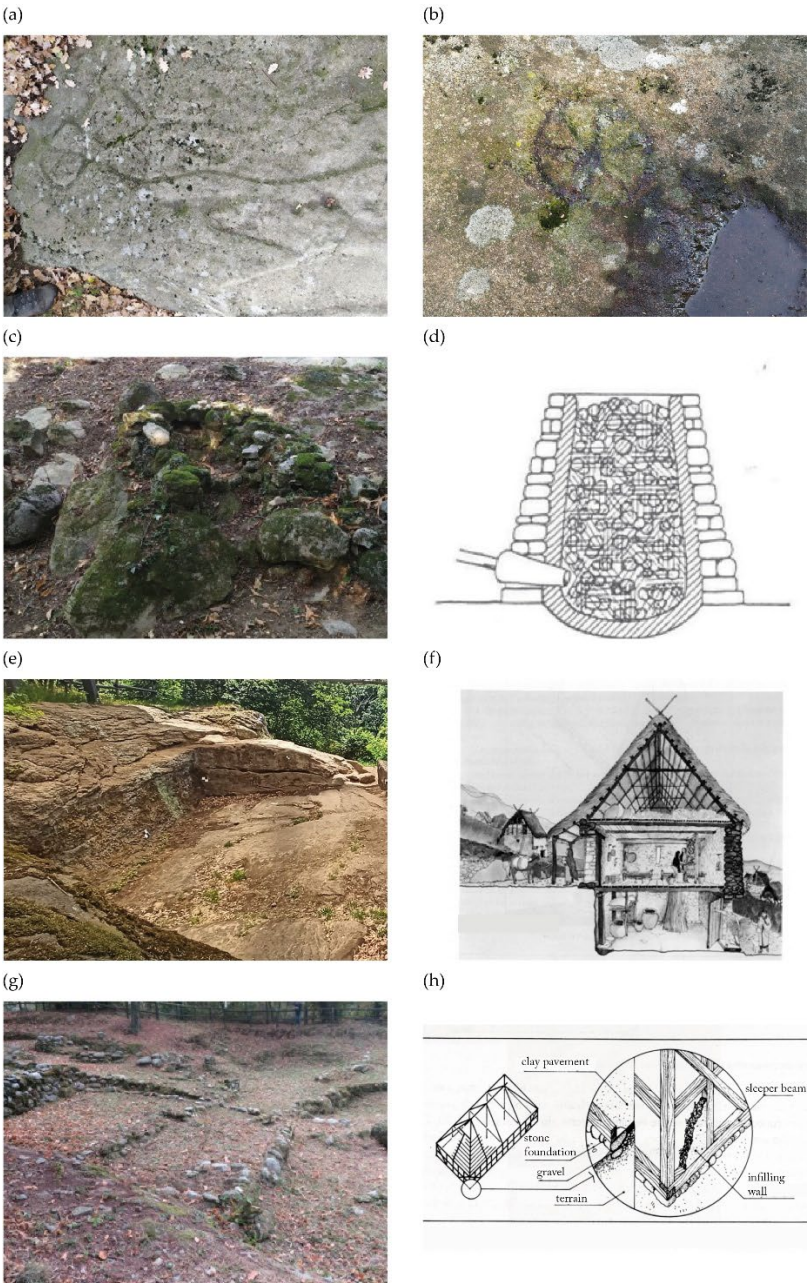

Figure 5. Examples of archaeological evidences from Spina Verde Park. Rock engravings depicting (a) human figure and (b) sun symbol. Metal working areas: (c) remaining furnace structures in Pianvalle settlement and (d) operating furnace schema (Catacchio et al., 2019). Construction typologies: (e) rock chamber "Camera Grande" site and (f) rock chamber construction hypothesis (Merlo & Frigerio, 1986); residential enclosure ("recinto") structure in Pianvalle settlement and (h) construction hypothesis (Merlo & Frigerio, 1986) – credits Università La Sapienza, LabG4CH.

Moreover, some of the hiking connections within the Park, which are essential for reaching archaeological sites and for the usability of the Park itself, are an active testament to the protohistoric ways that served as connections and communication routes between the various settlements. It is possible to observe the so-called "via glareata", covered in pebbles of different sizes, and the wagon tracks that are characterized by rock incisions generated by the continuous passing of wagons (Alivernini & Roncoroni, 2016). However, these trails are not always mapped in the regional geographic dataset, and the proposed methodology wants to move toward mapping these morphological elements.

Figure 6. Example of protohistorical routes: (a) cartwist track and (b) "via glareata" – credits Università La Sapienza.

Furthermore, the evolution of the urban settlement has also been accompanied by a stratification of defensive military structures, with evidence and initial confirmations dating back to the third century, significant activity during the Byzantine period (6th-7th centuries AD), and continuing through World War II (Società Archeologica Comense, 2013). In this framework, as mentioned in the previous section, spatial analysis and mapping are crucial issues for archaeological and defensive landscape heritage preservation (Figure 7). In this sense, landscape

morphologies are usually considered as linked characteristics to the physical condition of a territory portion, as well as the processing and relationship those create (Robinson, 1977). Specifically, these correspond to the landscape's material formation, including its shaping evolution, which is connected to the social and cultural structures with which it is associated.

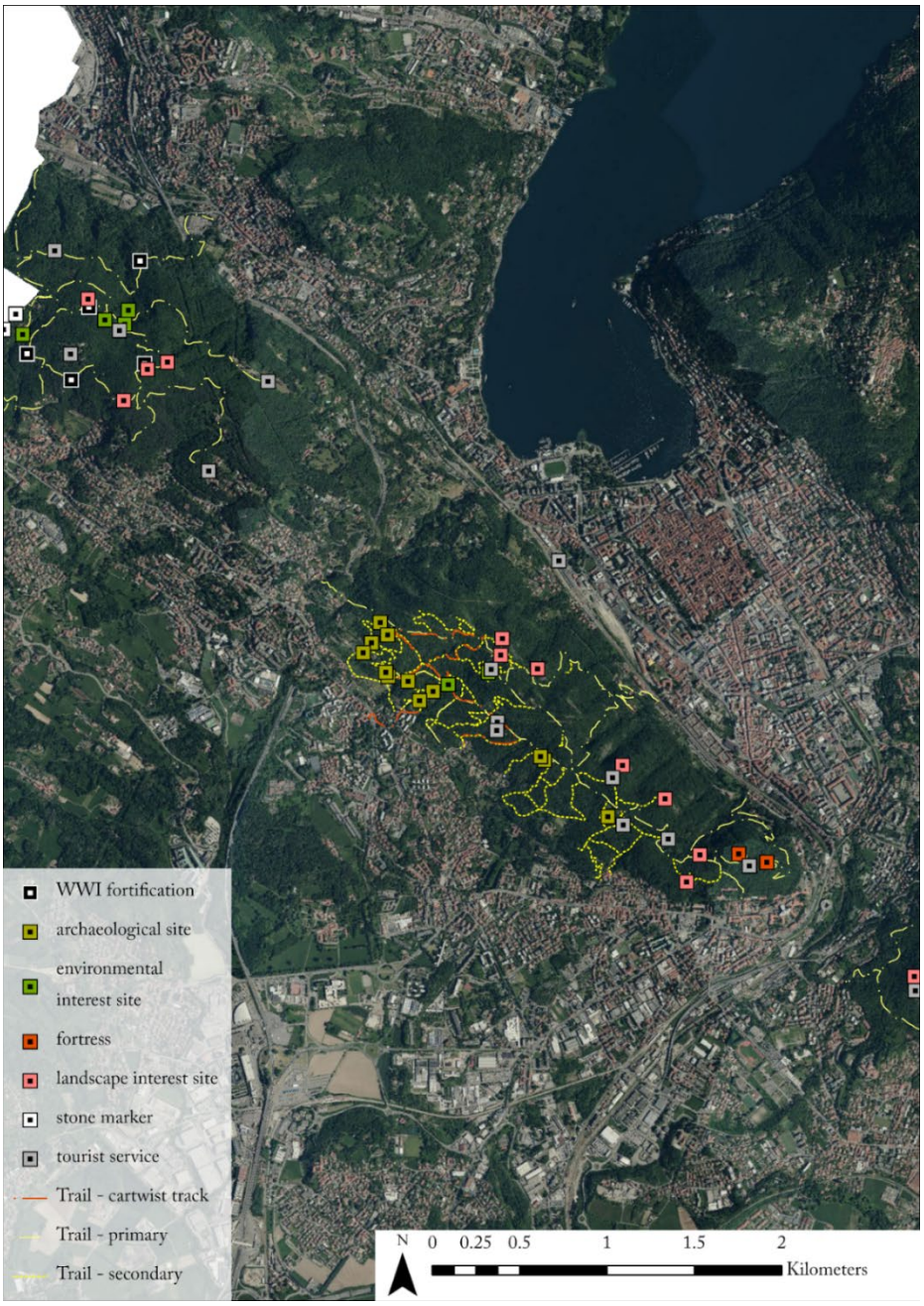

Figure 7. Map of the case study 1. The Spina Verde Park in Como (Lombardy). Datum RDN2008, projection UTM zone 32 N (EPSG: 7791) – credits LabG4CH, University La Sapienza (data), author (elaboration).

In this context, since the necessity was to enhance the knowledge of these sites, a project of archaeological research was integrated with a new survey funded by the regional Park of Spina Verde. The research takes origin from an agreement for multi-disciplinary investigation activities of the proto-urban site, coordinated by the local Superintendency of Archaeology, Fine Arts and Landscape, La Sapienza University of Rome, the Polytechnic University of Turin, and by the Turin unit of the Research Institute for Hydrogeological Protection of the National Research Council (CNR-IRPI) (Spanò, 2022).

In order to document the disseminated archaeological sites, and the complex territorial morphology, a low-altitude airborne LiDAR survey has been planned (75 pts/m^2). This has allowed for the rapid acquisition of homogeneous and widespread data that covered the full extension of the research area (Section 3.1.1 extensively describes the ALS primary dataset).

Furthermore, several ground-based 3D metric surveys were also planned to analyze and monitor individual archaeological areas, to be carried out in a widespread survey campaign.

Selected surveyed heritage sites

The terrestrial high-scale metric survey focused mainly on two areas: the Pianvalle proto-historical settlement and the Baradello castle (Figure 8, Figure 9), integrating UAS photogrammetry and LiDAR, terrestrial laser scanner (TLS), and mobile mapping systems (MMS) (Cappellazzo et al., 2023). Among the surveyed sites of the Park, these two areas have been selected because of methodological necessities. In fact, the surveys of Pianvalle and Baradello are characterized by several datasets acquired with different sensors, so to analyze and compare the resulting data.

The Pianvalle site (Figure 9a) is characterized by the presence of many typologies of archaeological evidence such as a huge rock engraving and several residential building typologies. The area was inhabited from the 6th to 4th centuries BC and abandoned until the end of the second century BC, becoming a sacred

burial place. Subsequently, the area was abandoned at the end of the first century BC, following the foundation of the Roman city of Como.

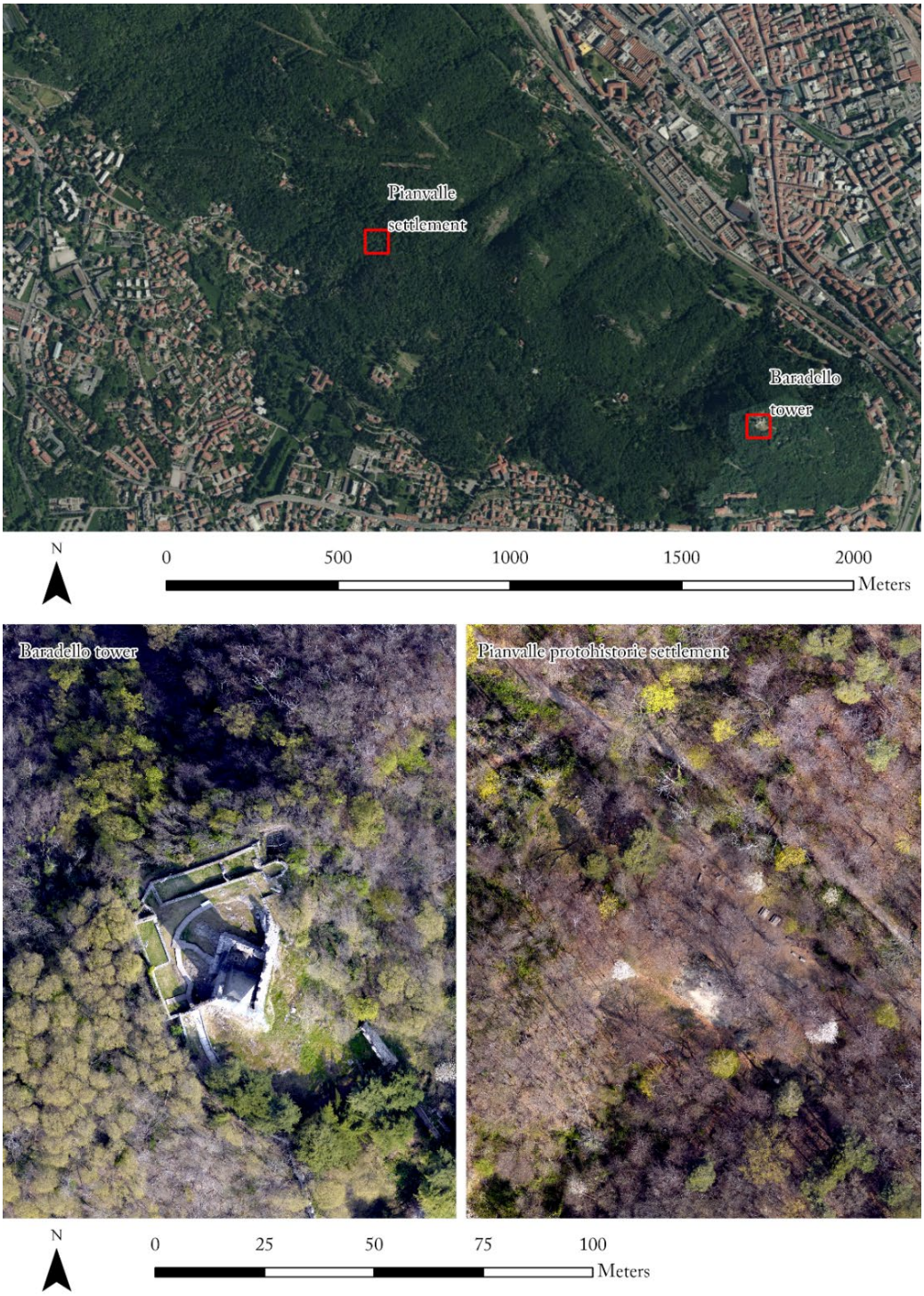

Figure 8. Integrated 3D metric survey areas from the Spina Verde Park: Baradello Castle tower and Pianvalle protohistorical settlement. Datum RDN2008, projection UTM zone 32 N (EPSG: 7791) – credits LabG4CH, CNR IRPI (Cappellazzo et al., 2023) (data), author (elaboration).

(a)

(b)

Figure 9. (a) Pianvalle protohistorical settlement and (b) Baradello Castle site – credits LabG4CH.

Still, Baradello castle (Figure 9b), situated on a hill overlooking Como, initially fortified in the late third century AD to defend against Germanic tribes, quickly became a key stronghold. During the 6th century, the Byzantines reconstructed the

fortifications during the Gothic War, marking the first major construction phase of the castle, then known as Castrum Baractelia. In the XIVth century, Azzone Visconti elevated a new quadrangular tower and strengthened the walls, further fortifying its defenses. However, in the XVth century, the Spanish governor of Como ordered its demolition, leaving only the tower standing as a testament to its storied past (Società Archeologica Comense, 2013).

The 3D metric integrated survey provided extended documentation of sites and ensured a multi-scale approach which is essential for a combined evaluation and comparison (Nex & Rinaudo, 2011, X) between the aerial LiDAR and photogrammetric/LiDAR UAS-terrestrial data.

Case Study 2: Sardinia Defensive Landscapes

As briefly discussed, the heritage framework section discussed the importance of enhancing the knowledge of historical defensive and military landscapes through its recognition, mapping, and documentation. In this context, the island of Sardinia represents a significant example of territorial defense development over time. Still, it should be underlined that Sardinia defensive systems have been widely studied, and the present doctoral dissertation is based on a knowledge-based approach that is developed starting from specific domain datasets and census that has been produced by other research groups or by the author.

Specifically, the datasets from other research groups are specifically acquired from different research projects listed below:

- Census of coastal military architecture conducted as part of the research project entitled "Military architecture in small islands", scientific directors Anna Maria Colavitti and Donatella Rita Fiorino, within the European project entitled "ISOS - Sustainable Islands: Réseau d'îles pour le développement durable et la préservation des patrimoines"

(http://interreg-maritime.eu/it/web/isos/progetto), funded by the call of the Cross-border Cooperation Programme Italy-France Maritime 2014 – 2020.

- Census of the Coastal Towers of Sardinia, scientific director Caterina Giannattasio, as part of the University of Cagliari research project entitled "Traditional masonry techniques: knowledge for conservation and performance improvement".
- Census of the military architectures of the Cagliari area, scientific director Donatella Rita Fiorino, carried out as part of the Collaboration Agreement signed on 18 September 2018 between the University of Cagliari and the Ministry of Defense – General Secretariat of Defense on research and training issues, in the field of engineering and architecture.
- Census of the military architectures of the Alghero Area. The census pertains to the master's degree thesis of the author (Cappellazzo, 2019).

These research experiments and works have then resulted in multidisciplinary publications (Deidda et al., 2015; Fiorino, et al., 2017b) and summary volumes (Fiorino, 2017, 2021; Giannattasio et al., 2020) that describe the military and defensive heritage context in Sardinia and the methodological practices for military heritage analysis and cataloging. Still, the generation of a geospatial database has been investigated in (Vacca et al., 2018) in order to catalog the Sardinian architectural military heritage. The architectural elements of Sardinia's historical defensive landscape are highly diverse, both in chronological and typological terms, as well as in their construction methods. These studies use interdisciplinary methodologies for chronological and typological analysis, providing a valuable tool for the conservation of this heritage.

From the 12th century to the 20th century, Sardinia's military architectural production has been directed towards constructing and improving the defensive

structure, especially along the coastal strip (Giannattasio et al., 2020). The heritage investigated consists of several elements, dating from the 12th to the 20th century. These could be classified among various typologies of defensive structures.

- Fortified villages – enclosed settlements often protected by walls and designed to defend the inhabitants from external threats.
- Defensive walls – perimeter walls built to protect cities, towns, or strategic sites.
- Forts and fortifications
    - fortified houses – residential buildings fortified for defense.
    - keeps – central, strong defensive towers in a castle, often serving as a final refuge.
    - castles – large, fortified sites of lords or rulers, combining defense, residence, and administration.
    - donjons – large defensive towers, often serving as an additional stronghold within a castle.
    - forts and strongholds – strong defensive structures designed for military use, typically larger and more strategic.
    - bastions – external projection parts of a fortification designed to offer defensive positions for artillery.
    - towers – standalone structures built for defense or observation, often part of larger fortifications.
    - ramparts – defensive earthworks or walls surrounding a fortified site.
    - redoubts – small, enclosed defensive positions within larger fortifications.
- 20th-century military installations
    - barracks – military buildings used to house soldiers and equipment.

        - batteries – anti-aircraft/navy artillery installations used for coastal or strategic defense.
        - bunkers – underground or partially buried structures used for protection from attacks.
        - pillboxes – small, fortified defensive bunkers, typically concrete built for infantry or machine-gun placements.
        - strongpoints – heavily defended positions established to hold strategic areas.
        - anti-aircraft lines – defensive alignments designed to protect against aerial attacks.
        - air-raid shelters: structures built to protect civilians and soldiers during aerial bombings.
    - Signaling or lookout posts
        - coastal towers – defensive towers built along the coast to monitor eventual maritime threats.
        - lighthouses – tall structures emitting light to aid navigation and sometimes used for signaling.
        - semaphore stations – communication posts using visual signals to transmit information across mid-long distances.
    - Prisons – former military prisons

Regarding the main historical periods, it is possible to underline five significant construction phases concerning the defensive and military structures of Sardinia. The first one is characterized by diffused architectural production between the 12th and 15th centuries AD. In that, one finds fortified villages, defense walls, and fortresses constructed along territorial borders and major lines of communication. Many of these were promptly abandoned, others adapted to new military needs, and still others were newly built. Starting from the 16th century, new elements enriched the complex medieval defensive system such as fortified walls and coastal

towers erected to protect from Saracen invasions (Murru, 2015). During the 18th century, with the Kingdom of Sardinia-Piedmont, building new royal strongholds, forts, and bastions was carried out with reinforcement along the coast. During the 19th century, building work focused on the construction of military barracks with the aim of maintaining and restoring public order in the newly founded Kingdom of Italy. The last step of construction is represented by the extensive military production during the Second World War: batteries, bunkers, strongholds, pillboxes, air-raid shelters, and watchtowers (Mameli & Sanjust, 2015).

Despite the severe risk of obliteration of these artifacts, there is the necessity of documentation and conservation plans, as well as consolidated methodologies for recognizing and mapping the multiple historical defensive systems (Fiorino et al., 2017a). It is thus important to underline the plurality of architectural systems that have been built and developed over the centuries.

In this framework, in this doctoral dissertation a particular focus has been given to two different systems:

- The Sardinian Coastal Defense System (13th-18th centuries AD).
- The Mediterranean Wall of World War II (1939-1943).

Concerning the coastal tower system, starting from the 13th century and especially from the 16th, mainly developed by the Spanish Crown, it has been particularly committed to the construction of coastal towers and bastions to be protected against Saracen and pirates raids. Active until their dissolution in the 19th century, the Spanish administration maintained an integrated defense network of fixed towers and mobile units. Moreover, the century-old fortification process appears properly documented thanks to the Crown Tower Administration institution establishment in 1583 (effective in 1587) (Murru, 2015).

Furthermore, concerning the WWII coastal containment arch, particular attention has been given to the construction of concrete pillbox bunkers and

strongholds as part of a system designed for Sardinia's most vulnerable coastal urban centers. These architectures are referred to as “difficult heritage” since they have been neglected for a long time due to their association with war traumatic events (Cherchi et al., 2023). Moreover, it is worth mentioning that, after losing their defensive function, some of these were completely obliterated, while the remaining “modern ruins” are awaiting appropriate documentation, preservation, and reuse processes.

As shown in Figure 10, the Sardinian case study is divided into two different areas: one in the southern major urban center of the island (Cagliari) and the other in one of the most important tourist locations of the northern part of the island (Alghero). The two case studies primarily differ in the chrono-typological heterogeneity of defensive heritage artifacts and the scale of datasets that have been exploited. In both case studies, the primary data ALS dataset pertains to a regional dataset derived from two 2008 airborne LiDAR surveys. The acquisition campaigns were planned and executed with different characteristics and sensors, resulting in point clouds with different superficial densities (Section 3.1.2 extensively describes the ALS primary dataset).

Figure 10. Map of areas pertaining to the Case Study 2. Sardinian Defensive Landscapes. Datum WGS 1984, projection UTM zone 32 N (EPSG: 32632) – credits ESRI, ISTAT (data), author (elaboration).

Area 1 (Figure 11) is related to the urban area of Cagliari Municipality in the southern part of the region. The density of regional data is 2 points per square

meter, and a balanced chrono-typological heterogeneity characterizes the present historical defensive artifacts. There are thus different object typologies distinguishable from towers, bastions, fortresses, bunkers, and batteries.

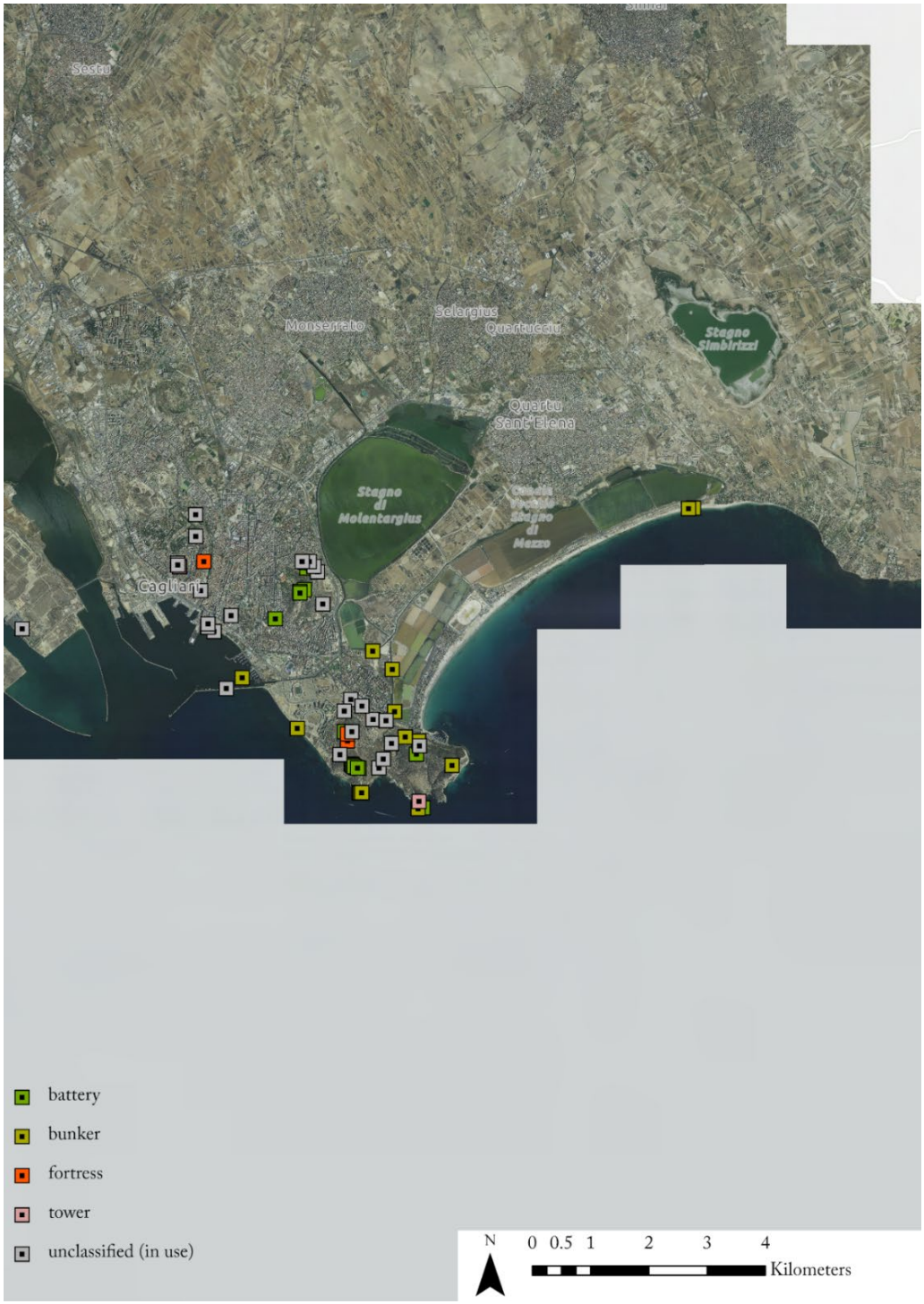

Figure 11. Map of Area 1 (Cagliari, Sardinia) pertaining to the Case Study 2. Sardinian Defensive Landscapes. Datum WGS 1984, projection UTM zone 32 N (EPSG: 32632) – credits Sardinia region, University of Cagliari (Fiorino, 2021) (data), author (elaboration).

The map in Figure 12, represents Area 2 in the Alghero municipality. In this case, the ALS point cloud density is 10 points/m^2, while the strong presence of WWII bunker artifacts characterizes the landscape.

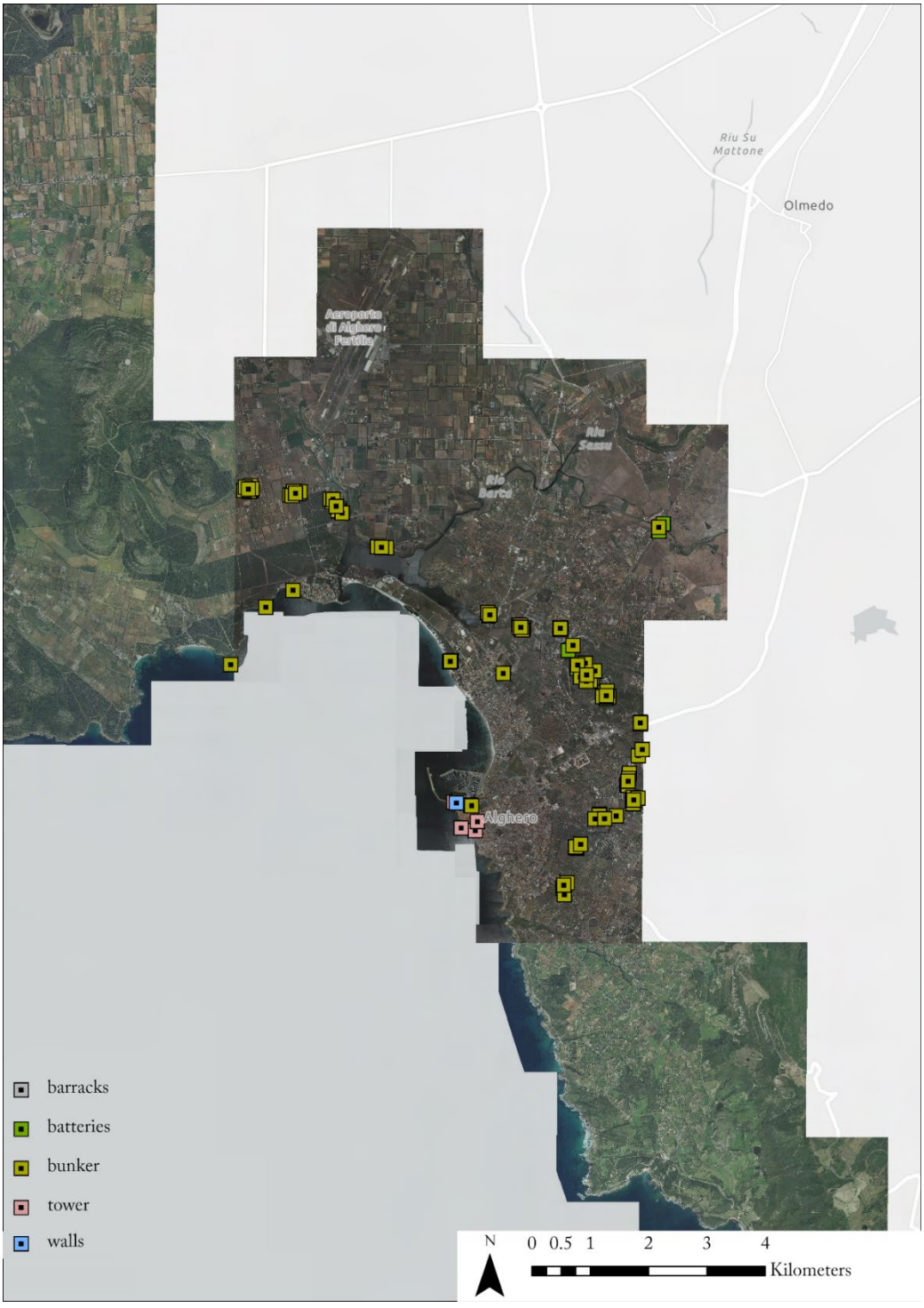

Figure 12. Map of Area 2 (Alghero, Sardinia) pertaining to the Case Study 2. Sardinian Defensive Landscapes. Datum WGS 1984, projection UTM zone 32 N (EPSG: 32632) – credits Sardinia region, author (Cappellazzo, 2019) (data), author (elaboration).

1.3 Dissertation structure

The Introduction section presents the heritage framework and emphasizes the study's relevance by introducing the research framework and explaining the objectives and the methodologies chosen to address the research questions.

The remaining structure of this doctoral dissertation is organized as follows:

- Chapter 2 – Literature review: Remote Sensing and machine learning techniques for data acquisition and structuring in landscape heritage contexts

This chapter reviews the literature concerning the methodologies and techniques that have been investigated for acquiring and analyzing data in Cultural Heritage contexts. The application of passive and active techniques, such as digital photogrammetry and LiDAR via airborne and spaceborne platforms, is increasingly crucial nowadays, as also briefly stated in the previous section. Additionally, subsection 2.1.3 evaluates the methods for organizing and categorizing such data, emphasizing unsupervised and supervised techniques for working with 2D raster and 3D point clouds. Furthermore, the chapter discusses relevant heritage documentation and data acquisition practices and examines the latest advancements in automatic classification and segmentation in the data processing and management framework.

- Chapter 3 – Materials and methods: Integration of multi-sensor Remote Sensing and Machine Learning methodologies for Landscape Heritage contexts applications

Chapter 3 discusses how remote sensing and machine learning techniques are integrated and applied to Spina Verde Park and Sardinia Defensive Landscapes case studies. The methodologies and workflows used for data processing are presented here, including macro-classification of point clouds, unsupervised filtering

techniques, and the development of Deep Learning models for semantic segmentation. Additionally, the chapter presents a preliminary investigation of the application of NN detectors for mapping heritage sites and the use of ML classifiers and visualization techniques in identifying man-made landforms.

- Chapter 4: Results and discussions

In the fourth chapter, the outcomes of the integrated methodologies are presented and analyzed from a critical point of view. Specifically, the chapter evaluates the effectiveness of unsupervised filtering approaches in preparing training data employed for the two Case Studies. It also presents the results of Deep Learning models for semantic segmentation, assessing the performance of ML classifiers for the classification of anthropogenic features within the study sites.

- Chapter 5: Conclusions

The final chapter summarizes the research's key contributions, emphasizing the significance of Remote Sensing and ML methodologies in advancing landscape heritage documentation, automation for data structuring, and analysis. It also reflects on the challenges faced during the study and the future perspectives for the research, suggesting ways to improve the integration of GeoAI technologies in Cultural Heritage studies.

Some of the content that has been presented concerning methodologies, key findings, and results insights have been previously published by the author in earlier works (Cappellazzo et al.,2023;2024a; 2024b).

Chapter 2 – Literature review

Remote Sensing and Machine Learning techniques for data acquisition and structuring in Landscape Heritage contexts

2.1 Methodologies and technologies

As briefly introduced in Section 1.2.1, in recent decades, RS and ML technologies have significantly advanced in several application fields, such as cartographic production automation (Savino et al., 2011), environmental and anthropic risk monitoring for post-emergencies (Boccardo & Giulio Tonolo, 2012b), and specifically the field of CH documentation (Bassier et al., 2018; S. Yang et al., 2023). In fact, the integration of these technologies allows for detailed, efficient, and non-invasive methods of recording and analyzing CH sites (Argyrou & Agapiou, 2022).

In this context, remotely sensed data have thus revolutionized data acquisition by offering both far-distance and close-range approaches. Methods can be classified into passive and active technologies, which could also be categorized depending on the acquisition platform, such as spaceborne, airborne, and terrestrial (Figure 13) (Luo et al., 2019). In this regard, the present dissertation considers UAS platforms as a separate aerial category of vectors, intending instead airborne solutions only those piloted by a human operator (e.g., airplane, helicopter).

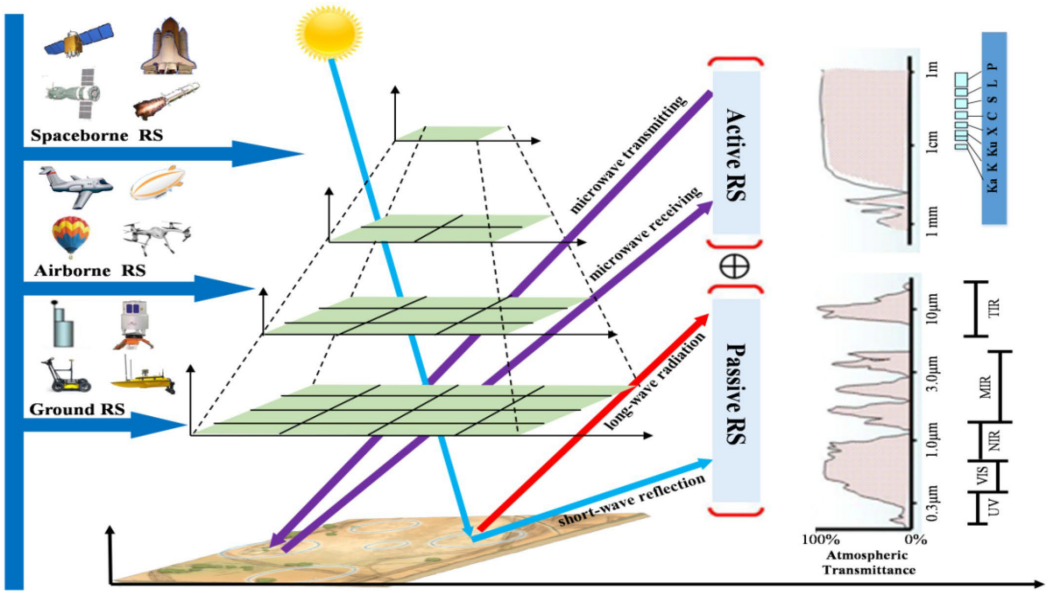

Figure 13. Schematic diagram of Remote Sensing – credits (Luo et al., 2019)

Since doctoral research focuses on the application of suitable techniques for the acquisition, processing, and analysis of 3D point cloud data and the interpretation of territorial context morphology via Digital Terrain Models (DTM), these will be presented in order to discuss different issues. In this sense, spatial and radiometric accuracy, echo return information, penetration capabilities, existing data availability, density, costs, and automation are significant arguments that are analyzed and evaluated to respond to the dissertation's expected results. Specifically, as highlighted in the introduction, the thesis aimed at the application of ML methodologies on heterogeneous scale Airborne Laser Scanner (ALS) point clouds and subsequent DHMs in order to develop support methodologies that can adequately describe the terrain and built morphology of the presented landscape

contexts. In fact, the technology review is focused on discussing the methodology related to territorial and landscape-scale context applications. Sub-section 2.1.1 provides an overview of the principal acquisition methodologies and describes the principal Remote Sensing technological component in the geomatic and information sciences framework for 3D data acquisition and processing, focusing on CH adaptability. Sub-section 2.1.2 describes the current potentials and issues of 3D ALS LiDAR data and model interpolation. The 2.1.3 sub-section instead illustrates the increasingly important GeoAI methodologies for the automatic classification and semantic enrichment of 3D/2D unstructured data.

2.1.1 Passive and active sensors for CH monitoring, mapping, and documenting

In the last decades, passive and active RS methodologies have risen and become crucial in several application fields, such as cartography production, forestry sciences (Iglhaut et al., 2019), agricultural sciences (Candiago et al., 2015), and, of course, archaeological and heritage monitoring and documenting (Luo et al., 2019). In the following paragraphs are presented some of the acquisition techniques that have been evaluated in the present dissertation to acquire complete 3D data about extended landscape contexts.

Structure-from-Motion digital photogrammetry

In this framework, Structure from Motion (SfM) digital photogrammetry techniques certainly occupy a privileged place. This technique involves using digital cameras to capture multiple overlapping images of a 3D scene or object. These are then processed to estimate the internal parameters of the camera, and thus the camera position, by solving the relative exterior orientation of the photogrammetric

block by image matching through homologous point identification (Granshaw, 2020; Sweeney et al., 2015) (Figure 14).

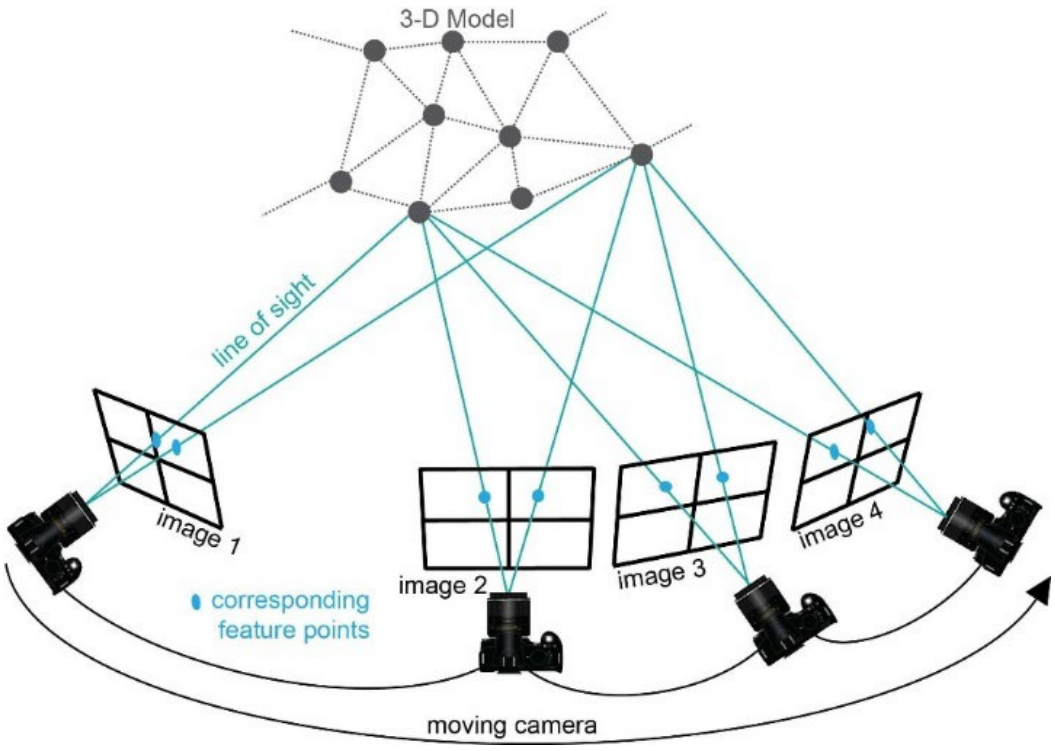

Figure 14. Schematic acquisition methodology and geometrical principles for SfM digital photogrammetry – credits Katherine Shervais (Department of Geoscience, Colorado State University)

The 3D model is subsequently processed to solve the absolute orientation by translation, rotation, and scalation matrixes (bundle block adjustment), which are usually calculated by Ground Control Points (GCPs) employment (James & Robson, 2012).

This technique allows the generation of high-resolution 3D models from relatively simple and cost-effective equipment (Westoby et al., 2012). SfM techniques, and especially UAS digital photogrammetry, are particularly useful for documenting large areas and complex structures, maintaining at the same time a very high spatial and radiometric resolution (Colomina & Molina, 2014). Still, digital photogrammetry largely benefited from the integration of GNSS real-time kinematic (RTK) sensors on remotely piloted vehicles and cameras, allowing the direct georeferencing (DG) of the camera center positions (Carbonneau &

Dietrich, 2017). In this framework, UAS photogrammetry can also be evaluated as a valuable tool for the generation of dense and accurate DTMs for microtopography analysis and monitoring (Johnson et al., 2014). However, it should be noted that DTM generation could be accomplished while working with data acquired in optimal conditions and not in forested areas.

Furthermore, even CH documentation has largely benefited from the technological development of digital photogrammetry sensors, and especially vectors, such as Unmanned Aerial Systems (UAS) (Aicardi et al., 2018; Remondino, 2011; Rinaudo et al., 2012). In fact, it is possible to accurately describe immovable and movable heritage features in several scales and different contexts (Lovitt et al., 2017; Patrucco et al., 2023; Spanò et al., 2018; Vavulin et al., 2021), from museum artifacts to building and landscape sites. Still, the importance of radiometric and spatial resolution richness is a crucial issue for the analysis of CH sites and buildings. In this sense, SfM techniques allow the generation of high-resolution 3D models. In order to underline the importance of this topic, in these sections some of the processing results of the surveys are presented from the Spina Verde Case Study. In fact, Figure 15 shows the dense photogrammetric point cloud of the Baradello castle area obtained from a low-altitude UAS survey. In this regard, it is possible to observe that the spatial and radiometric resolution of the model allows to analyze features such as the masonry texture and identify eventual decays or inconsistencies.

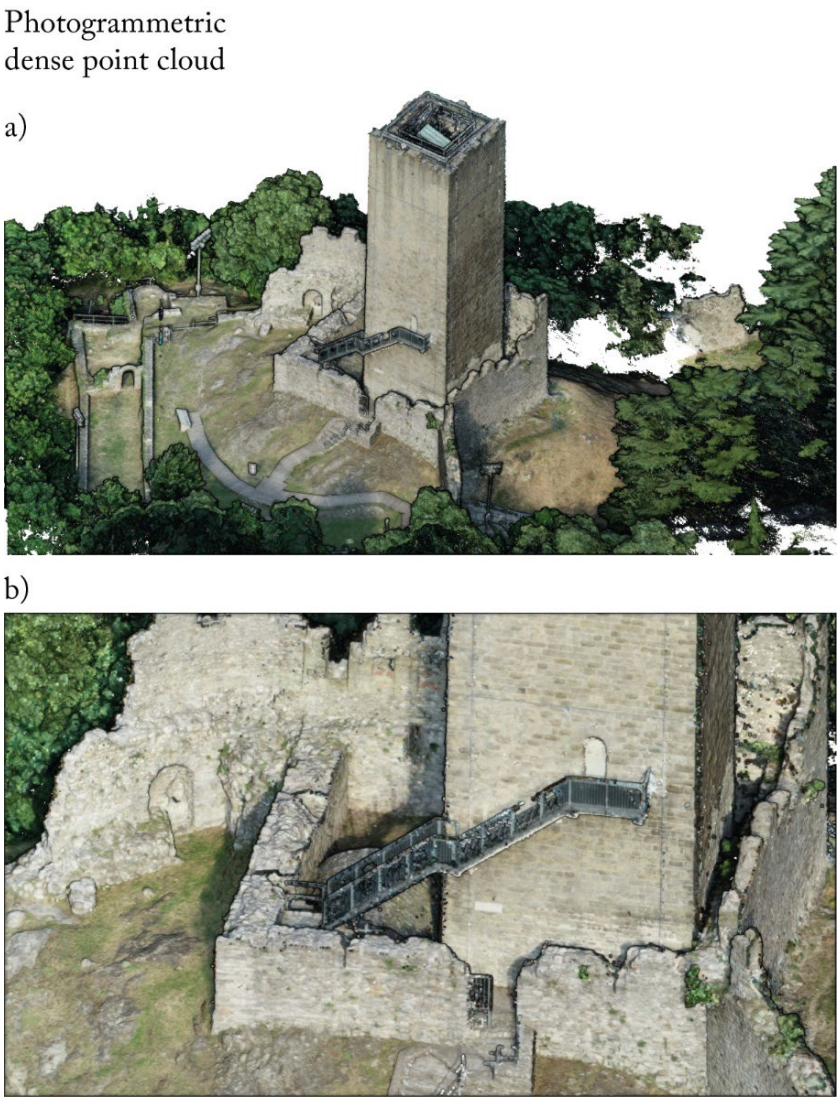

Figure 15. Colored densified point cloud from UAS photogrammetry from Case Study 1 integrated survey (Como, Spina Verde Park). (a) Contextual view of the Baradello medieval tower. (b) Close-up view of the southeast façade of the tower. Sensor: CMOS 1" equipped on DJI Phantom 4 Pro. Processed with Agisoft Metashape Pro – credits LabG4CH (data); author (elaboration).

Digital photogrammetry and imagery products derived from spaceborne and aerial platforms

Among the acquisition platforms, in spaceborne remote sensing, sensors are carried by orbiting satellites. In this case, altitude ranges are much higher than airborne vectors (typically over 250 km), and the acquisition covers the earth's surface at fixed intervals, depending on the satellite's orbit. In the framework of

territorial morphologies analyses, since the beginning of the 21st century, the leverage of available stereoscopic images from satellite platforms has allowed the generation of low-resolution DHMs using homologous point coordinate extraction. These have achieved spatial resolution accuracies ranging from 5 to 10 meters in open and flat areas (Jacobsen, 2003). In this sense, in (Borgogno Mondino et al., 2004), several tests have been conducted to validate the accuracy of DTMs generated from 15 m Ground Sampling Distance (GSD) stereoscopic satellite imagery in sloped mountain regions, estimating a 20 m absolute accuracy. Instead, in (Takaku et al., 2014), the leverage of a stereoscopic triplet (2.5 m GSD) allowed the semi-automatic processing of a DSM that has been validated with GCP and reference DSM estimating a RMSE (Root Mean Square Error) of 5 m. Furthermore, (Bhushan et al., 2021) exploited commercial VHR triplet stereo imagery to automate the generation of DHMs, validating the model with an absolute vertical accuracy ranging from 3 m to 5 m. Although the generation and validation of height models is a relevant topic in satellite imagery, the reliability of open-access satellite DTMs for monitoring archaeological and CH sites has not been considered suitable for the present research. Instead, starting from the end of the 20th century, spaceborne Synthetic Aperture Radar (SAR) techniques have proven to be more accurate for micro-topography analysis of the terrain (Massonnet & Rabaute, 1993), although pertaining to active sensors. In particular, Interferometric SAR (InSAR) could be employed for subsidence monitoring and prospection due to the sensor's capacity to sense a target with any light or weather condition and eventually penetrate soil and vegetation depending on amplitude and phase frequencies (Franceschetti & Lanari, 2018). In this context, (Barreca et al., 2020) demonstrated that the analyses of ground deformation from multi-temporal InSAR (MT-InSAR) are coherent with the displacement measurements from traditional GNSS techniques, confirming the technique to be suitable for macro-topography monitoring. Still, InSAR techniques have also proven their capabilities

in detecting buried and terrain features for archaeological purposes, and they also show better results when compared to optical imagery (Luo et al., 2019).

On the other hand, spaceborne imagery techniques can surely be considered still suitable for various applications by leveraging multispectral and hyperspectral data, which allows the capture of information in the non-visible range of the radiometric spectrum. Specifically, spectroscopy imaging consists of co-registering images related to contiguous spectral channels (Schaepman et al., 2009). In this sense, the disambiguation between multispectral and hyperspectral imaging is crucial where the definition of a material by the identification of spectral signature is much more accurate where it is possible to access more numerous and thinner spectral channels (Luo et al., 2019). Although the very first civilian satellite program, including multispectral imagery (Landsat 1-1972), had a resolution of 15 m, contemporary spectral imaging sensors can easily reach a higher GSD, ranging from 50 cm to 10 m, and manage multiple spectral channels. In this framework, Sentinel 2 mission data represents a valuable open-access solution (Drusch et al., 2012) (Figure 16). However, the low GSD from the Sentinel 2 data makes them not suitable for archaeological and heritage monitoring unless adopting super-resolution algorithms, as presented in (Lanaras et al., 2018).

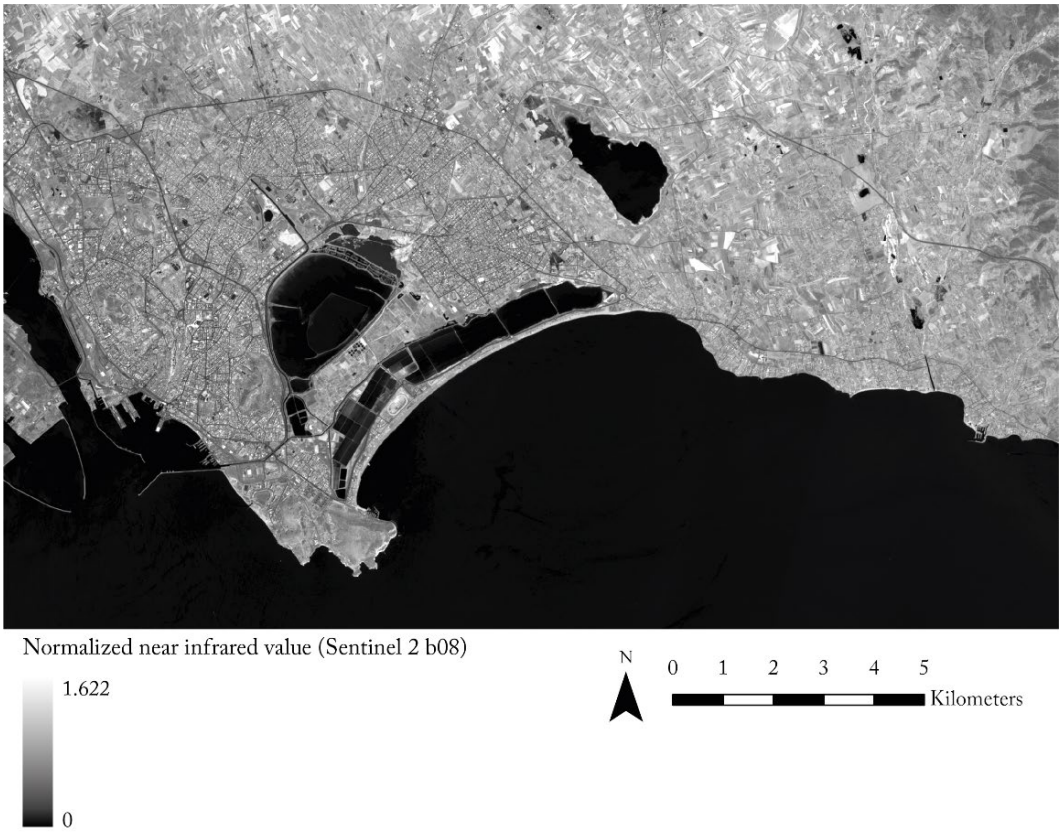

Figure 16. Normalized near-infrared band from Sentinel 2. (Level 2A – bottom atmosphere). Sample data from Case Study 2 – Area 2 (Cagliari, Sardinia) – credits Copernicus, (Drusch et al., 2012) **(data) author (elaboration).**

Moreover, it is worth mentioning that UAS equipped with photogrammetric sensors offer flexible, cost-effective, and high-resolution data acquisition capabilities, enhancing the documentation of both large and small sites (Kalacska et al., 2021). In this framework, Very High-Resolution (VHR) multispectral and hyperspectral imagery represent highly adaptable approaches, providing rich datasets that capture a wide range of information about the condition and composition of the territory and landscape (Batar et al., 2017; Santoro et al., 2023). In fact, providing valuable information about the composition of materials has been proven to be essential for preserving heritage sites (Chane et al., 2013; Picollo et al., 2020). However, although VHR airborne or terrestrial multispectral data fusion is considered particularly valuable for building/object-scale CH applications (Adamopoulos & Rinaudo, 2020), it is worth noting that extended landscape

contexts, such as those presented for Case Study 2, are difficultly surveyable with terrestrial and UAS SfM solutions.

Data acquisition with active sensors: LiDAR

Among the sensors from remote sensing techniques, active sensors represent a valid solution for acquiring 3D data. In contrast to passive sensors, where absorbing existing radiation is used to take measurements (e.g., the sun), active sensors, such as LiDAR, directly emit radiation for measurements. These systems, which have been the basis of one of the most important surveying methodologies that have been largely diffused and consolidated in the present millennium, can collect extensive and accurate 3D data that can be exploited for various applications.

LiDAR sensors operate by emitting laser pulses, which bounce on objects or surfaces and return to the sensors (Boehler & Mars, 2004; Shan & Toth, 2018). These systems can be categorized depending on the operating principle of the sensor. Essentially LiDAR sensors can be categorized into two classes, which also pertain to the sensor typologies that have been employed in the surveys of the two case studies.

- Phase shift (PS) sensors
- Time-of-flight (TOF) sensors

In PS methods (multiple-frequency phase comparison), the range value is derived by the comparison of transmitted and received sinusoidal wave patterns (Figure 17). Thus, by the difference between transmitted and received signals, the fractional part of the total distance is calculated ($\Delta\lambda$). Due to the medium acquisition range (300-400 m) and millimeter accuracies, PS systems are usually used by terrestrial laser scanners (TLS) for building scale surveys (Shan & Toth, 2018).

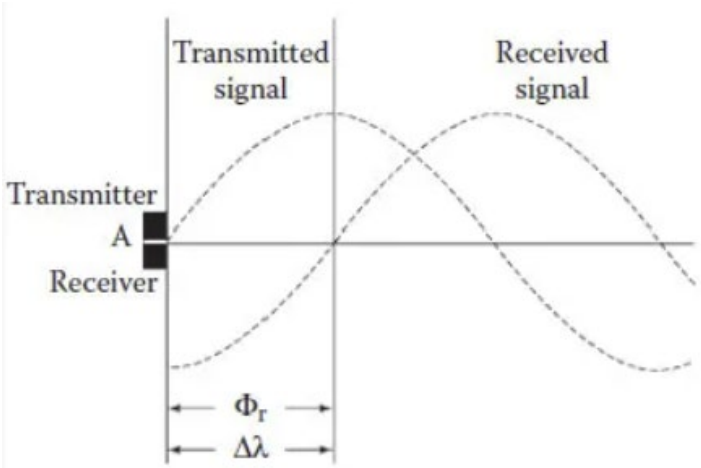

Figure 17. Phase comparison of the sinusoidal wave from transmitted and reflected signals – credits (Shan & Toth, 2018).

TOF methods involve the accurate measurement of the time that the transmitted laser pulse radiation employs to reach the ground object and the time the reflected pulse employs to return to the instrument (Figure 18). Through the calculation of the time interval that has passed between the pulse emitted by the laser and the pulse returning from the object, it is possible to calculate the distance and position of the point on the object (Shan & Toth, 2018).

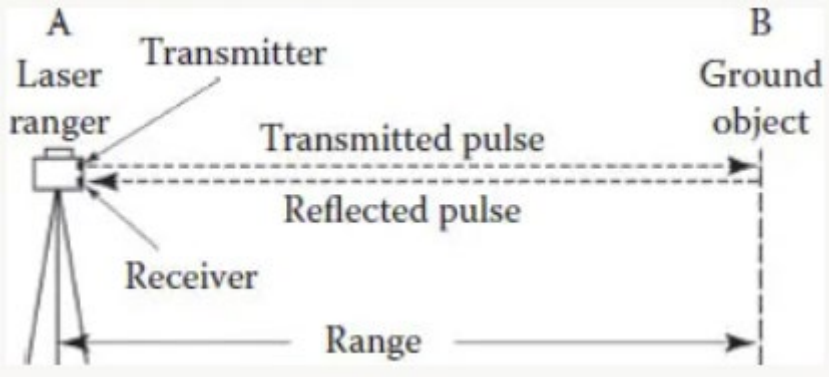

Figure 18. Operating scenario of a Time-of-Flight laser sensor – credits (Shan & Toth, 2018).

TOF systems are usually equipped on airborne platforms due to the high range allowed (> 1 km). In fact, these are particularly suitable for territorial-scale applications (Maas & Vosselman, 2010).

Furthermore, the evolution of technologies has led to the consideration of integrating LiDAR sensors using UAS vectors. These compact solutions now optimize the on-flight stability issues and improve the estimation of the navigation path with differential real-time kinematic (D-RTK) Global Navigation Satellite System (GNSS). Moreover, the potential to estimate the ground surface is comparable, if not superior, to that obtainable using SfM-based UAS photogrammetry, such as demonstrated by (Kalacska et al., 2021) focusing on environmental monitoring applications.

Still, the recent diffusion of commercial UAS platforms equipped with compact LiDAR sensors (e.g., DJI Zenmuse L1/L2, RIEGL miniVUX) increases accessibility to technologies as well as provides cost-effective solutions for experimentation on landscape and heritage high-scale 3D mapping (Diara & Roggero, 2022; Mazzacca et al., 2022).

Furthermore, these systems have proven particularly effective in dense urban areas (Figure 19), as described in (Kölle et al., 2021), where a UAS LiDAR system has been used to generate a point cloud and mesh semantic segmentation benchmark dataset for urban contexts.

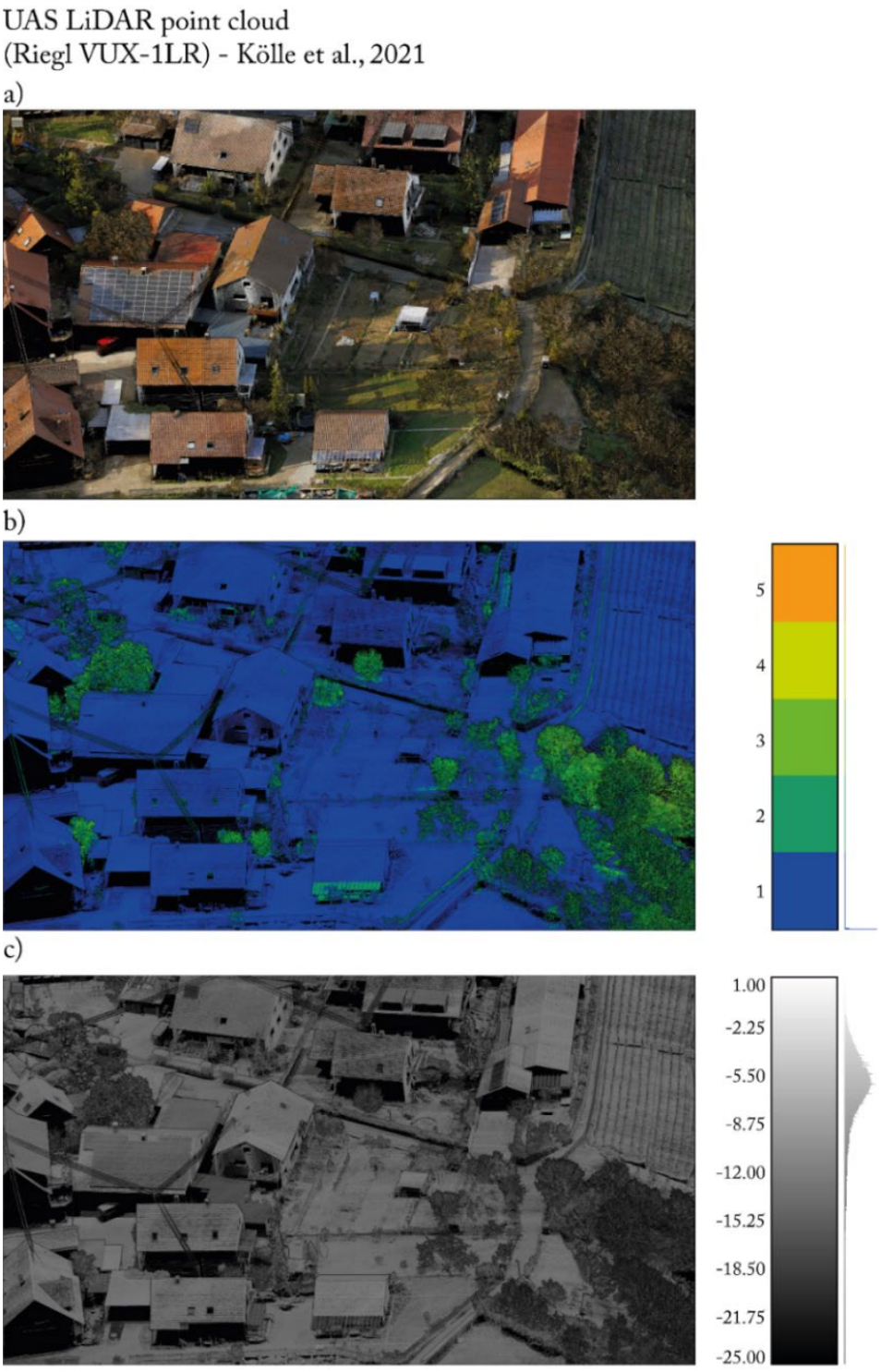

Figure 19. Sample data from Hessigheim 3D (H3D) benchmark, acquired from a UAS platform. (a) RGB colored point cloud (2 oblique Sony Alpha 6000 cameras). The echo information of (b) number of return and (c) corrected intensity have been recorded from a Riegl VUX-1LR LiDAR sensor – credits (Kölle et al., 2021) **(data).; author (elaboration).**

2.1.2 DHMs generation from airborne LiDAR

If compared to terrestrial and other techniques, such as the discrete points measurement using the GNSS technique or digital photogrammetry, LiDAR technologies have predominantly innovated 3D mapping and vegetation penetration capabilities, acquiring accurate data from sensors equipped on aerial-based vehicles (e.g., planes, helicopters, and drones). However, unlike in digital photogrammetry and phase shift TLS, it is impossible to derive the ground coordinates of the laser point solely with the range points (Maas & Vosselman, 2010). In fact, although UAS photogrammetry techniques could benefit from RTK positioning for the estimation of precise sensor coordinates, this is not an essential condition for the accomplishment of surveys. The reconstruction of the sensor trajectory is thus possible with the employment of integrated Global Navigation Satellite Systems (GNSS) and Inertial Measurements Units (IMUs) georeferencing systems. These can estimate the airborne platform position and altitude with an accuracy ranging between 4 and 7 cm and 20-60 arc seconds, respectively (Shan & Toth, 2018). The use of airborne platforms is traditionally related to the most varied application sectors, reducing time acquisition and ensuring high and accurate productivity, especially for urban 3D modeling or terrain morphology analysis. Furthermore, the recent advancements in full-waveform LiDAR (Mallet et al., 2011) have enhanced the pulse return number recording and reflectance accuracy, facilitating better analysis of micro-topographic features (Mancini et al., 2013). In Figure 20 and Figure 21, it is particularly evident that the integration of full-waveform LiDAR and digital photogrammetry represents a valuable tool for extended areas monitoring, being able to obtain accurate data with an adequate spatial resolution coherent to mid-scale spatial analysis, also targeting heritage sites.

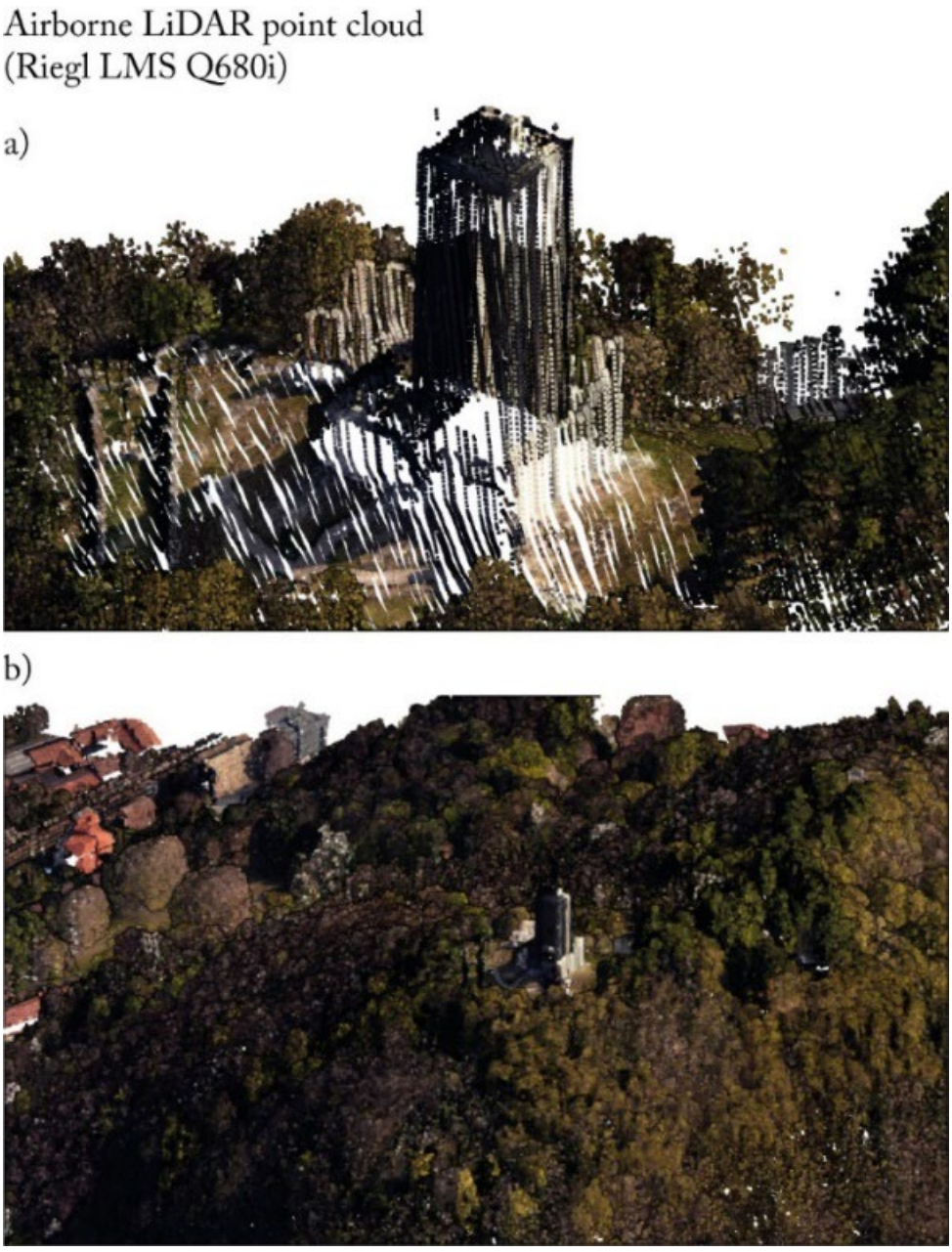

Figure 20. Sample data of the airborne LiDAR acquisition from the survey planned in Case Study 1 (Como, Spina Verde Park). (a) Close view of Baradello medieval tower from Case Study 1. (b) Contextual view of the tower. The survey has been conducted using a Litemapper 6800 LiDAR system (Riegl LMS-Q680i – PhaseOne iXM medium format aerial camera) – credits LabG4CH and CNR IRPI (data); author (elaboration).

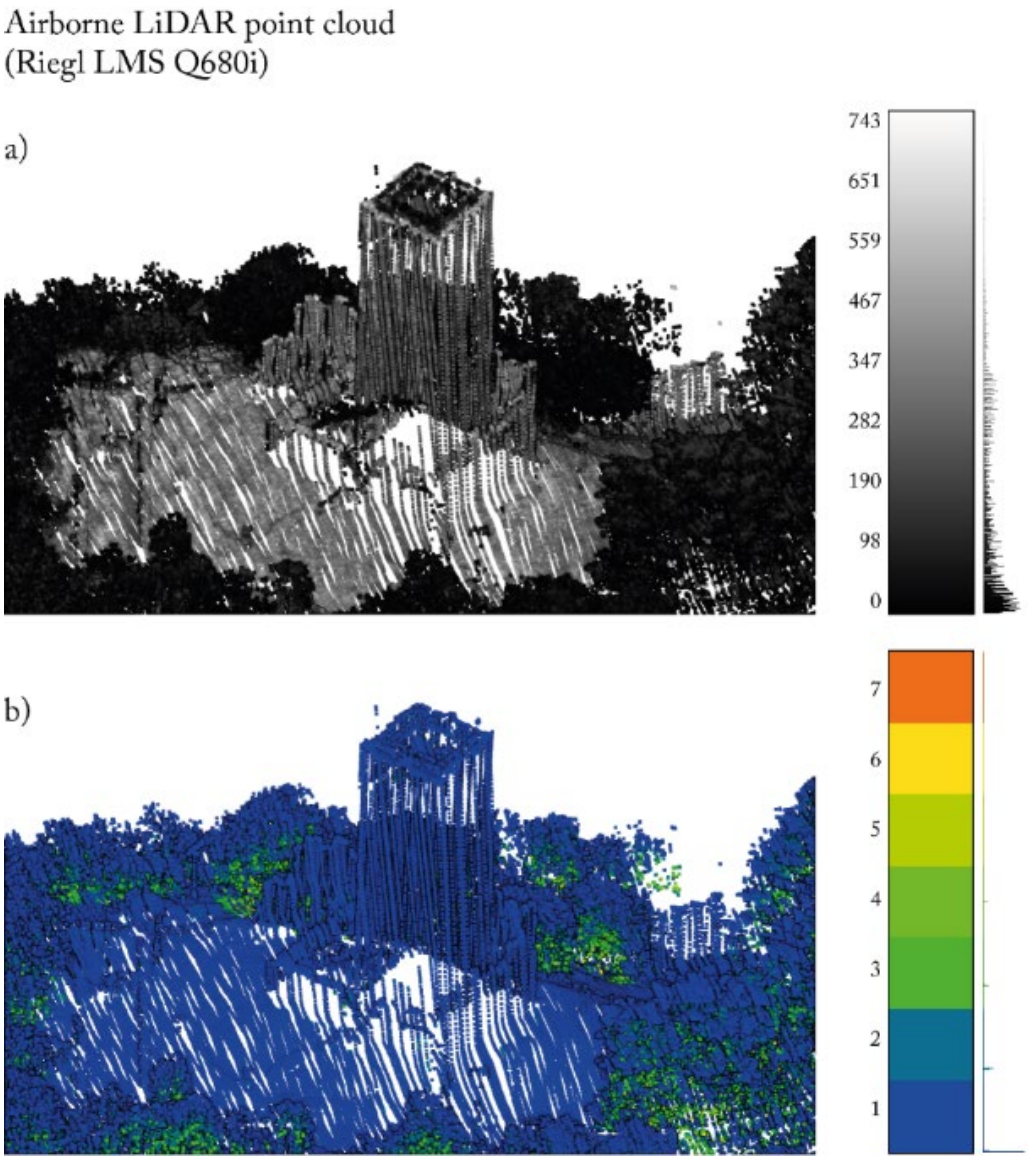

Figure 21. Sample data of the airborne LiDAR acquisition from the survey planned in Case Study 1 (Como, Spina Verde Park). (a) Reflectance intensity and (b) return number information. The survey has been conducted using a Litemapper 6800 LiDAR system (Riegl LMS-Q680i – PhaseOne iXM medium format aerial camera) – credits LabG4CH and CNR IRPI (data); author (elaboration).

However, it should be underlined that one of the critical challenges in using RS data for archaeological and heritage monitoring derives from interpolation processing to generate DTM. In this sense, terrain models in densely forested areas are usually generated with higher densities and accuracy using airborne LiDAR technology rather than digital photogrammetry or UAS LiDAR (Wieser et al., 2016). In fact, the generation of DTMs and the spatial accuracy of raster

interpolation techniques depends on the application context, the sensor penetration capacity, and the density of ground points (Adedapo & Zurqani, 2024).

Given the importance of DTM generation for CH sites mapping and analyses, in Figure 22, it is possible to observe the raw data comparison between UAS LiDAR and manned airborne LiDAR.

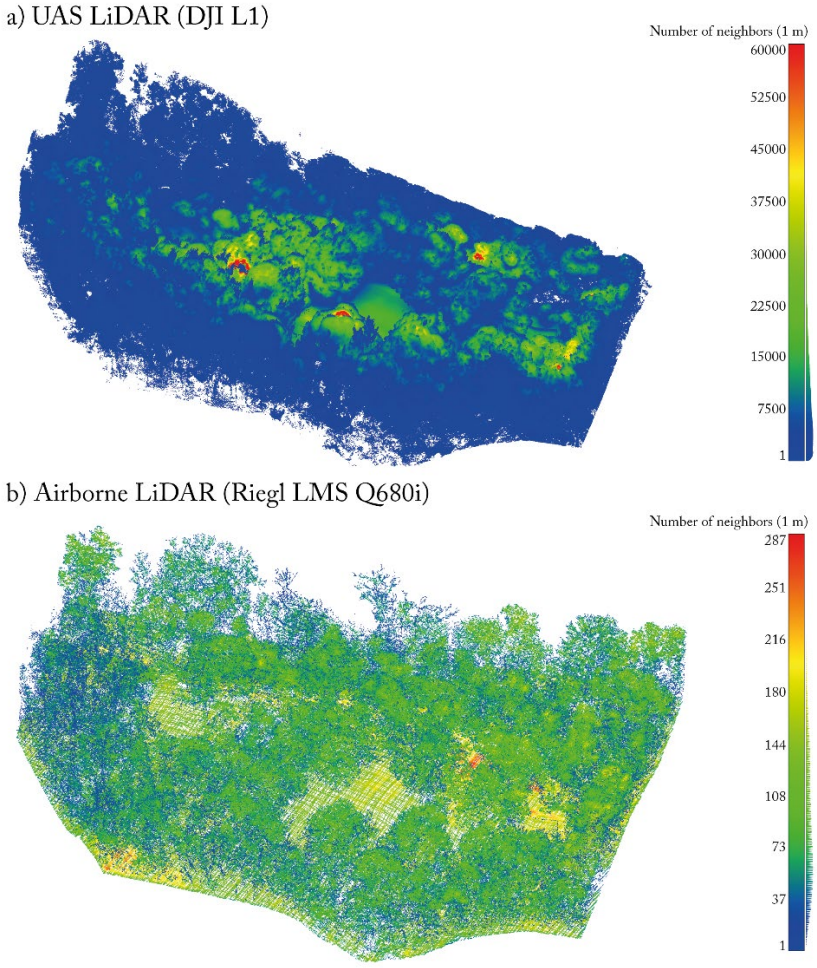

Figure 22. Sample data comparison between the UAS LiDAR point cloud and ALS point cloud number of neighbors (1 m radius) from Case Study 1 in Spina Verde Park. The sample is taken from the Pianvalle protohistorical settlement, where a (a) UAS LiDAR survey has been conducted with a DJI L1 (Livox) sensor equipped on a DJI Matrice 300 k. (b) The ALS survey has been conducted with a Riegl LMS Q680i from a helicopter platform – credits LabG4CH and CNR IRPI (data); author (elaboration).

In this case, the difference in above-ground level (AGL) height is particularly evident in terms of the calculated number of neighbors and, thus, spatial resolution. However, since the cruciality of DTM generation has been underlined, the two

different techniques should also be evaluated in terms of the consistency of ground point data, especially in such a forested context. In fact, in Figure 23, it is possible to observe that the application of ground-filtering algorithms showed the manned airborne LiDAR to have a major penetration capability rather than UAS LiDAR. In this regard, segmentation and filtering are fundamental steps towards the semantic classification of 3D point clouds, and they are even useful for an accurate analysis of primary data. For this specific reason, the manned solution represents the preferred primary data acquisition approach, which is necessary to operate preliminary extended analysis in forested heritage sites.

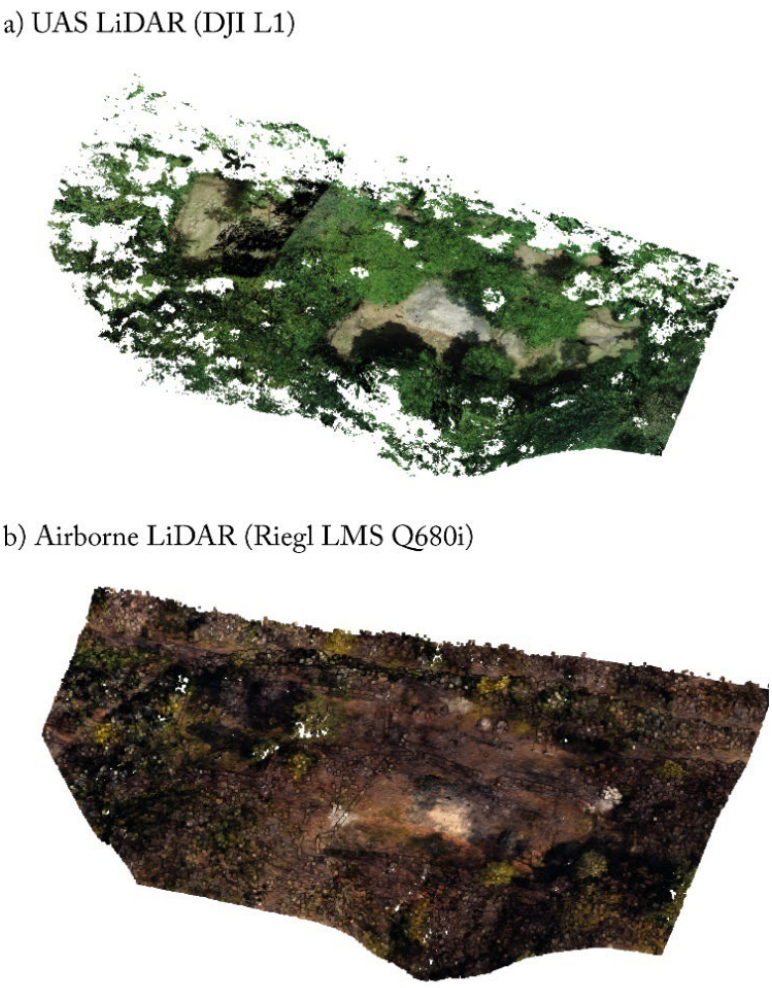

Figure 23. Sample data comparison between the UAS LiDAR point cloud and ALS point cloud from the Case Study 1 in Spina Verde Park. The sample is taken from the Pianvalle protohistorical settlement, where a (a) UAS LiDAR survey has been conducted with a DJI L1 (Livox) sensor equipped on a DJI Matrice 300 k. (b) The ALS survey has been conducted with a Riegl LMS Q680i from a helicopter platform – credits LabG4CH and CNR IRPI (data); author (elaboration).

2.1.3 Structuring and classifying data: unsupervised and supervised approaches for 2D grid and 3D point data

Much attention has been devoted in recent epochs to the study of automated classification algorithms to structure geospatial data. In this framework, Artificial Intelligence (AI) is nowadays widely studied for the optimization of classification and documentation pipelines. Numerous ML and DL methods have been developed and tested to increase automation and ensure classification workflow accuracy. Specifically, nowadays, machine learning is considered a branch of computer science where algorithms learn and improve knowledge to perform several tasks without explicit programming. Meanwhile, deep learning is conceived to be a branch of ML that approaches artificial intelligence and automates tasks on the basis of data. In fact, since DL models the real world using hierarchical structures of concepts and representations, it can construct complex representations from simpler elements and achieve remarkable flexibility and effectiveness (Goodfellow, 2006). The efficiency of single algorithms or layered algorithms (NNs) is usually controlled by setting the algorithm during the learning stage, which is called hyperparameters. Specifically, hyperparametrization is a critical step in optimizing machine learning models for tasks such as object detection, pixel classification, and object classification. Hyperparameters are settings that influence the training process and the model's performance. Some examples include learning rate, batch size, number of epochs, early stop settings, and model-specific parameters. In Sections 3.3.1 and 3.3.2, hyperparameter settings are extensively described for the training of the deep learning models.

In this context, data structuring, labeling, and annotation represent important research topics that can be integrated into several application domains. As also shown in Figure 24, interest in the data labeling and annotation topic has been graphically represented across a five-year term period.

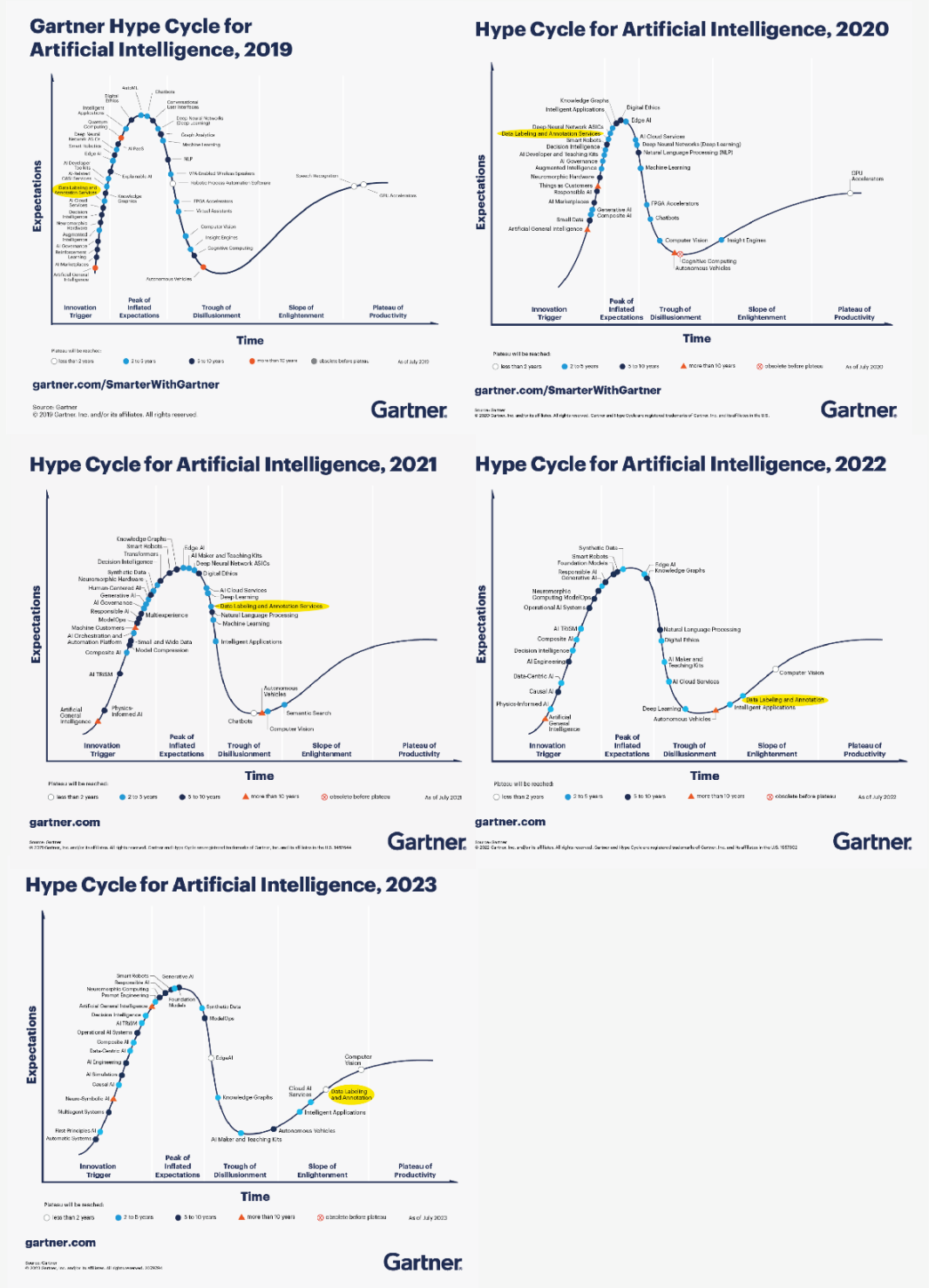

Figure 24. Gartner Hype Cycle graph for Artificial Intelligence (2019-2023). In the present comparison, a focus is represented by data labeling and annotation of the AI applications topic, which, starting in 2019, has moved across the curve, almost reaching production stability. The graph helps the user by providing an objective map that allows them to understand the real risks and opportunities of innovation. Every Hype Cycle includes five phases: the innovation cycle begins with a breakthrough or launch that sparks interest. Excitement peaks as usage grows, but hype often exceeds actual results. Disillusionment follows as early adopters face issues, but with time, users start seeing benefits and refining their approach. Eventually, the innovation reaches widespread adoption, delivering tangible, real-world value – credits Gartner (www.gartner.com).

Specifically, Gartner Hype Cycles are graphic representations of the maturity, relevancy, and adoption rate of emerging and mainstream innovations. Focusing on the data labeling topic, it is possible to understand how research has investigated the automation of semantic segmentation, detection, and classification of data. In addition, the countless variety of LiDAR or Image-based methodological approaches developed in literature in the last tens of years demonstrates that automated and integrated data structuring approaches based on multi-source data prove to be a successful approach (Z. Chen et al., 2017).

The following paragraphs specify the two main categories of ALS data classification that the author considered. The first subsection is related to image-based classification approaches using raster data. Furthermore, a review of methodologies for structuring 3D point clouds is provided, which has been so far less investigated.

Raster-based classification approaches

The necessity to enhance the automation of image classification tasks led to the development of various methodologies depending on the aims and the specific criteria assumed by different algorithm applications.

Considering the different categories of image classification methods deeply examined by (D. Lu & Weng, 2007), the high efficiency of non-parametric, per-pixel, and supervised strategies for remotely sensed imagery and DHM has been established. Literature research demonstrates de facto that AI techniques based on Machine Learning classifiers (MLCs) are particularly suitable for geospatial imagery (Maxwell et al., 2018). However, some recent studies have investigated ML classification techniques adopting an integration strategy on DHM using optical sensor data and ALS 3D data (Alifu et al., 2020; Maxwell & Warner, 2015).

These classification algorithms belong to the supervised learning category, where a predictive model is generated from an input set of training samples. Additionally, it is widely acknowledged that MLCs can handle large datasets

effectively, producing more accurate results for complex data than parametric classifiers (Maxwell et al., 2018). Parametric classifiers, such as Maximum likelihood, require the assumption of a normal data distribution and are slightly influenced by training data. Moreover, the landscape's morphology complexity led to noisy classification results (D. Lu & Weng, 2007). Among the variety of available ML algorithms, Random Forest (RF) (Breiman, 2001) and Support Vector Machine (SVM) (Cortes et al., 1995) are two extensively used approaches.

- **SVM** is a machine learning method based on supervised statistical learning theory exploiting the theory of small samples (Pal & Mather, 2005). For classification learning tasks, SVM evolved as a nonlinear probabilistic algorithm focusing on the distribution and distinction of training samples (support vectors) among two classes based on optimal hyperplane (Cortes et al., 1995). SVM thus efficiently suits remote sensing applications for high-dimension pattern recognition and binary classification tasks (Pal & Mather, 2005).

- **RF** combines multiple Decision Tree classifiers (DTs) (Breiman, 2001). Each DT uses a random sample of the training data to reduce the variance, assigning finally a unique class. The final prediction is then assigned by considering all the DT results through the majority voting method.

ML classification approaches have been efficiently investigated for the treatment of SAR data based on SVM methods (Maity, 2016). For the classification of satellite data (Maity, 2016) presented Sentinel-2 Time-Series exploiting the Google Earth Engine computational platform. Moreover, (Zhou et al., 2021) effectively used SVM for hills micro-landform classification based on grid DTM.

A specific category of raster processing and interpretation related to the present research is the use of Geomorphological layers (GMLs) methods, composite raster data, and visualization techniques (VTs) (Gawior et al., 2017). It is identified for DTM analysis and classification tasks and employed as a training dataset for machine learning classification algorithms. (Mukherjee & Singh, 2020) presented an application of ML and multiple layer combination (n°12) for a multicollinearity analysis for the classification of potential areas for groundwater, with an accuracy of almost 80%. Furthermore, as preliminarily investigated in (Cappellazzo et al., 2023; Cappellazzo et al., 2024a), ML and VTs have already been experimented with for supervised automated classification of territorial micro-topography characteristics.

Moreover, artificial Neural Networks (NNs) (Rosenblatt, 1958; Rumelhart et al., 1986; Vargas et al., 2018) also represent a valuable tool for image detection and classification. Currently, several specific disciplinary sectors have widely explored the potential connected to DL applications related to image classification. Recent studies have also investigated DL research for multi-class semantic classification, as in (Kirillov et al., 2023) where, starting from 1 billion masks on 11 million images, a classification model characterized by a significant generalization capability has been developed, enabling the possibility to segment a massive variety of images with heterogeneous features. Concerning environmental studies, (Brusco et al., 2023) developed a solution to detect crop pest species, implementing also semantic enrichment and comparing then the results obtained using both RGB and near-infrared UAS imagery. Also, heritage and archaeological domains have widely benefited from the advancement of technology in the automatic classification framework. For example, (Patrucco & Setragno, 2021), starting from a manually annotated dataset, a fully convolutional network (FCN) has been trained aiming at the enhancement of the photogrammetric pipeline for the 3D reconstruction of heritage objects. Moreover, (Felicetti et al., 2021) exploited an integration of a convolutional neural network (CNN) UNet-3 and Watershed algorithm while

defining a methodological pipeline aiming at generating a digital vectorized representation of decorative apparatus.

3D point cloud semantic segmentation and object detection

In the framework of semantic enrichment, classification and segmentation of 3D data have been proven to be crucial aspects of the RS technique. A large category of classification methods is based on 3D point cloud data. The features and challenges related to the performance of points-based classification methods differ from those of raster-based approaches for imagery classification, mainly due to the unstructured nature of the primary data (Xu et al., 2014; Y. Zhang et al., 2022). In this regard, the framework of point cloud semantic segmentation and classification is a crucial task that nowadays is characterized by continuous technological and methodologic advancements (Sarker et al., 2024).

In this framework, DL networks and unsupervised algorithms are able to implement learning tasks directly on the 3D point cloud data.

Among the available solutions, the geometric voxel analysis defines one of the most diffuse approaches (Poux & Billen, 2019). A broad spectrum of unsupervised ground filtering algorithms related to geometric and voxel relationship features can be mentioned. The competition among them is mainly based on the accuracy of the results related to the context-related capabilities, the nature of starting data, and the objectives of the application. In this context, Simple Morphology Filter (SMRF) aims to segment the ground class points, operating a division of the point cloud into grids along an XY plane (Pingel et al., 2013). Moreover, in this framework, in (W. Zhang et al., 2016) a method based on the cloth simulation technique is used to extract the ground points. A combination of geometric features can be used to recognize, extract, and label contour detector candidates from 3D point clouds based on geometric features (Grilli et al., 2019). Still, geometric unsupervised filtering is also directly linked to 3D modeling purposes (Hackel et al., 2016). In fact, this research topic is crucial nowadays to overcoming the need for Digital Twin

Cities (DTCs) or, eventually, 3D city models (Nurunnabi et al., 2022). In this regard, several experiments on the ISPRS H3D benchmark dataset (Kölle et al., 2021) have been conducted to enhance the segmentation of urban 3D unstructured data and to ensure the correctness of the semantic content in imbalanced class frequency datasets. For example, in (X. Zhang et al., 2022), the integration of generalized-class point-transformer segmentation and a refined object-based approach fully address the imbalanced class distribution problem. Additionally, in (Laupheimer & Haala, 2022) a RF model has been trained using geometric, radiometric, and echo support features derived from point clouds and mesh data.

Also, concerning supervised methods, several recent approaches explore DL techniques applied to 3D point cloud data, showing effective results (Hu et al., 2019; Li et al., 2018; Nong et al., 2023; Qi et al., 2016). Following the necessity of DTCs to constantly update 3D point cloud urban data, (Ballouch et al., 2022) trained a semantic segmentation model using the RandLA-Net architecture for urban point cloud data.

However, in this framework, a significant bottleneck is represented by the generation of reference data for the training and validation issues of a DL model. In fact, this task is onerous and time-consuming, requiring significant efforts. Furthermore, the training process requires Python libraries that need powerful and updated graphic hardware (CUDA enabled). The memory consumption is thus a relevant issue while training a DL model (Guo et al., 2019). In (Varney et al., 2020), a methodological example for training and validation data generation is addressed. Also, a reference dataset preparation strategy has been proposed in the literature for DL 3D points classification model evaluation, balancing the Training and Validation dataset in 80%-20% (Matrone et al., 2020b).

Moreover, DL algorithms, specifically artificial Neural Networks (NNs), are increasingly used for object detection and semantic labeling in several application fields (Kirillov et al., 2023). These techniques, being applied also to LiDAR 3D data (Guo et al., 2021; Wu et al., 2021), allow for the automated identification of

particular elements, artifacts, and other features, enhancing the efficiency of the automatic identification process. However, it is essential to note that point cloud object detection is predominantly developed for applications in autonomous driving and indoor modeling (Li et al., 2021; Xiong et al., 2013). Therefore, most of the benchmark datasets, such as KITTI (Geiger et al., 2012) and H3D (Patil et al., 2019), have been designed and generated for these purposes, consisting of tens of thousands of labels, divided into several classes (Table 1), making them less directly applicable to heritage contexts without significant adaptation (Hahner et al., 2020).

Table 1. Summary of existing open benchmark datasets for 3D object detection, showing data type, number of classes, and annotated 3D bounding boxes.

Dataset	Reference	Year	Data	Type	Object classes	Annotated 3D boxes
KITTI	(Geiger et al., 2012)	2012*	RGB + LiDAR	Autonomous driving	8	200K
ApolloScape	(Huang et al., 2018)	2018	RGB + LiDAR	Autonomous driving	6	70K
H3D	(Patil et al., 2019)	2019	RGB + LiDAR	Autonomous driving	8	1.1M
Waymo Open	(Sun et al., 2019)	2020	RGB + LiDAR	Autonomous driving	4	12M
nuScenes	(Caesar et al., 2019)	2020	RGB + LiDAR	Autonomous driving	23	1.4M

In fact, heritage assets are usually characterized by typology heterogeneity, and thus not coherent with the number of annotated labels useful for training a NN detector model. In this framework, Deep NNs that exploit LiDAR data can be divided into three main categories relating to the point cloud representation. Projection-based methods apply 2D Convolutional Neural Networks (CNNs) on a 2D projection of the point cloud, such as Scanet and MV3D (X. Chen et al., 2016; H. Lu et al., 2019). Voxel-based methods (Lang et al., 2019; Yan et al., 2018) are designed to structure the disordered point clouds into a 3D voxel structure, forming multiple Bird's Eye View (BEV) feature maps, where 2D CNNs are applied. Point-

set methods extract point-wise features from the unstructured point clouds by neighbor cluster aggregation (Z. Yang et al., 2019, 2020).

2.2 Landscape-scale heritage applications related works

This section presents some related works that concern specific applications of remote sensing and machine learning methodologies and techniques aiming at knowledge enhancement and mapping of heritage sites and focusing on extended landscape-scale contexts.

2.2.1 Remote Sensing techniques for environment and Heritage documentation

As briefly introduced, in recent decades, RS technologies have significantly advanced the field of CH documentation (Bassier et al., 2017; S. Yang et al., 2023).

Several applications have been developed for the CH domain to detect land or subsurface features and monitor site conditions at a landscape scale. For example, (Abate et al., 2021) have applied multispectral imagery enhancement and analysis to investigate potential buried structures in the medieval monastic settlement of San Vincenzo al Volturno, Italy. In fact, in this framework, providing valuable information about the material and ground composition has been proven essential for preserving heritage sites (Agapiou & Skarlatos, 2023). Furthermore, the potential for data fusion between point clouds and multispectral UAS photogrammetry has been demonstrated in (Santoro et al., 2023). Specifically, fusion between Mobile Mapping Systems (MMS) data and multispectral imagery has allowed for an extended and comprehensive mapping and understanding of military heritage. Since two of the main characteristics of the fortified built heritage are often inviolability and inaccessibility, (Barazzetti et al., 2023) exploited DG UAS photogrammetry for the digital documentation of Italian Alps fortifications.

Still, the work also compared the traditional SfM reconstruction techniques with Neural Radiance Fields (NeRF) to generate dense point clouds, aiming at the 3D modeling of the heritage objects.

Following this multi-sensory approach, active RS technologies, including Terrestrial Laser Scanning (TLS), MMS, and Airborne LiDAR, have become essential tools in CH domain study. In fact, multi-sensory and multi-scale acquisition methodologies have been particularly adopted in heritage documentation processes (Martino et al., 2023). Airborne LiDAR, in particular, has shown great potential in densely vegetated extended areas where other survey methods are less effective (Luo et al., 2019). Such systems can penetrate forest canopies to reveal underlying archaeological or landscape features (Wieser et al., 2016), making them an invaluable tool for extended CH sites mapping, study, and analysis (Cappellazzo et al., 2023). For instance, in (Masini et al., 2011), ALS data in several heritage case studies have been conducted and analyzed, demonstrating the Airborne LiDAR capabilities in specific heritage contexts, specifically mapping unknown features and detecting landforms in dense woodland areas. Among others, Golden et al. (Golden et al., 2021) collected 331 km^2 of high-resolution airborne LiDAR data, demonstrating ALS point clouds to be suitable for extended heritage contexts, where the necessity was to detect unmapped rural Centro-American heritage artifacts and infrastructures.

Specifically, it is also important to consider that ALS point clouds are particularly suitable for DSMs and DTMs. In fact, in (Albrecht et al., 2020), it is underlined how interpolation techniques directly impact the utility of the data for archaeological analysis.

In the framework of active sensors application to heritage contexts, in recent years, the increasing progress of UAS has allowed the equipping of high-resolution sensors with relatively low-cost solutions. For example, (Mazzacca et al., 2022), a UAS LiDAR survey has been conducted for archaeological documentation in a densely forested area. Also, (Diara & Roggero, 2022; Kersten et al., 2022; Maté-

González et al., 2022) have investigated the accuracy performances and geometric quality of commercial LiDAR sensor L1 from DJI by comparing L1 data with full-waveform ALS sensors, TLS, and Simultaneous Localization and Mapping (SLAM) data. This allowed the demonstration of the potential of UAS LiDAR technologies for built Heritage documentation.

2.2.2 Automatic classification and segmentation approaches: enhancing data processing and structuring for semantic enrichment

Since several research studies from the previous section demonstrated the importance of integrated multi-sensor and multi-scale data, it is also important to underline that raw 3D data comes in an unstructured form. In fact, since semantic structuring methodologies are essential to analyzing and processing remotely sensed data, the following paragraphs present related research works that have worked towards automating landscape-scale CH sites data structuring.

Applying ML and DL techniques in analyzing remotely sensed data has opened new avenues for the analysis and interpretation of CH sites (Argyrou & Agapiou, 2022). In fact, several experiments have been carried out to enhance heritage documentation and data structuring. Moreover, in such a complex application field, semantic accuracy and specificity are crucial for evaluating automation approach performances both in ML and DL directions (Matrone et al., 2020a).

Although automatic learning approaches are being increasingly studied nowadays, leveraging both raster-based data and 3D data, the classification of optical imagery and grid-based DHMs has been more extensively explored, particularly within the context of remote sensing applications for CH applications.

In this sense, in (Orengo et al., 2020) a ML algorithm has been developed for archaeological mounded site detection in the Cholistan Desert (Pakistan). The

work exploited Sentinel 1 Synthetic Aperture Radar (SAR) and Sentinel 2 multispectral data, extracting thus georeferenced vector polygons. Yet also (Soroush et al., 2020) exploited a FCN inspired by the U-Net model architecture for pixel classification, aiming at the mapping of anthropogenic wells (or qanat) systems in Erbil (Iraq). Moreover, also the exploitation of DHMs data and visualizations has proven to be effective for archaeological and landscape heritage artifacts and earthworks mapping, as demonstrated by (Davis et al., 2021). Specifically, airborne LiDAR point clouds have been exploited to generate 1.5 meters DTM and different visualizations such as Hillshade and Slope analysis to train a Res-Net-50 DLM for the detection of Native American underground deposits (shell ring) in Florida.

Since the majority of presented applications leverage optical or grid-based data, it should be underlined that also the classification and segmentation of raw point clouds are essential tasks for generating semantic content and extracting meaningful information from unstructured data (S. Yang et al., 2023). In fact, ML techniques such as semantic segmentation and raster classification of landscape and archaeological contexts represent a valuable tool for enhancing sites knowledge and processing automation (Grilli et al., 2018). An instance of this is represented by the work of (Mazzacca et al., 2022), where a UAS LiDAR system has been used for a 3D metric survey of an archaeological area under a densely forested area. Specifically, ML algorithms such as Random Forest have been used to detect ground-level archaeological features leveraging point cloud data and Visualization Techniques (VTs) using shaded interpolation of ground class points. (Bundzel et al., 2020), tested several CNNs for the semantic segmentation of the Pacunam LiDAR Initiative (Guatemala) airborne survey in order to generate accurate DTMs. The aim was yet again to detect archaeological remains by training a DLM exploiting U-Net CNN and Mask R-CNN networks.

Finally, given the research background, it should be clear how machine-learning techniques applied to CH contexts are nowadays becoming crucial tools

for mapping and data structuring automation, supporting heritage domain experts (Fiorucci et al., 2020). Specifically, the research topic for automation in data structuring and labeling has probably reached a high degree of maturity, being highly investigated in several research areas and real-world field applications. However, as previously mentioned in Section 1.1.2, applications regarding the CH domain are not fully investigated, and still, the various methodologies presented are often exploited singularly. Given this important and complex methodological background, the present doctoral research aims to develop an integrated GeoAI approach for airborne LiDAR data semantic structuring. In this sense, it is worth reiterating what was stated in Section 1.1.3: the present dissertation originality consists of the study, design, and adoption of different methodologies of heterogeneous data (both 3D and 2D) structuring methodologies for cultural heritage field applications, aiming to build a specific and transferable workflow. Specifically, the objective is also to address the issue of big spatial data processing automation through deep learning model training and traditional machine learning OBIA algorithms, where the necessity is the analysis of cultural landscape contexts and the detection of non-mapped built artifacts or landscape anthropogenic earthworks. The primary data and methodologies exploited in the doctoral research are deepened in the following Chapter 3.

Chapter 3 – Materials and methods

Integration of multi-sensor Remote Sensing and Machine Learning methodologies for Landscape Heritage context applications

The integrated methodologies that have been investigated in the present doctoral research involve applying semi-automatic segmentation and classification approaches on aerial LiDAR datasets based on machine learning technologies through a combination of methods. As mentioned in the 1.2.2 section, the aim is to adequately document the landscape morphology of the territorial context and to detect and map ground-related features (e.g., anthropogenic landforms) and historical defensive heritage systems. Specifically, mapping these non-documented landscape morphological features and heritage systems has been intended to bridge the gap in the existing geographic datasets and update and enrich the domain-related spatial database. In fact, within the complex framework of Cultural Heritage documentation and data structuring, this work aimed at integrating comprehensive,

current methodologies for the semantic classification and object-detection of 3D LiDAR point clouds (S. Yang et al., 2023) and raster data (Maxwell et al., 2018). Therefore, the whole research is evaluated and validated, considering each approach from a holistic perspective.

After the first phase related to the primary data acquisition and collection (Section 3.1), the second part of the methodology consists of integrating unsupervised geometric filters (Section 3.2) with supervised Neural Network (NN) models for a generalized macro-class automatic segmentation of 3D point cloud data (Section 3.3.1). The macro-classes are intended to be compatible with the American Society for Photogrammetry and Remote Sensing (ASPRS) specifications (Graham, 2014) (Table 2).

Table 2. ASPRS Standard LiDAR point classes from The LAS 1.4 Specification (Graham, 2014).

Classification value	Meaning
0	Created, never classified
1	Unclassified*
2	Ground
3	Low Vegetation
4	Medium Vegetation
5	High Vegetation
6	Building
7	Low Point (noise)
8	Reserved
9	Water
10	Rail
11	Road Surface
12	Reserved
13	Wire - Guard (Shield)
14	Wire - Conductor (Phase)
15	Transmission Tower
16	Wire-structure Connector (e.g., insulator)
17	Bridge Deck
18	High noise
19-63	Reserved
64-255	User definable

In this regard, although an overgeneralized class scheme could be nowadays defined as insufficient for semantic segmentation purposes, in such a complex research context, it has been crucial to define a semantic classification scheme that could equally meet both the mapping and data structuring necessities dictated by the objectives and the constraints imposed by the data scales. In fact, the methodology aims firstly to test semantic structuring techniques on high-scale data from low-altitude airborne LiDAR surveys. These preliminary tests are then useful to verify if the leverage of the existing regional ALS dataset as primary data for ML analysis of the defensive landscape could allow a robust and comprehensive analysis of fortification systems without the necessity of acquiring new data.

Moreover, a preliminary investigation for the development of LiDAR object detection methodologies for heritage defensive systems and artifacts mapping has been addressed. In this regard, since the developed integrated method is conceived as a multi-scale approach, the integration of landscape scale macro-classification DLM and artifact scale 3D detection could represent a significant research direction. Therefore, the semantic segmentation method has been developed at a lower scale for land cover classification and subsequently combined with a higher scale approach for mapping heterogeneous defensive architectures. In fact, Section 3.3.2 consists of the preliminary investigation answers and training data generation for the DL object-detection strategies aiming at the identification of specific point cloud objects. In this last sense, a class schema has been prepared for the generation of training labels for the object detection DL approach (Table 3).

Table 3. Historical Defensive Heritage object-detection and land cover schema. This class schema has been created to provide a basic semantic structure for the DL object-detection approach. For each class is also listed the number of elements in each area.

Class value	Class name	CS2 Area 1 objects	CS2 Area 2 objects	Description
0	not classified	28 out of 62 45%	28 out of 113 25%	This class contains all the points remaining from the other classes.
1	coastal tower	2 out of 62 3%	6 out of 113 5%	This class integrates all kinds of objects related to military observation towers and outposts.
2	bastion	-	1 out of 113 1%	This class must be intended as objects pertaining to fortification walls and bastions.
3	pillbox	14 out of 62 23%	66 out of 113 58%	This class contains objects related to pillbox-fortified structures. These structures must be intended as a special type of concrete camouflaged guard post.
4	battery	15 out of 62 24%	12 out of 113 11%	This class contains objects related to military batteries, whether those be antiaircraft or antinavy.
5	fort	3 out of 62 5%	-	This class contains objects pertaining to fortresses and strongholds.

Finally, the integrated workflow inquiries about the application of ML classification techniques using unconventional non-optic imagery data, such as DTM and geomorphological analysis (Section 3.4).

3.1 Primary data and Case Studies Territorial contexts

Following the analysis of the literature pertaining to RS techniques applied to CH contexts, several considerations based on primary data evaluation should be issued. Firstly, the employment of terrestrial platform sensors could provide dense and accurate data compatible with object-scale heritage documentation objectives. Nevertheless, integrating multiple sensors and exploiting terrestrial and aerial platforms is usually recommended for a 3D metric survey of CH sites in the direction of comprehensive multiscale documentation. Still, while working in an extended landscape context, it should also be considered that airborne sensing techniques are preferred platforms for the rapid collection of more data. Moreover, the necessity to generate DTMs that are widely used for CH analysis and monitoring requires evaluating the primary data in terms of the sensor's ability to penetrate surface elements (e.g., vegetation) and, consequently, the ground point density. In this regard, the airborne (helicopter or UAS) LiDAR and SfM datasets from the Spina Verde Park case study will be presented and subsequently evaluated in the following sub-section.

3.1.1 Spina Verde Park

The research area of Case Study 1, located on the southern side of the Como Lake, features a vast dimension (almost 36 km^2), with dense and irregular forest coverage of the Spina Verde Park and evergreen plants in certain areas, resulting in varying densities of point clouds. The area elevation is between 164 m and 597 m, and it is featured by steep gradient slopes of 0° min, 66° max, and 13° mean (Figure 25). Given these characteristics, a low-altitude integrated LiDAR/Photogrammetric flight survey has been meticulously planned to facilitate the efficient acquisition of comprehensive and uniform data and achieve an optimal point density for the micro topography investigation.

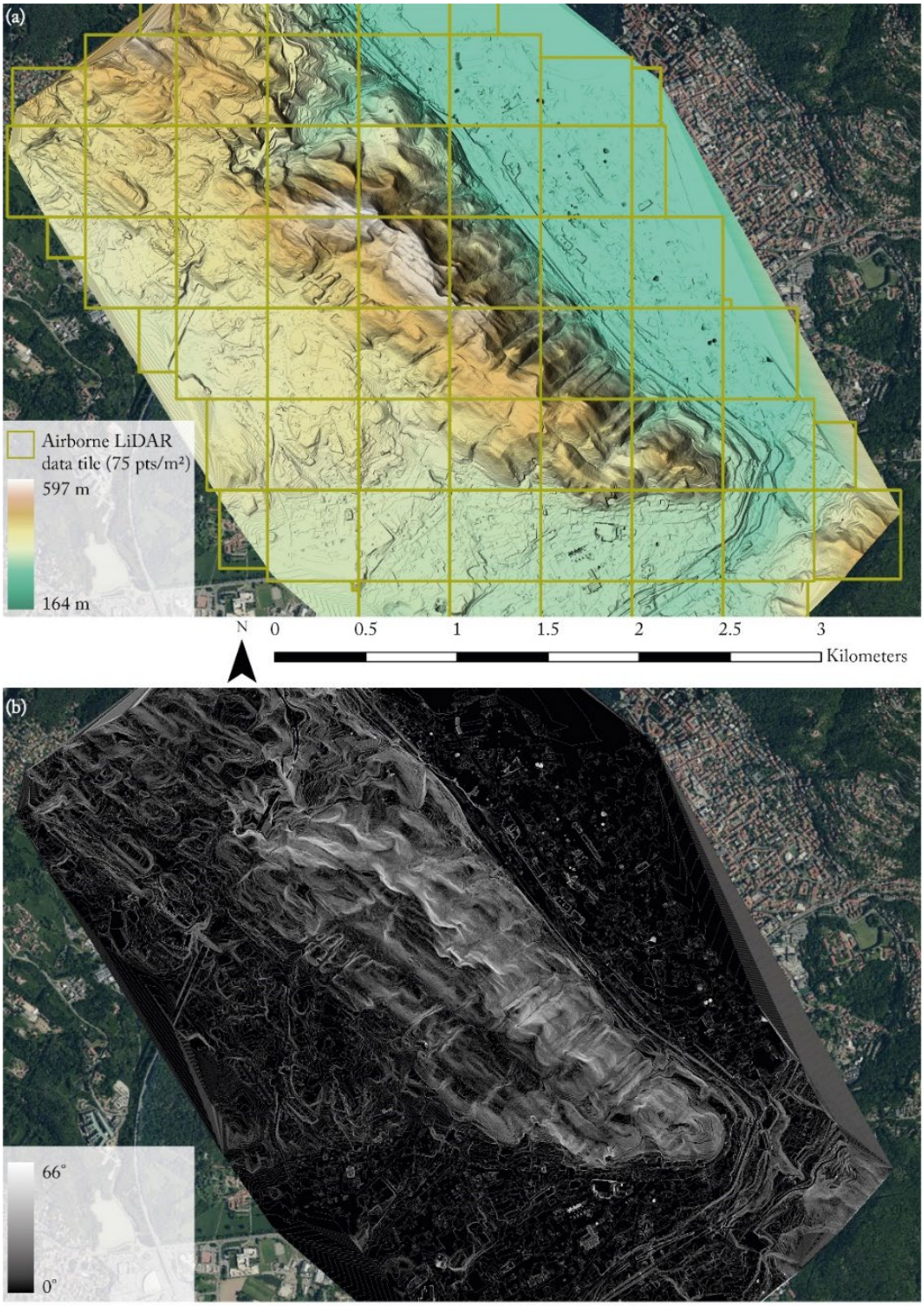

Figure 25. Area of the airborne LiDAR acquisition for case study 1 and site's morphology: (a) DTM, (b), and slope direction analysis. The DTM has been calculated from the filtered point cloud that has a density of 75 points per square meter (not filtered). The ground class has an average point spacing of 20 centimeters. Datum RDN2008, projection UTM zone 32 N (EPSG: 7791) – credits LabG4CH, CNR IRPI, Lombardy region (data); author (elaboration).

As mentioned in the introduction to the case studies (Section 1.2.1), the airborne data that has been leveraged in the Spina Verde Park Case Study 1 has been acquired in 2022 within a collaboration project with the CNR research institute for hydrogeological protection (Cappellazzo et. al, 2023).

To mitigate the effects of dense vegetation on hilly terrain, the acquisition has been performed before the spring season to minimize vegetation growth. The flight was performed using a Eurocopter/Airbus AS350 (Figure 26a) equipped with multi-sensor hardware composed by Litemapper 6800 LiDAR System with a RiEGL LMS-Q680i full waveform laser head operating with a maximum laser pulse repetition rate (LPRR) of 400 kHz at 60° of scan angle, with nominal laser beam divergence < 0.5 mrad. The aerial flight positioning and altitude computation is performed using an IGI AEROControl GNSS/IMU composed of a 256 kHz IMU and a full GNSS Septentrion. Finally, a 150 MP PhaseOne iXM-RS150F medium format aerial camera (50 mm focal length) for stereo pair images is equipping the platform.

(a)

(b)

Figure 26. (a) Picture of the Eurocopter/Airbus AS350 used for the survey and (b) LiDAR pod containing the Litemapper LiDAR system, the GNSS/IMU platforms and the full frame PhaseOne camera – credits CNR IRPI.

Since the external aerial LiDAR pod (Figure 26b) is engineered to be removed each time, a dedicated calibration flight is mandatory to obtain a reliable dataset. For this reason, after takeoff, a special pattern composed of 8 cross-flight strips at different AGLs over the helipad base was executed to calculate boresight calibration. The helipad is fully resolved from a topographic/geodetic point of view

through ground control points, checkpoints, and tie points useful for estimating boresight misalignments (different for each flight) and solving camera parameters.

The flight has been planned to provide a 70%-50% overlap in front and lateral directions, considering an average AGL of 490 m. The flight pattern comprised 11 flight strips, 9 with NNE-SSO and 2 orthogonal to them, used for on-site boresight calibration purposes (Figure 27).

Figure 27. Flight pattern over the Spina Verde Park Case Study – credits CNR IRPI (data); CNR IRPI (Cappellazzo et. al, 2023) (elaboration).

Two cross-strips were added over the survey area to check and improve boresight (roll, pitch, heading, and mirror scale) parameters. The area was overflown to obtain high spatial resolution images with a GSD between 3 and 4.8 cm/pixel. Finally, a dense raw point cloud was generated with an approximate density of 40-50 pts/m^2 over border areas and more than 100 pts/m^2 over the top hilly area (with smaller AGL). The average density of data is thus estimated at 75 pts/m^2.

In this case, the trajectory on aerial LiDAR application is solved in post-processing using Precise Point Positioning (PPP) e.g., when no GNSS ground station of a geodetic reference frame is present. The presence of a GNSS CORS (Continuously Operating Reference Station) over the survey area permitted to solve aerial N, E, H separation (256 Khz IMU with two epochs per second) with an RMSE (Root Mean Square Error) of +/- 0.030 (ETRF2000 – ellipsoidal). After that, to reduce the ellipsoid height to a local orthometric datum, an official geoid model provided by the IGM (Italian Military Geographic Institute) based on the ITALGEO2005 geoid model was applied (Declared accuracy is +/- 0.035 m at 1σ or +/- 0.100 m at 3σ).

Moreover, as a terrestrial complement, an extensive survey campaign made by ground-based surveys has been planned to monitor individual archaeological sites. These ground-based data ensured a multi-scale approach and enriched the comparative analysis between aerial and terrestrial datasets, as already extensively discussed in (Cappellazzo et al., 2023). An integrated UAS photogrammetric and terrestrial/UAS LiDAR campaign was carried out to document the Park landscape and its archaeological sites. In the specific framework of this research, the campaign primarily delivered GNSS measurements that have been used to validate the ALS dataset. The terrestrial survey was planned to integrate the ALS survey on specific archaeological sites and to provide a collection of ground control points for the validation of the ALS data. This has been done by collecting 27 GCPs (average accuracy ≈ 0.03 m) taken with GNSS real-time positioning techniques all around the survey areas, used to check the plano-altimetric consistency of the point cloud. Furthermore, a rubber-sheet algorithm based on GCPs Z-axis residuals was used to smooth the altimetric fluctuation of the point cloud (Table 4). The GCPs have been used as East-North constraints for the absolute orientation of the photogrammetric block. Consequently, a model keypoint ground surface was generated and used for image projection and the final orthomosaic generation.

Table 4. Rubbersheet algorithm and GCPs Z-axis residual weighted average have been used as parameters for the algorithm (The control points are thus not absolutely fixed but have a variable variance to guarantee best fitting over the local plane.)

Minimum absolute ΔZ [m]	Maximum absolute ΔZ [m]	RMSE [m]	Std. Deviation [m]
0.001	0.12	0.052	0.052

Concerning the documentation of the specific sites, both the Pianvalle site and the Baradello castle area were documented, integrating terrestrial LiDAR (TLS), UAS LiDAR, and UAS photogrammetry methodologies. As it is possible to observe in Table 5, the accuracies ranging from 1 to 4 cm – are consistent with the prefixed aims of the survey, thus granting a multi-scale data collection.

Table 5. Resume table of the collected data and the post-processing accuracy assessment.

Methodology		Pianvalle	Baradello
TLS	sensor	Faro Focus 120	Faro Focus 330
	n° scans	24	22
	accuracy assessment	ICP 6.5 mm target 10 mm	ICP 6 mm target 11 mm
UAS SfM	sensor	CMOS full frame camera DJI Matrice M300	CMOS 1” camera DJI Phantom 4 pro
	n° images	73 (AGL 5.5 m)	631 (AGL 42.5 m)
	accuracy assessment	GCP 2.1 cm CP 3.3 cm	GCP 4.1 cm CP 3.8 cm
UAS LiDAR	sensor	Zenmuse L1 (Livox) DJI Matrice M300	
	n° scans	2	
	accuracy assessment	N/A	

The acquisition of heterogeneous data has allowed thus to evaluate the consistency of the acquired datasets. Although the spatial and radiometric resolution of digital photogrammetry and UAS LiDAR appear to be more consistent, following the literature studies these techniques were not considered suitable for the territorial scale analysis of the area. Furthermore, in addition to the

several processing of acquired datasets, these have been extensively compared to confirm the state-of-the-art best practices for DTM generation in extended forestry contexts. Following the carried-out analyses, it is visible from Figure 28 that despite a superior spatial resolution, digital photogrammetric techniques could not adequately describe the ground morphology. If compared to the employment of a manned airborne full-waveform LiDAR sensor operating from a higher AGL (400 m vs. 42.5 m) SfM-based data can be considered useful for the tower documentation. However, considering the necessity to derive and analyze the site topography, the photogrammetric dataset is not sufficient to describe the terrain under the canopies.

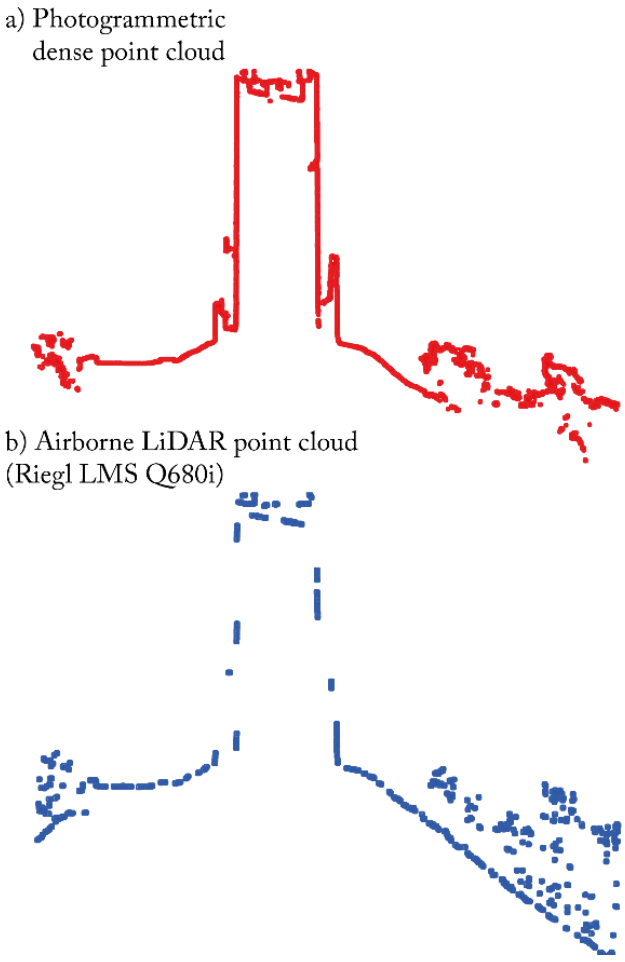

Figure 28. Sample section comparison between the SfM dense point cloud and ALS point cloud from the Case Study 1 in Spina Verde Park. The sample is taken from the Baradello tower, where a UAS photogrammetric survey has been conducted with a CMOS 1" camera equipped on a DJI Phantom 4. The ALS survey has been conducted with a Riegl LMS Q680i from a helicopter platform – credits LabG4CH and CNR IRPI (data); author (elaboration).

A similar behavior is noticeable from the comparison between ALS data and UAS LiDAR data, as observed in Figure 29. In this case, in addition to the superior penetration capability of the sensor operating from the manned platform, several issues have been identified regarding the resolution of the sensor's trajectory and, therefore, the registration of the acquired data. This is partly due to the black-box nature of the commercial system used, which does not ensure controlled workflows during data processing stage.

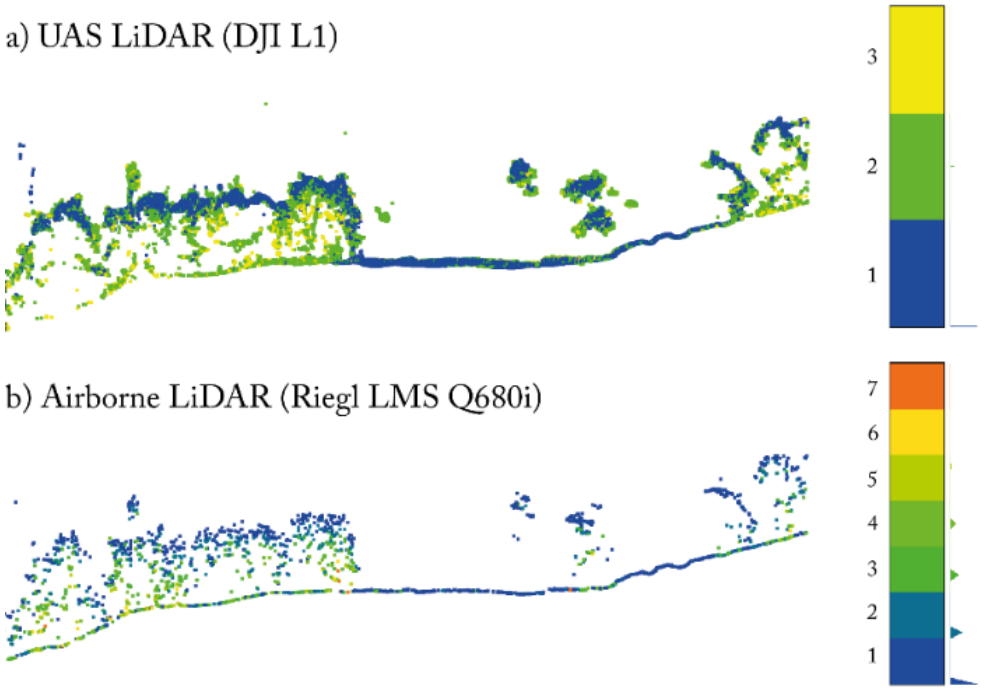

Figure 29. Sample section comparison between the UAS LiDAR point cloud and ALS point cloud from the Case Study 1 in Spina Verde Park. The sample is taken from the Pianvalle protohistorical settlment, where a UAS LiDAR survey has been conducted with a DJI L1 (Livox) sensor equipped on a DJI Matrice 300 k. The ALS survey has been conducted with a Riegl LMS Q680i from a helicopter platform – credits LabG4CH and CNR IRPI (data); author (elaboration).

Moreover, some issues have been encountered while evaluating reflectance intensity acquisition, as shown from the comparison with full-waveform ALS data in Figure 30. In this case, almost the entirety of the data coming from the UAS LiDAR sensor shows null reflectance values (0 values are approximately 26% of total data).

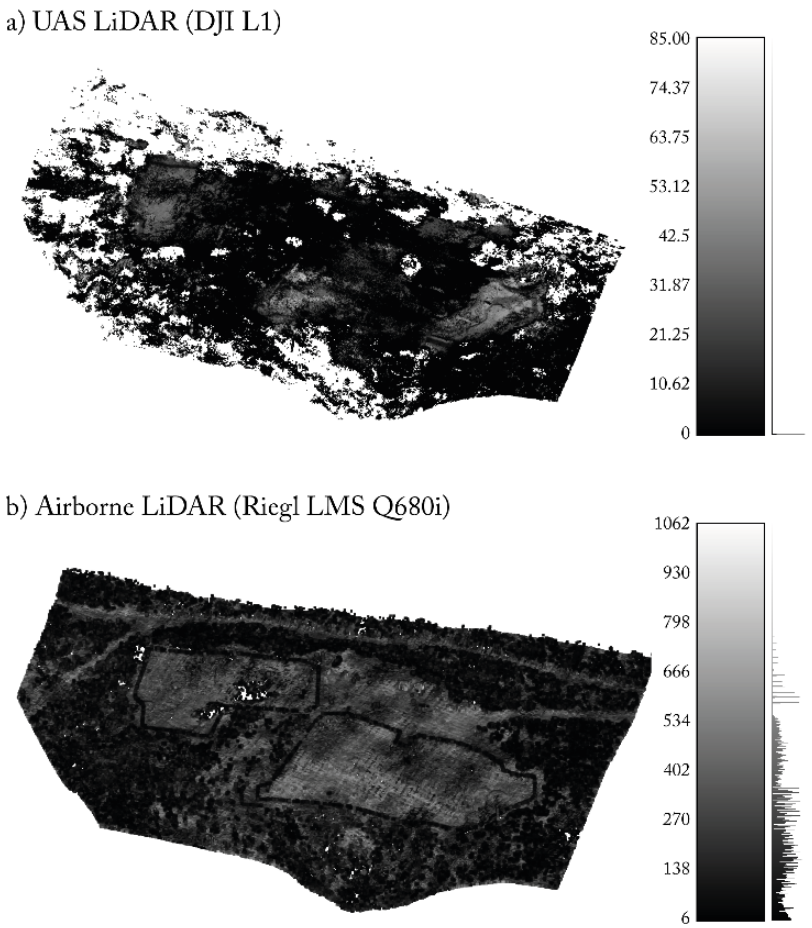

Figure 30. Sample data comparison between the UAS LiDAR point cloud and ALS point cloud from the Case Study 1 in Spina Verde Park, showing non-normalized reflectance intensity values of ground-class points. The sample is taken from the Pianvalle protohistorical settlment, where a UAS LiDAR survey has been conducted with a DJI L1 (Livox) sensor equipped on a DJI Matrice 300 k. The ALS survey has been conducted with a Riegl LMS Q680i from a helicopter platform – credits LabG4CH and CNR IRPI (data); author (elaboration).

3.1.2 Sardinia Defensive Landscapes

As presented in Section 1.2.1, the research sites of Case Study 2 pertain to two different coastal areas of Sardinia. Specifically, the first area pertains to the main urban settlement of the island, Cagliari. The designed contextual area of the city extends almost 180 km^2, alternating dense urban fabric, rural and salt pans areas, and dense low-vegetation shrub cover in the coastal part. The area elevation is between 0 m and 247 m, and it is featured by steep gradient slopes of 0° min, 57° max, and 9° mean (Figure 31).

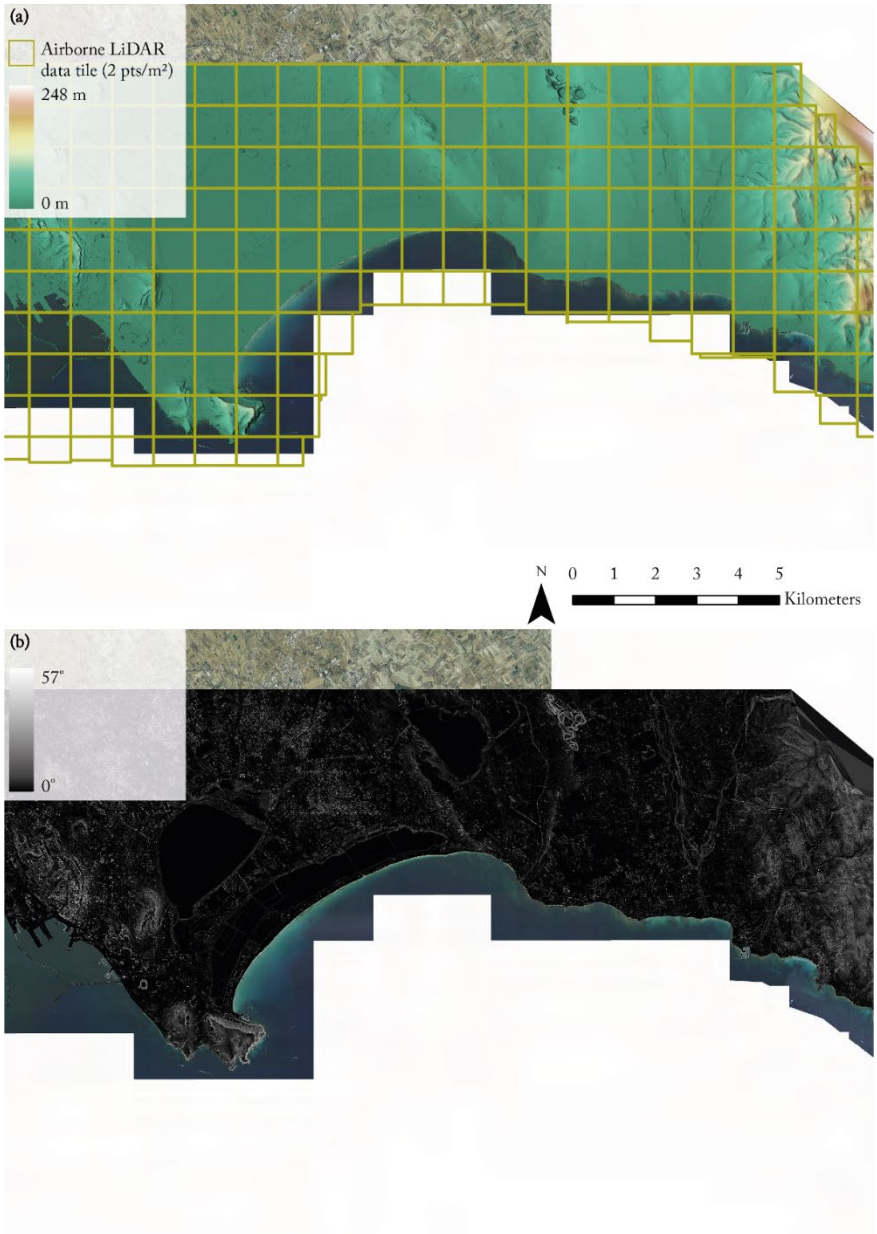

Figure 31. Area of the airborne LiDAR acquisition for case study 2 (Area 1 – Cagliari, Italy) and site's morphology: (a) DTM, and (b) slope direction analysis. The DTM has been calculated from the filtered point cloud that has a density of 2 points per square meter (not filtered). The ground class has an average point spacing of 1 meter. Datum WGS 1984, projection UTM zone 32 N (EPSG: 32632) – credits Sardinia region (data); author (elaboration).

The second area context is related to one of the most important urban settlements of the island's northwest, Alghero (Figure 32). With a higher maximum elevation than Area 1 (331 m) and a higher average slope (12°), the Alghero areas are characterized by distinctive karst morphology, caves, sinkholes, fractures, and channels, particularly visible along the coast where the dense shrub vegetation recedes.

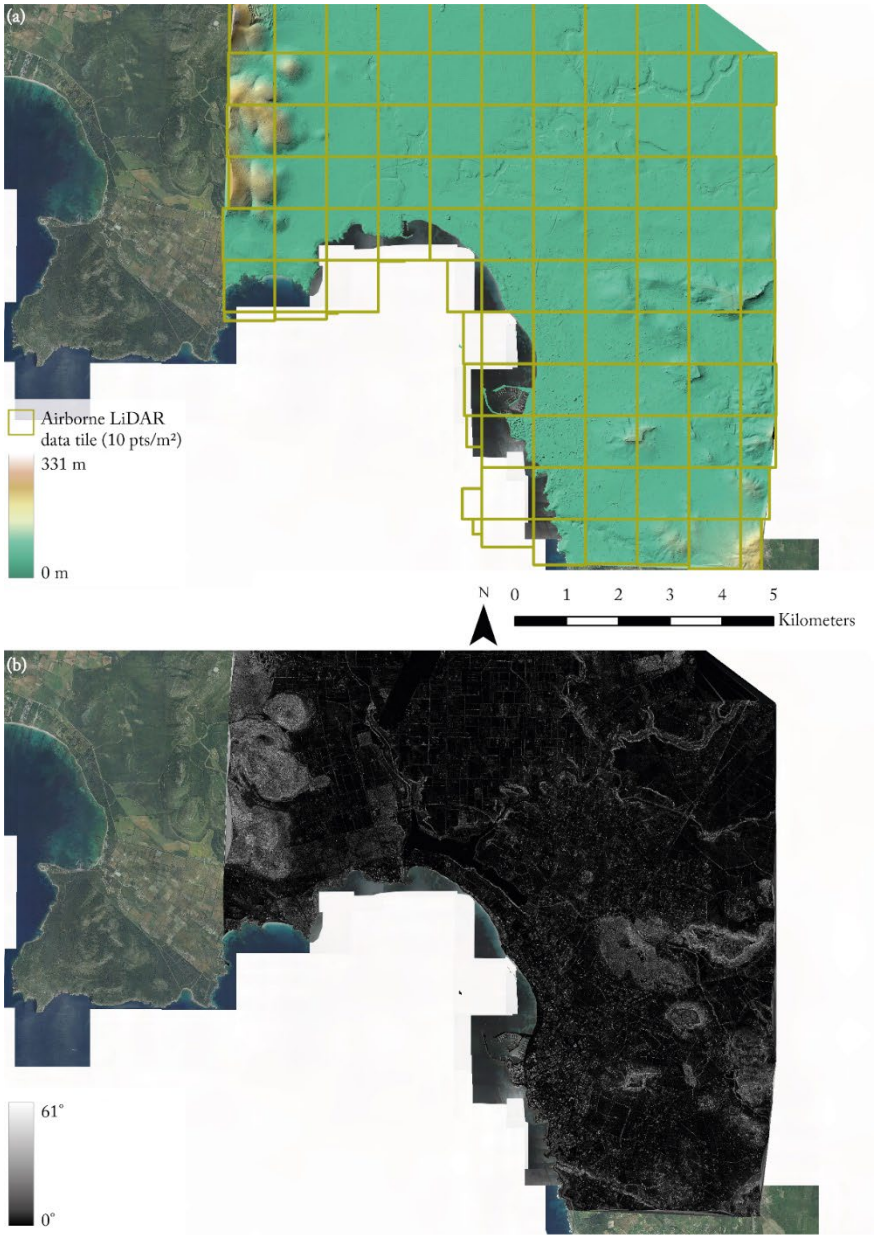

Figure 32. Area of the airborne LiDAR acquisition for case study 2 (Area 2 – Alghero, Italy) and site's morphology: (a) DTM, and (b) slope direction analysis. The DTM has been calculated from the filtered point cloud that has a density of 10 points per square meter (not filtered). The ground class has an average point spacing of 50 centimeters. Datum WGS 1984, projection UTM zone 32 N (EPSG: 32632) – credits Sardinia region (data); author (elaboration).

Given the vast dimension of the research areas and the widespread diverse typologies of fortifications (presented at the beginning of the chapter in Table 3), the necessity was to acquire sufficient data that would be useful to document the territorial context of defensive heritage systems adequately.

In 2007, the Autonomous Region of Sardinia issued a series of tenders for implementing an integrated LiDAR and photogrammetric aerial survey over the coastal areas of the Sardinian territory. The aim of the survey was to obtain georeferenced orthoimages, DSM, and DTM, specifically focused on the coastal strips and particularly on the major urban centers facing the sea. In this sense, it is possible to understand how much the coasts are considered the primary touristic economic driver for this territory and how coastal landscapes represent thus a crucial asset for the regional administration and inhabitants' wealth.

After a brief analysis of the grid DTM products in the catalog of the Sardinia Geoportal website (Sardinia Geoportal - Autonomous Region of Sardinia, 2024), the datasets of the research areas selected in Section 1.2.1 have been made available by the Cartographic Information Sector of Sardinia region. The ALS point cloud pertains to two surveys (Table 6) conducted in 2008.

Table 6. Surveys details. This table provides information about the sensor used and the survey and post-processing characteristics.

Survey	Sensor	LPRR [kHz]	Target echoes	Overlap	Vertical accuracy [m]	Ground speed [kn]	AGL [m]	Average density [pts/m^2]
1*	ALTM Gemini	125	4	30%	25	140	1400	2
2*	Riegl LMS-Q560	240	unlimited**	60%	10	110	500	10

* Survey 1 is intended to be the sum of the acquisitions that have been completed in several weeks.

** The stored echo information is practically limited only by the maximum data range allowed by the data recorder of the LiDAR system.

The total extension of the acquisitions (Figure 33) covers almost the entire waterline length.

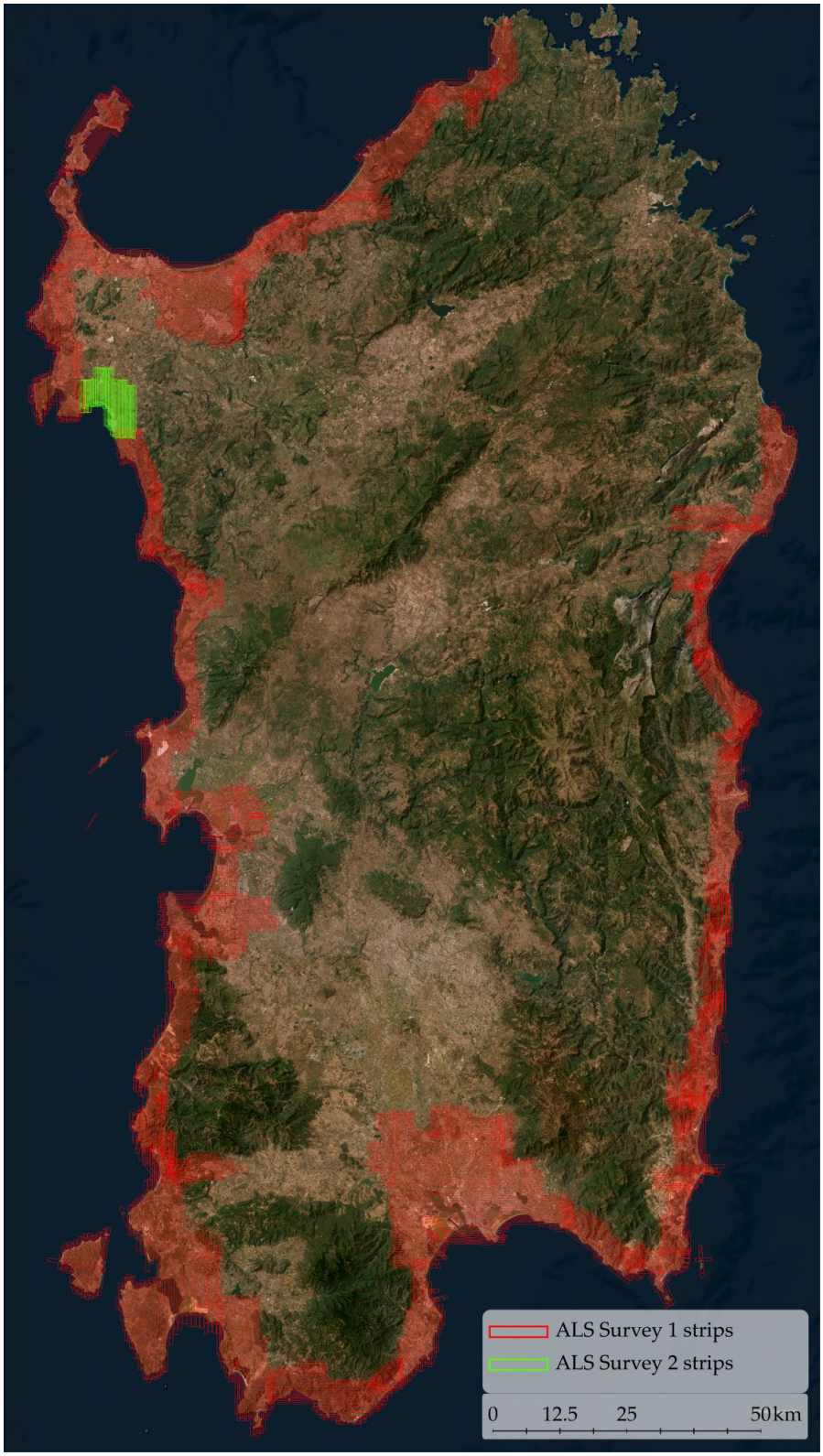

Figure 33. Map of the data provided by the Sardinia Region. The stripes available from the two airborne LiDAR surveys are located on this map. The two surveys were carried out using two different sensors, as detailed in Table 2. Datum WGS 1984, projection UTM zone 32 N (EPSG: 32632) – credits Sardinia region (data); author (elaboration).

Survey 1 represents most of the acquisitions and has thus been planned and executed at 1400 m AGL and a ground speed of 140 knots (≈ 260 km/h). This results in a point cloud dataset with an average density of 2 points per square meter, which is the primary data from Area 1. Contrarily, Survey 2 has been planned to focus only on the Alghero municipality area (Area 2). In this case, the acquisition has been conducted with a low AGL (500 m) and a 110-knot ground speed (≈ 200 km/h), resulting in a density of approximately 10 pts/m^2. Besides the flight characteristics, it is possible to observe from the available information that the sensors and the operating conditions were significantly different.

In fact, the sensor from Survey 1 was a multi-echo (Mallet & Bretar, 2009) laser scanner head system operating with a 125 kHz Laser Pulse Repetition Rate (LPRR). The point cloud datasets strips (Figure 27) have been obtained from the regional Cartographic Information Sector in a LAS file format, storing sensor information as intensity and echo returns (incomplete).

Instead, the sensor from Survey 2 was a full-waveform topographic LiDAR (Mallet & Bretar, 2009) laser head and operated at a 240 kHz PRR frequency. Despite the technological superiority of the second sensor, these point cloud strips have been given in an XYZ file format, not storing significant information regarding the multiple echo returns.

For this specific reason, the unsupervised and supervised semantic segmentation methodologies for the Sardinian case studies have been developed considering this issue, exploiting thus only the geometrical information of the point clouds.

3.2 Point cloud macro-classification: unsupervised filtering approaches for DHMs generation and Machine Learning training data preparation

Concerning the LiDAR data structuring methodologies, the two case studies have followed two different unsupervised approaches for the semantic segmentation of the ALS point clouds. These are extensively described in the following sub-sections. In this context, unsupervised filtering methodologies have been evaluated from the perspective of accurate DHM generation, yet also as a possibility for automating the reference data preparation for the application of 3D point cloud semantic segmentation (3DPCSS) techniques.

3.2.1 Spina Verde Park: unsupervised filtering of acquired high-scale LiDAR data

In this regard, the intention was to establish a methodological low-time consumption pipeline to semantically classify an ALS LiDAR point cloud into a highly generalized model, following the ASPRS LAS specification (Lewis Graham, 2012). However, it is crucial to specify that for Case Study 1 the vegetation class was not intended to contain only the points referring to the vegetation but also all the other points remaining from the ground and building classes (e.g., powerlines). In this sense, a 3-class semantic segmentation schema has been used (Table 7).

Table 7. Semantic segmentation class schema description for Case Study 1.

Class value	Class name	Description
2	Ground	This class contains all the points pertaining to the ground surface.
5	High vegetation	This class contains objects recognized as trees, and other points remaining from the ground and building classes.
6	Buildings	This class contains points related to human-made artifacts, such as buildings, ruins, etc.

Regarding the unsupervised approach that has been developed for Case Study 1, the objective was to evaluate the effectiveness of combining different unsupervised filters: the consolidated SMRF filter (Pingel et al., 2013) for the ground extraction step (Figure 34) and a tailored geometric filter to distinguish between buildings and vegetation.

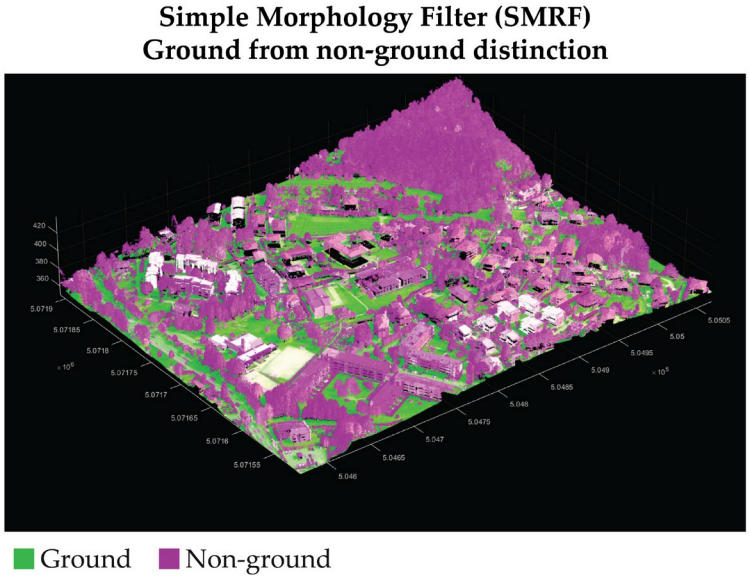

Figure 34. First step: ground from non-ground filtering with SMRF – credits (Cappellazzo et al., 2024a)

The SMRF filter divides the point cloud into grids along an XY plane. The lowest elevation value is computed within each grid element to create a minimum elevation surface map. Through an iterative segmentation of the surface map and the elevation and slopes calculation from an estimated DTM, it is possible to

distinguish between ground and non-ground pixels referring to the optimal threshold for elevation difference and slope tolerance. The segmentation mask obtained from this process is then applied to the original point cloud, removing non-ground points. The integrated unsupervised filter uses the eigen-based geometric features of normal (λ_3) and curvatures (1 m radius neighborhood) to distinguish among points pertaining to vegetation or building classes. In this function, the variance in normals and curvature values has been used to differentiate between buildings and vegetation. Buildings typically exhibit greater planarity conditions than vegetation, resulting in less curvature variation and relative normals differences among neighboring points in a certain cluster. In contrast, vegetation points are scattered, leading to higher curvature variations than buildings. In this regard, the contemporary condition of low normal values (< 0.05) and low mean curvature (< 0.1), represents buildings, as shown in Figure 35.

The result of the filtering process returns a classified point cloud. The filtering process could then be optimized for every case study, using eigenfeatures to disambiguate with more accurate results. The final structure of the point cloud is *x, y, z, I, C*, where:

$$I = Intensity$$
$$C = Classification\ ground\ truth\ label$$

In this case, a reduced field structure has been conceived to generate light reference data for the training of a transferable DLM for ALS point clouds. One of the aims is in fact, the evaluation of automation strategy using the least number of parameters possible, avoiding storing radiometric and return pulse values. Yet, the evaluation of the application of an unsupervised filter has been done from the perspective of DHM generation from the segmented point clouds.

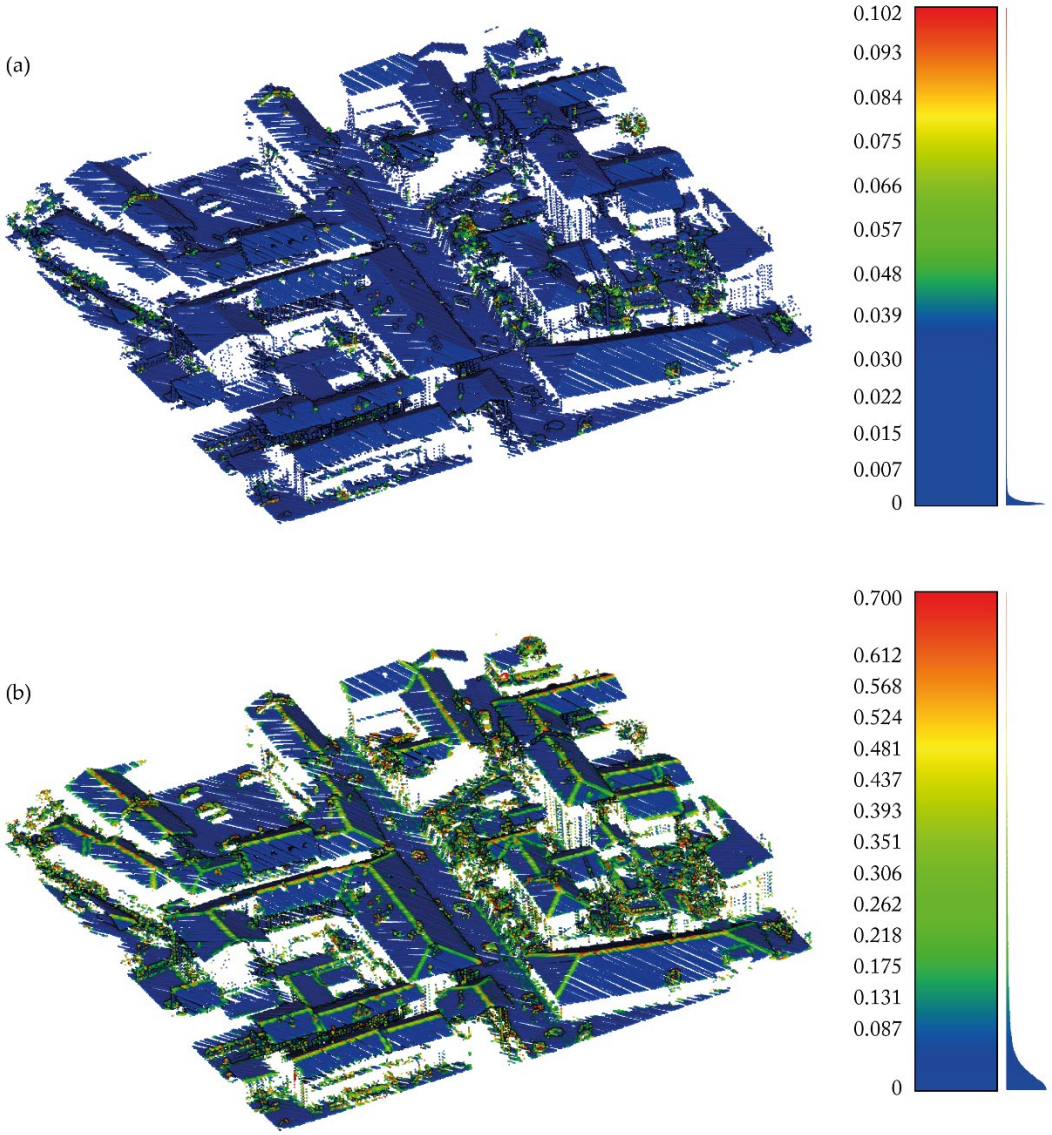

Figure 35. Computed normals – λ_3 (a) and mean curvature (b) values. The geometric features have been computed on a 1-meter radius.

3.2.2 Sardinia Defensive Landscapes: existent mid-scale LiDAR data

In order to document the coastal landscapes from Case Study 2, an adequate structuring of ALS point cloud datasets has been essential.

In such a complex research context, it has been crucial to define a semantic classification scheme that could equally meet both the mapping and data structuring

necessities dictated by the objectives and the constraints imposed by the data scales. For this reason, a 5-class scheme has been proposed (Table 8).

The classification scheme consists of 5 classes, which, given the scale and thus the data density, are based on the LAS specifications of the American Society for Photogrammetry and Remote Sensing (ASPRS) standard (Graham, 2012). In the framework of the present research, it should be underlined that since the application of ML analysis is directed toward the comprehension of fortification architectures, particular attention has been given to the building class that embeds most of the studied artifacts.

Table 8. Semantic segmentation class scheme description for Case Study 2.

Class value	Class name	Description
1	Unclassified	This class contains all the points remaining from the other classes. It particularly refers to low vegetation (e.g., bushes), cars, etc.
2	Ground	This class contains all the points pertaining to the ground surface.
5	High vegetation	This class contains objects recognized as trees.
6	Buildings	This class contains points related to human-made artifacts, such as buildings, ruins, etc.
9	Water	This class contains water surface points.

The class scheme's aim is to provide an efficient macro-class segmentation of unstructured point clouds, distinguishing between terrain, trees, buildings, and water. Moreover, the Unclassified class is developed to host object classes that are not identifiable due to the scarce density issues. In fact, points pertaining to low vegetation, urban furniture, and cars are not clearly distinguishable from one another.

Since it has been defined the classification scheme, the first step in structuring the data has been the employment of unsupervised filtering approaches. First, a preprocessing phase was necessary for the entire dataset, from which data blocks organized into 2000 m by 2000 m tiles were generated. After organizing the data

for both areas, it was decided to generate a reference ground-truth dataset using the point clouds from Area 1 (Cagliari). In fact, using low-density data (2 pts/m^2) would allow training a classification model with significantly representative data while avoiding GPU memory overflow errors (Matrone, Lingua, et al., 2020). The preliminary analyses of a part of the ground truth have thus been conducted, similarly to previous research work. The eigenvalues of the geometric vectors (normals - λ3, curvature, sphericity, number of neighbors, surface density, surface variation) of the point clouds have been calculated with a radius of 1, 2.5, 5, and 10 meters. These indices were used for an unsupervised segmentation of the points (non-ground) remaining from applying the Simple Morphological Filter (SMRF) algorithm (Pingel et al., 2013). Moreover, while evaluating different filters, the Cloth Simulation Filter (CSF) (W. Zhang et al., 2016), despite its accuracy capabilities, has been yet considered less effective in this context.

Multi-sensor data integration techniques provide rich datasets that allow capturing a wide range of information about the condition and composition of the territory and landscape (Batar et al., 2017). In fact, these have risen in several application fields, such as cartography, forestry sciences, and agricultural sciences (Candiago et al., 2015; Iglhaut et al., 2019). Moreover, providing valuable information about the material composition has been proven to be essential for the study of heritage sites (Picollo et al., 2020). Since spaceborne imagery has been proven efficient in several water and vegetation resource studies, this contribution proposes a data fusion approach to enhance the automation of the point cloud labeling process. Specifically, an integration of ALS point cloud data with Sentinel-2 missions near-infrared band (NIR) (Drusch et al., 2012) has been developed to support manual labeling activities in this coastal landscape heritage context. However, it is worth mentioning that due to the resolution difference between the ALS point cloud and spaceborne imagery, an upsampling strategy has been essential to match the spatial resolution of the Sentinel-2 bands (10 m) with the average point spacing of the ALS point cloud data (1 m). For this necessity, a cubic

resampling algorithm has been selected to accurately achieve the point cloud spatial resolution while avoiding sharp interpolation resulting from the Nearest Neighbor algorithm (Roy et al., 2016). However, despite the spatial resolution resampling algorithms being a consolidated approach, those do not provide an efficient solution for radiometric resolution enhancement. In fact, the integration of point cloud data with the NIR band has been exploited for the segmentation of the water class. In this sense, two different approaches have been tested to segment the water class points, as shown in Figure 36.

The first approach consisted of generating a vector 2D mask to be used in Cloud Compare for a semi-automatic areal water segmentation. The Normalized Difference Water Index (1) (McFeeters, 1996) has been calculated, generating thus a 2D polyline vector.

$$\mathrm{NDWI} = \frac{\mathrm{Green\ (b03)} - \mathrm{NIR\ (b08)}}{\mathrm{Green\ (b03)} + \mathrm{NIR\ (b08)}} \tag{1}$$

Additionally, a second approach has been tested to directly integrate ALS data with the near-infrared information as a point cloud scalar value. In this case, the NIR band has been projected on a 3D mesh triangulated from the DSM, and thus, a point cloud scalar field has been generated with a Majority Voting Nearest Neighbors (6 points) algorithm. However, despite the successful integration of NIR semantic information, the enriched ALS point clouds have not been declared sufficient for the identification or discrimination of other elements (e.g., vegetation and buildings), not coherent with the original spatial resolution of the Sentinel 2 data (10 m). Therefore, this approach has led to an efficient automatic segmentation of water class points, thus granting the generation of accurate DSMs and DTMs.

Moreover, after a rapid manual correction of the data classification resulting from the unsupervised approaches, it has been generated valid ground-truth reference data for the training of a DLM for semantic segmentation.

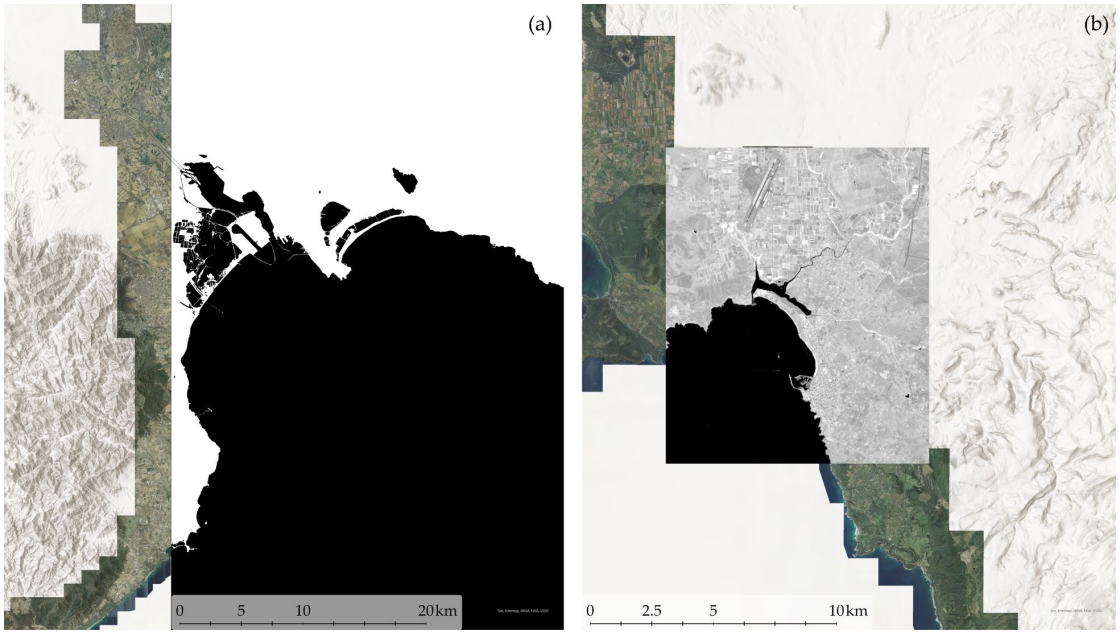

Figure 36. Sentinel-2 data fusion approaches. Vector water mask generation for areal segmentation (a). Band 8 NIR projection on DSM mesh for scalar value interpolation (b). Datum WGS 1984, projection UTM zone 32 N (EPSG: 32632) – credits Sardinia region, Copernicus, (Drusch et al., 2012) (data); author (elaboration).

3.3 Machine Learning for LiDAR point clouds

The use of unsupervised filters, which have been described in the previous sections, has been useful in validating an automatic approach for the generation of DHM. However, the focus on the use of the filters is here studied as a replacement or aid for manual segmentation in data preparation to train NN semantic models of ALS point clouds. The study of DLMs training methodology for extended landscape heritage context is presented in Section 3.3.1. Moreover, since one of the aims has been intended to be the historical defensive systems mapping, the methodology thus explored the solutions for fortification classes automatic identification from existing airborne LiDAR point clouds. In this framework, Section 3.3.2 describes the preliminary investigations that have been done toward the application of LiDAR DL object-detection techniques.

In this specific framework, it has been evaluated the method's reliability using the graphical user interface solution in ArcGIS Pro instead of a common code-based solution. Nowadays, software houses like ESRI are deepening the research of

integrating Machine Learning tools inside software to allow spatial data scientists to easily include GeoAI processing tasks in the same environment. Regarding the processing, two different workstations were used to train the models (Table 9), both with CUDA-enabled NVIDIA RTX graphic cards.

Table 9. Workstation specifics comparison

Workstation	GPU	VRAM [GB]	Accessible RAM [GB]
1	NVIDIA RTX A4000	**16**	32
2	NVIDIA RTX A5000	**24**	32

3.3.1 Macro-classification: training data and deep Neural Networks

Following the unsupervised approach that has been described in Section 3.2, with the reference ground truth data generated by geometrical filter application, the second step was to train semantic segmentation DLMs aiming at converting unstructured 3D datasets into a semantically organized dataset. This dataset contains significant semantic information about the class of each point, which is used as primary data input for the NN.

Two separate neural architectures have been used in the training process: RandLA-Net (Hu et al., 2019) and PointCNN (Li et al., 2018). A CE (Cross-Entropy) loss function has been used for both architectures that pertain to point-based approaches. As previously mentioned, RandLA-Net and Point CNN significantly differ for two reasons. Firstly, PointCNN is a point convolution network using only coordinates as input, while RandLA-Net is a point-wise multilayer perceptron architecture. Moreover, PointCNN is particularly suitable for analyzing small-scale object clouds. At the same time, RandLA-Net is designed to efficiently process urban or territorial-scale data, incorporating a random sampling phase for each network node. For this reason, and specifically for Case Study 1, the primary datasets have been employed, adopting different downsampling strategies and normalization techniques for the point cloud values. In fact, in this framework,

it is extremely crucial to have access to adequately structured LiDAR data and process the dataset in such a way as to save computational power. Especially concerning DL approaches, as widely demonstrated by the state of the art (Matrone et al., 2020b), using original-resolution LiDAR point clouds with global coordinates and non-normalized scalar fields can impact processing times and consume excessive memory.

Spina Verde Park: a first test approach toward point cloud data structuring with low resource consumption

As briefly discussed in the previous paragraph, different downsampling strategies have been explored in Case Study 1 to prepare training data to avoid excessive GPU memory consumption. The PointCNN models have been trained using subsampled data (2 pt/m^2) with a minimum distance subsample strategy, while the RandLA-NET models have been trained using the original resolution data (75 pt/m^2). The main reason for adopting this subsample strategy was to reduce the inferential training time and memory consumption. Additionally, the intention was to evaluate the methodology's scalability using a strong subsample strategy. Moreover, the classification of "older" datasets with lower density > 10 pts/m^2, such as those presented in Case Study 2 represents a crucial issue in the environmental and heritage data structuring and landcover mapping framework.

One of the aims was also to evaluate the impact of geographic coordinates in the training process. Despite previous research experiences, this aspect has been considered extremely important to avoid memory exceeding failure (Matrone et al., 2020a). The training data has thus been generated using shifted classified point clouds resulting from the integrated unsupervised filter, where some checks and few corrections related to the building class have been applied. In this case, the aim was to limit the manual operator intervention, working on a reduced dataset that will be used as a training dataset. Three different training datasets have been generated,

which differ in data quantities, area, and the balance percentage between training and validation data for each set (Table 10). The impact of these aspects has been then evaluated during the training phase. These TV datasets have thus been tested for the models training, using only the intensity value as an additional parameter.

Table 10. Training data preparation for Case Study 1 semantic segmentation model training.

Dataset	Training/Validation	Tiles number (100m*100m)	Total Area [km²]	Training/Validation percentage	TV on total dataset percentage
Spina Verde	Total		36.00		
TV-1a *	Train	100	1.00	71%	3.9%
	Validation	40	0.40	29%	
	Total	140	1.40		
TV-1b *	Train	22	0.22	69%	0.9%
	Validation	10	0.10	31%	
	Total	32	0.32		
TV-1c **	Train	20	0.20	80%	0.7%
	Validation	5	0.05	20%	
	Total	25	0.25		

* Testing with workstation 1 (Table 9)

** Testing with workstation 2 (Table 9)

The TV-1a dataset has been generated by selecting the 140 blocks (100 m x 100 m) with the highest density within the Spina Verde dataset (Figure 37). These have been thus randomly split into training and validation data. In this regard, the automatic selection of point cloud blocks based on higher density has, on the one hand, been reducing the time required to prepare the two datasets, but on the other hand, it has proved ineffective in preventing class frequency imbalances, as shown in Table 11. Starting from the first training tests with both NNs leveraging the TV-1a dataset, some critical issues have emerged during the conversion phase of the 3D data LAS standard to H5 (Hierarchical Data Format version 5) (Folk et al., 2011) required by the technical python pipeline. Since the graphical interface did not allow controlled management of the conversion to *h5, each original square block

was separated during the conversion, generating multiple round blocks. Therefore, the final number of converted blocks does not correspond to the original number of 140 tiles, chosen for the training and validation of the models, generating thus critical issues as following reported.

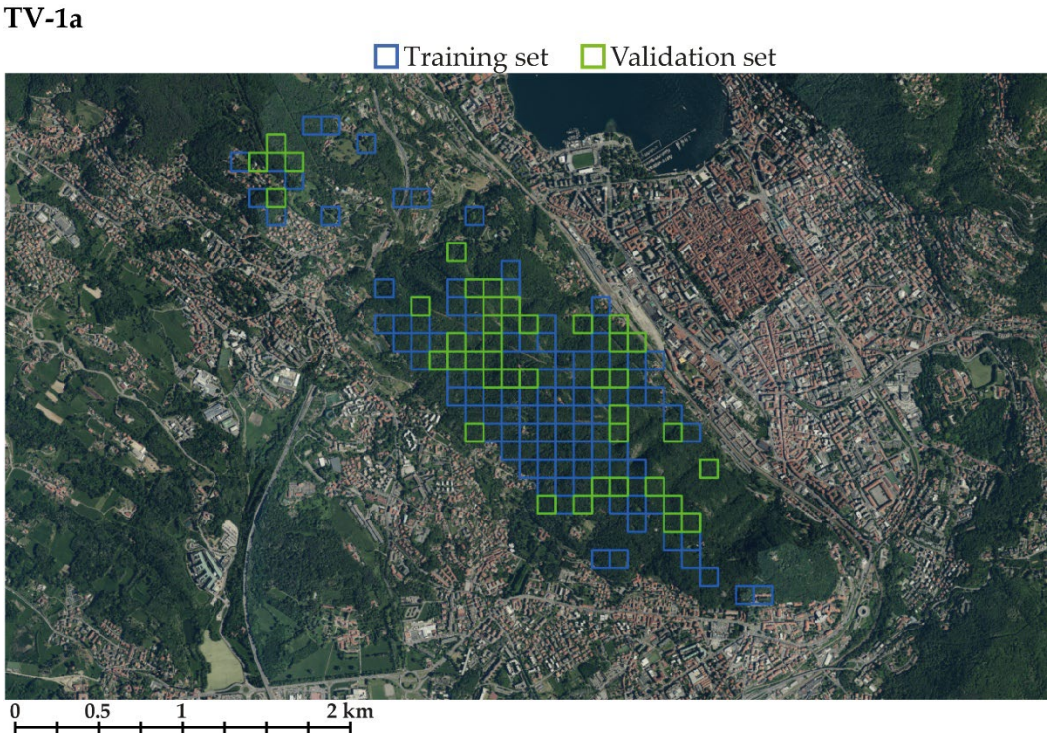

Figure 37. TV-1a location map. Datum RDN2008, projection UTM zone 32 N (EPSG: 7791) – credits CNR IRPI, author (data); author (elaboration).

Table 11. Data consistency and class distribution of the training dataset (TV-1a) that has been used for training and validating the predictive segmentation model.

TV-1a	Data Percentage	Class	Class Distribution
Training	80%	Ground	30%
		High Vegetation	68%
		Building	2%
Validation	20%	Ground	31%
		High Vegetation	68%
		Building	1%

In this case, the models had linear learning until the 5th epoch, decreasing the errors on both training and validation datasets at each epoch despite observing an abnormal increase in errors on the validation set in the 6th epoch. However, the

gradual learning loss of the two subsets does not coincide with a systematic increase in the model's accuracy values.

The TV-1b dataset (Figure 38, Table 12) enabled a more accurate selection of the tiles to ensure a representative sample of data, partially preventing class imbalances and reducing the number of batches to be processed. For both NNs, the learning rate of the models appeared promising in the first epochs. However, both models eventually overfit, memorizing the reference data without effectively learning from it, resulting in poorly generalizable predictions. The excessive errors on the validation set were induced, once again, by inaccuracies in the input data conversion of the 32 original data square tiles (Table 10) that did not reflect the number of converted round blocks. Moreover, the issues with out-of-memory errors were still present, leading to the impossibility of training a working semantic segmentation model.

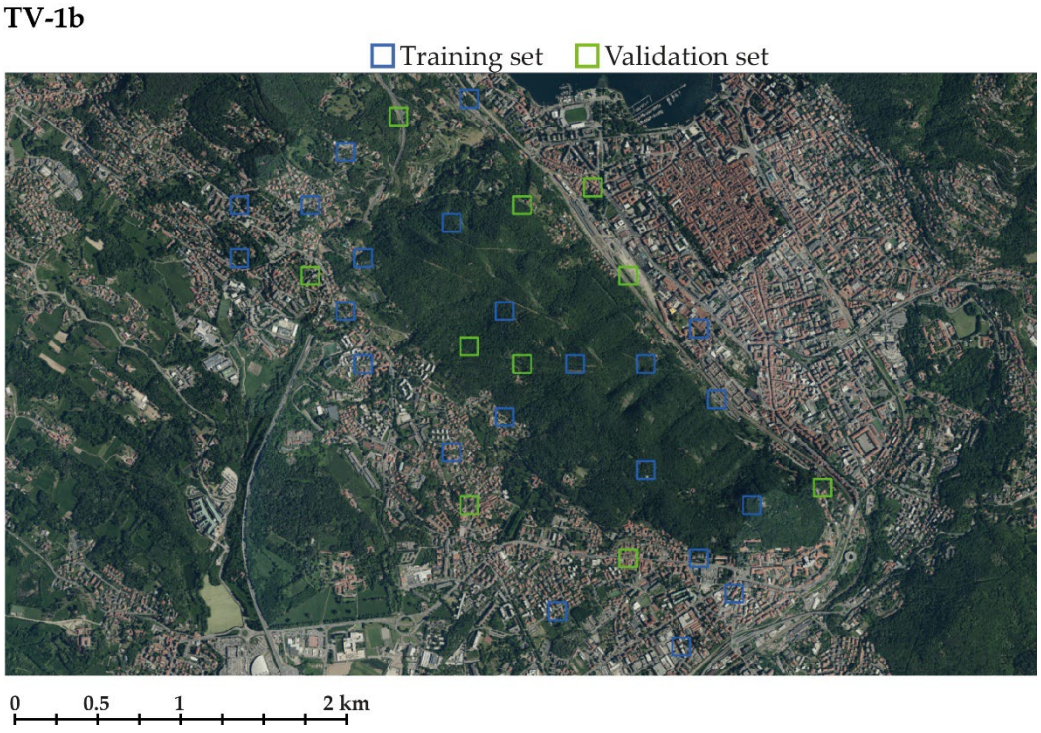

Figure 38. TV-1b location map. Datum RDN2008, projection UTM zone 32 N (EPSG: 7791) – credits CNR IRPI, author (data); author (elaboration).

Table 12. Data consistency and class distribution of the training dataset (TV-1b) that has been used for training and validating the predictive segmentation model.

TV-1b	Data Percentage	Class	Class Distribution
Training	79%	Ground	42%
		High Vegetation	49%
		Building	9%
Validation	21%	Ground	45%
		High Vegetation	45%
		Building	10%

For this reason, new training data (TV-1c) has been accurately prepared and extensively analyzed, slightly reducing input data (Figure 39).

TV-1c

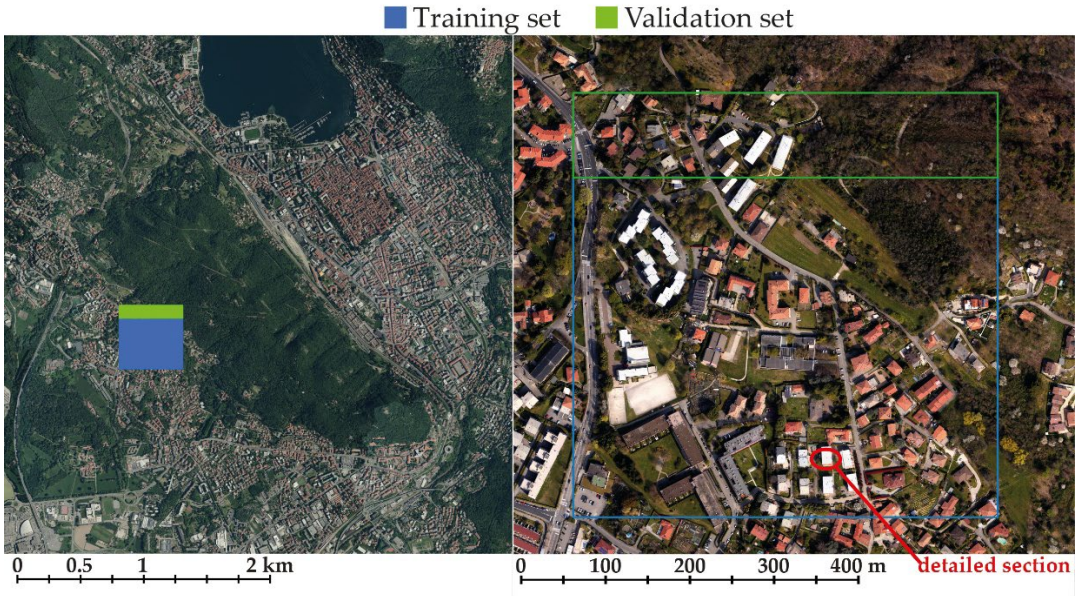

Figure 39. TV-1c location map. Datum RDN2008, projection UTM zone 32 N (EPSG: 7791) – credits CNR IRPI, author (data); author (elaboration) (Cappellazzo et al., 2024a).

Since the Park area is characterized by dense vegetation, the TV-1c dataset has been chosen to adequately represent the class distribution of the area. In fact, it is possible to observe from Table 13 that the most populated class is the one pertaining to high vegetation. The class imbalance issue observed in this dataset and its generalized class scheme is a well-known problem. This issue also arises when working with denser datasets (Kölle et al., 2021), where there is a need to provide a less generalized class schema (Niemeyer et al., 2014).

Table 13. Data consistency and class distribution of the training dataset (TV-1c) that has been used for training and validating the predictive segmentation model.

TV-1c	Data Percentage	Class	Class Distribution
Training	79%	Ground	34%
		High Vegetation	54%
		Building	12%
Validation	21%	Ground	36%
		High Vegetation	53%
		Building	11%

Finally, two final predictive DLMs have been thus trained for TV-1c and will be discussed in Section 4.2.1:

- DLM 1, trained original resolution data (NN architecture: RandLA-Net);
- DLM 2, trained using subsampled data (NN architecture: PointCNN).

The final training stage was set using the model hyperparameter specification. Both the DLM 1 and DLM 2 segmentation models have been trained without any pretraining on transfer learning backbones. The starting base learning rate was fixed at 0.0014, and rather than using a fixed rate, optimization has been implemented to dynamically adjust the learning rate by analyzing the learning curve loss. Early stopping was also employed to end training when it recorded the highest F1 score, aiming the model to reach its best validation performance. All these choices and spaces for hyperparameter tuning were essential for achieving convergence efficiency with robust segmentation accuracy over the point cloud data. The loss plots for PointCNN and RandLANet highlight key aspects of their training behavior and generalization ability. In the case of PointCNN (Figure 40), the training loss steadily decreases, showing that the model effectively reduces errors within the training set. However, an important observation is the behavior of the validation loss that, after initially declining, starts to rise. This increase is a strong indication of overfitting. In fact, while the model continues to improve on the training data, it gradually loses its ability to generalize new, unseen data. The growing gap between training and validation loss suggests that beyond a certain

point, additional training no longer enhances generalization but instead leads to memorization of the training set. This pattern emphasizes the importance of strategies like early stopping, dropout, or other regularization techniques to prevent overfitting.

RandLANet plot (Figure 39), on the other hand, exhibits a different trend, particularly in its first training phase. Here, both training and validation losses decrease in a synchronized manner, indicating that the model is not only learning effectively but also maintaining its ability to generalize throughout the process. The fact that the gap between the two loss curves does not widen suggests that RandLANet is not overfitting under these conditions, which could mean that its architecture or design inherently supports more stable learning. Additionally, the model appears to reach convergence relatively quickly, requiring fewer training batches to achieve a comparable reduction in loss. This efficiency is an important factor, especially when computational resources are limited.

PointCNN

Backbone: None

Learning Rate: 0.0014

Training and Validation loss

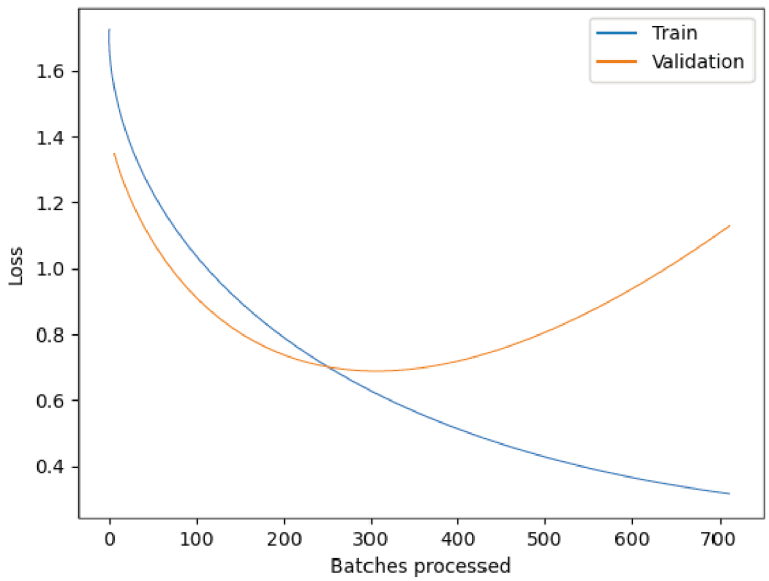

Figure 40. Hyperparametrization and learning loss curves for DLM 2.

RandLANet

Backbone: None

Learning Rate: 0.0014

Training and Validation loss

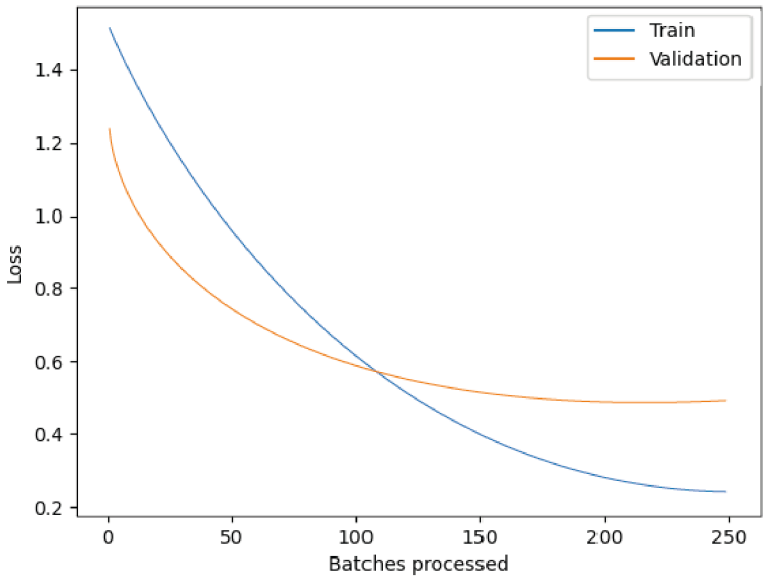

Figure 41. Hyperparametrization and learning loss curves for DLM 1.

The models have then been subsequently tested on four areas (100m*100m test dataset) (Figure 42), using both original resolution and sub-sampled data, in order to evaluate the classification in different morphological and urban contexts. In fact, these specific test areas have been chosen to analyze the model's behavior in different regions of the area, which accurately represent two main characteristics of the Como area: the dense urban fabric areas that embed the Park and the forested, less anthropized areas of the Park itself, as observable in class distribution (Table 14).

Table 14. Class frequency of the Como case study test datasets used to evaluate the trained predictive model. This dataset has been selected to evaluate the model performances in 4 different contexts than the training dataset.

	Ground	High vegetation	Building
1	39%	19%	42%
2	60%	25%	15%
3	31%	29%	40%
4	40%	58%	2%

Figure 42. Map of the Como case study test areas location. The presence of heterogeneous features and morphology characterizes the considered areas – credits (Cappellazzo et al., 2024a).

Sardinia Defensive Landscapes: toward an interoperable semantic segmentation Deep Learning Model for mid-scale airborne LiDAR point clouds

Following the unsupervised approach that has been described in Section 3.2.2, with the reference ground truth data generated by geometrical filter application, the second step was to train semantic segmentation DLMs aiming at converting unstructured 3D datasets into a semantically organized dataset. Moreover, the DL methodologies application largely benefited from the lesson learned during the Case Study 1 experiments.

The training dataset for Case Study 2 (TV-2a, Figure 43) has been selected from the ALS data of Area 1 (Cagliari) and consisted of training and validation datasets balanced at 78%-28% (Table 12). Furthermore, particular attention has been given to the selection of data to ensure both the representativeness of the urban and landscape morphology of the area and a homogeneous distribution of classes between the two parts of the dataset.

TV-2a

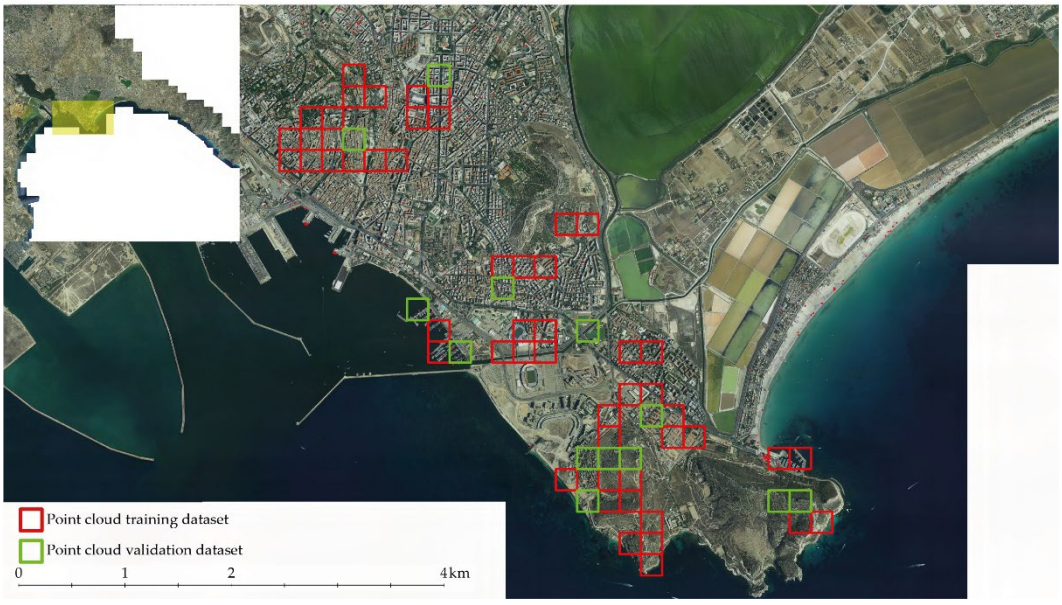

Figure 43. Map of the location of the TV-2a (Case Study 2 – Area 1, Cagliari). The red tiles are about the training set, while the green blocks relate to the point cloud tiles used to validate the model – credits (Cappellazzo et al., 2024b).

Table 15. Data consistency and class distribution of the training dataset (TV-2a) that has been used for training and validating the predictive segmentation model.

TV-2a	Data Percentage	Class	Class Distribution
Training	78%	Unclassified	5%
		Ground	58%
		High Vegetation	10%
		Building	26%
		Water	2%
Validation	22%	Unclassified	6%
		Ground	67%
		High Vegetation	8%
		Building	18%
		Water	1%

Finally, a predictive segmentation DLM (DLM 3) has been trained using the Training dataset from Area 1 (Cagliari). The training process employed RandLA-Net (Hu et al., 2019) neural network architecture, which has been selected due to its capacity to efficiently handle large-scale datasets, incorporating a random sampling phase for each network node. A cross-entropy loss logarithmic function has been used to validate the model.

Similar to DLM 1 and 2, DLM 3 has been trained without incorporating any backbone model and setting the starting learning rate to 0.0014. The adapting learning rate optimization has been implemented as well in order to initially take relatively large steps to accelerate convergence and then progressively refine the model's parameters following the decrease in the loss curve.

Regarding the DLM 3 training, where training extends over a significantly larger number of batches, the behavior of the model (Figure 44) remains largely consistent for most of the training duration. Both loss curves decrease steadily, demonstrating continued learning. However, towards the later stages, a slight increase in validation loss becomes apparent while the training loss continues to decline. This suggests that given enough training time, even RandLANet is susceptible to overfitting, though to a lesser extent than PointCNN. The key

takeaway from this observation is that, while RandLANet generally maintains better generalization properties, prolonged training can still introduce overfitting if not carefully controlled.

RandLANet

Backbone: None

Learning Rate: 0.0014

Training and Validation loss

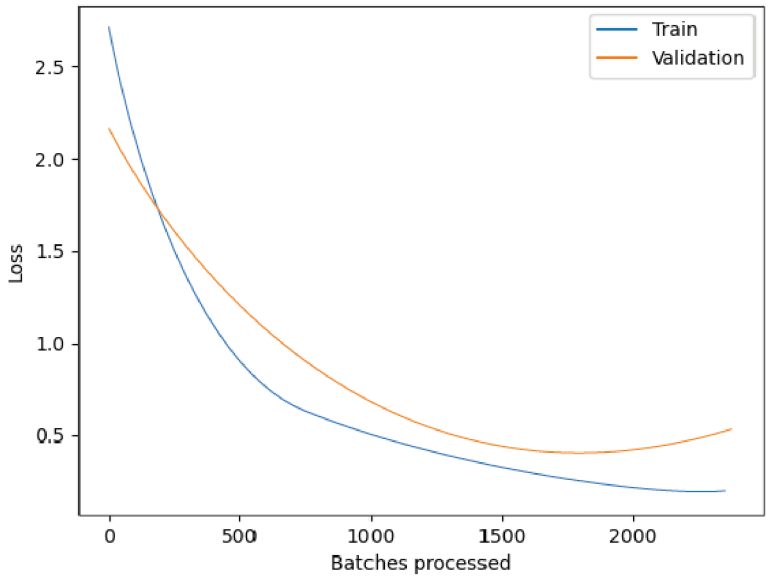

Figure 44. Hyperparametrization and learning loss curves for DLM 3.

Comparing DLM 1-2-3, it is evident that PointCNN exhibits overfitting much earlier, whereas RandLANet is able to maintain a more balanced learning process over shorter training durations. However, neither model is entirely immune to overfitting, and both could benefit from adaptive training strategies such as dynamic learning rate scheduling or regularization techniques tailored to their specific architectural characteristics. These observations highlight the importance of carefully managing training duration and hyperparameters to ensure that models not only learn effectively but also retain their ability to generalize to new data.

Moreover, to evaluate the predictive model performance, 4 test datasets have been selected (Table 16). For example, test area 7 is characterized by many points

related to the building class (80%), while test area 8 has a more balanced frequency but with more points related to vegetation (36%).

Table 16. Class frequency of the Sardinia case study test datasets used to evaluate the trained predictive model. This dataset has been selected from Area 2 (Alghero).

	Unclassified	Ground	High vegetation	Building	Water
5	2%	52%	2%	38%	6%
6	4%	43%	9%	44%	-
7	1%	19%	1%	80%	-
8	3%	41%	36%	20%	-

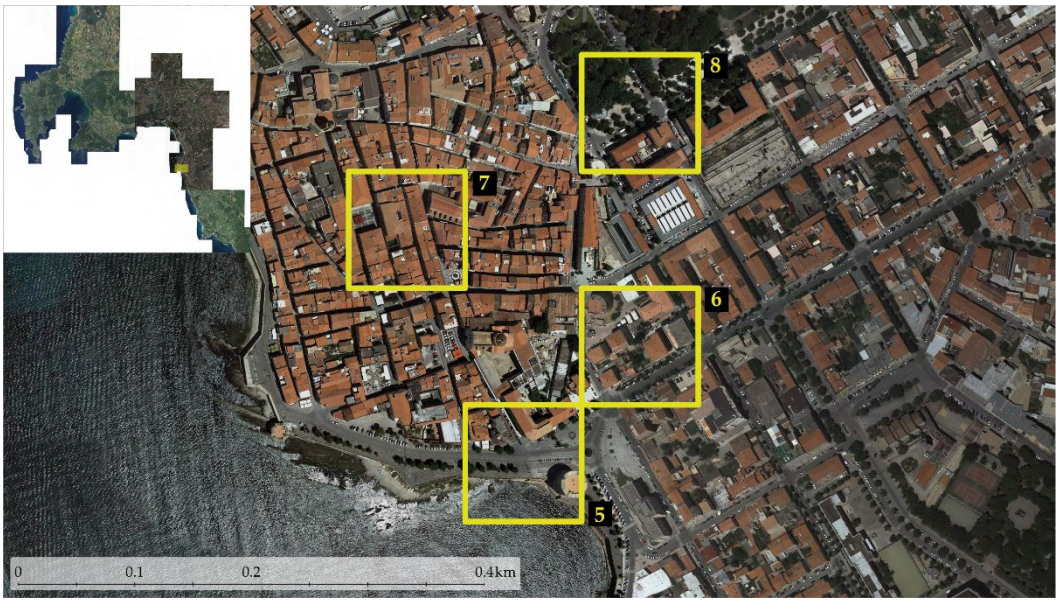

Figure 45. Map of the test dataset areas. The test point clouds have been selected from the Case Study 2, Area 2 (Alghero) – credits (Cappellazzo et al., 2024b).

The evaluation of the Model 3 results will be further discussed in Chapter 4.

3.3.2 Deep Learning detectors: a preliminary perspective test aiming at mapping automation for defensive and military Heritage artifacts leveraging mid-scale existing point clouds

Since one of the aims has been intended to be the development and application of an integrated methodology for historical defensive landscapes, it has been necessary to evaluate the priorities, challenges, and issues related to the

identification of fortifications. Due to the high number of fortification sites and buildings and the accessibility challenges of their location, a preliminary investigation regarding the automatic object detection approach exploiting the semantic segmented point clouds has been addressed.

Therefore, in this research framework, this part of the methodology thus explored the solutions for fortification automatic identification from existing airborne LiDAR point clouds. However, it should be underlined that input data density, training data preparation, and predictive model training require several specific capabilities.

As mentioned in Section 2.1.3 Deep 3D object detection NNs for LiDAR data are increasingly being studied due to LiDAR spatial capture capabilities. Contrarily to 2D detection based on imagery data, the spatial comprehension given by active LiDAR techniques of an environment is a great benefit for recognizing 3D objects. Yet several challenges in 3D detection are present, because of the sparsity of LiDAR point clouds (Wu et al., 2021).

Moreover, the preparation of a reference dataset requires analysis of data characteristics, scene typology, and the number of object classes and annotations. In fact, this doctoral research addressed two essential preliminary technical questions: input point cloud data and reference data preparation. In order to test the label generation process, the research focused on bunker architectures of the WWII coastal containment arch system that are widespread in Alghero's territory (Area 2).

Moreover, the ALS data from Area 2 has been considered dense enough (10 pts/m^2) to recognize bunker objects that were easily distinguishable from other elements (e.g., bushes). Relatively to this context, Area 2 was characterized by a relatively high number of bunker artifacts, as reported in Table 3. Comparing the numerosity of the presented objects with the number of annotations in the object-detection benchmark datasets, it is evident that the data augmentation challenge should be addressed. These issues are further discussed in the conclusion chapter.

The generation of reference data was completed in a GIS environment, starting from point geometries of different census domain datasets (Fiorino, 2021; Cappellazzo, 2019). The label generation workflow consisted of extruding the squared buffers of the object centroid between two altimetric levels (Figure 46). The base height of the 3D bounding box has been calculated from the average reference DTM height. Consequently, the extrusion value has been summed to base height, generating the 3D bounding box for the training labels stored in ASCII format.

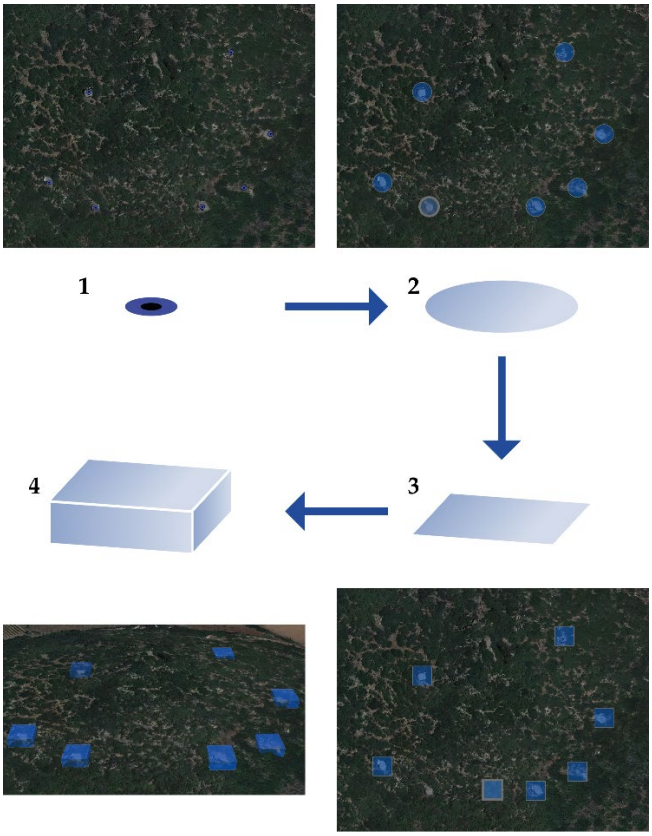

Figure 46. Label generation workflow: from a point feature class to a 3D geometry – credits (Cappellazzo et al., 2024b).

Section 2.1.3 has presented different types of 3D detectors NNs, that have precise characteristics and limitations. In fact, the projection and voxel methodologies result in the loss of LiDAR data information. However, the application of 3D CNNs in voxel-based methods still allows for the extraction and learning of local features from the 3D representation (Wu et al., 2021). Yet, point-based approaches fully exploit the 3D geometry without significant information loss

(Guo et al., 2021), despite some limitations that occur for point-wise feature generation.

In the framework of the present contribution, it has been conducted a preliminary training experiment exploiting the SECOND (Sparsely Embedded CONvolutional Detection) detector with arcpy 2.9 libraries. Specifically, hyperparameters have been set to optimize the learning process by concentrating on all the relevant data. The minimum points per block have been set to 0, ensuring that all data blocks were considered for training. The model focused on blocks containing objects of interest, optimizing the learning process by concentrating on relevant data. Similar to the point cloud segmentation models described in the previous sections, the learning rate strategy was set to dynamically adjust the learning rate to enhance convergence and model performance.

Batch size has been set to 2, allowing for frequent updates to the model parameters and facilitating faster convergence.

Early stopping was enabled to prevent overfitting. This mechanism allowed the halt of the training process, ensuring the model maintains generalization capabilities. Additionally, voxel settings were meticulously configured to define the granularity and computational limits of the voxel grid used in training. These settings included parameters such as voxel width (0.30 m) and height (0.30 m).

3.4 Machine Learning Classifiers and raster Visualization Techniques (VTs) for anthropogenic landforms classification

In the framework of CH mapping, it is worth underlining that when using an Airborne Laser Scanner (ALS) technique to investigate archeological landscapes in highly forested areas, also features such as trails, standing stones, walls, roads, canals, earthworks, and similar features must be reflected in the final DTM.

Starting thus from the segmented point clouds and after density evaluation analysis, the subsequent step has been addressed toward generating an accurate DTM. In addition to the elevation model, also geomorphological analysis and composite geomorphologic raster have been used to define and evaluate the best strategies to be adopted for the application of OBIA-supervised automatic classification methodologies.

3.4.1 LiDAR data interpolation: DTM generation and Geomorphological Layers (GMLs) for Heritage sites comprehension

As long as the average spacing through the ground class points was 20 cm, a DTM was calculated with a 20 cm GSD corresponding to the initial data density. Generally, various features related to the ground surface can be detected, such as trails, human earthworks, and similar elements present, even if not well represented, in the raw DTM. Considering the research aims, interpreting visual features related to the ground surface, such as anthropogenic elements, represents a relevant challenge. Therefore, the issues connected to difficulties in identifying and interpreting these visual features became evident when studying the DTM. In fact, it was not easy to unambiguously detect these features in ALS point cloud data and the subsequent raster interpolation of DTM. It is indeed clear from Figure 47 that both the orthoimage and raw DTM did not help reach the research aims. Concerning the RGB orthoimage, the vegetation covers almost the entire underlying terrain, even though aerial photogrammetric acquisitions have been performed during the leafless period of the year.

To address the issues related to ground feature identification, an investigation was carried out to generate geomorphological raster datasets that could enhance the interpretation of traces in the terrain morphology.

Different geomorphologic analyses have been conducted to determine the most significant geometrical and numerical signatures and to detect the significant ground shapes (Figure 47). The shaded visualization and the slope, aspect, and flow direction analyses have been generated from the DTM surface.

Moreover, from a Focal Statistic (FS) analysis on a 5-pixel neighborhood cluster of the DTM, a Relative Roughness index r_i (Jenson & Domingue, 1988) raster has been estimated using the raster calculator.

$$r_i = \frac{(FS_{mean} - FS_{min})}{(FS_{max} - FS_{min})} \quad (2)$$

From a spatial analysis of the 3D point cloud, the direction value of the magnetic north was calculated for each point. This function calculates the orientation angle for each point using the supplementary attributes of Magnetic North vectors acquired during the flight (Pomerleau et al., 2012). The resulting scalar field is then interpolated to create a shaded false-color visualization. From this visualization, human artifacts such as trails become more visible. This method is considered an effective alternative to simple DTM Hillshade, which often fails to highlight man-made paths, especially under vegetation.

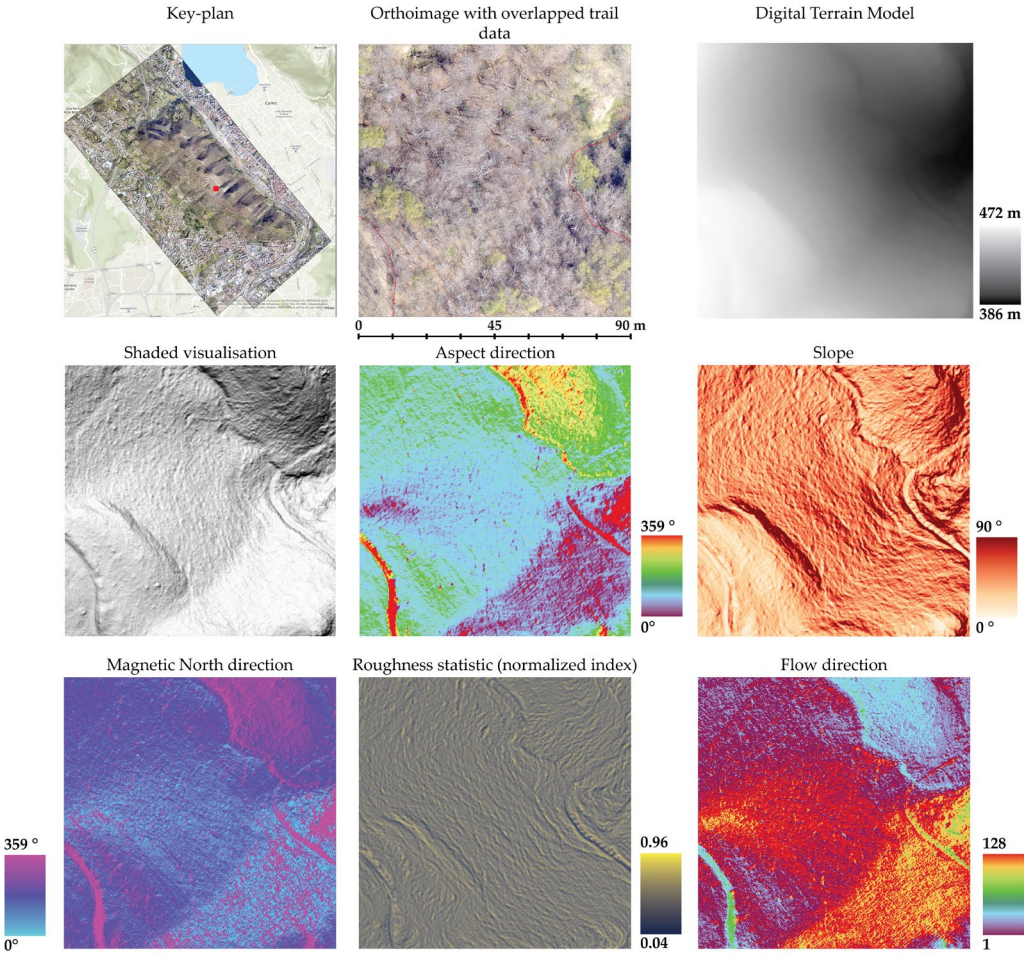

Figure 47. A comparison of orthoimage, DTM, and subsequent geomorphological analyses was performed on a sample site, showing the park's trails. Each raster analysis has been visually inspected, considering a sample area, in order to understand its suitability for the rapid identification of the anthropogenic shapes of the terrain – credits (Cappellazzo et al., 2024a)

From the visual inspection of the geomorphological analyses (Figure 47), it is evident how specific ground features such as trails, depressions, and rock formations are detectable. On the contrary, the elevation model and the orthoimage have not proven suitable for this type of task since the searched features are not unambiguously evident. Therefore, Geomorphological Layers (GMLs) have been used as training datasets for applying Machine Learning (ML) classification algorithms.

After the classification accuracy evaluation (Section 4.3*)* using the individual geomorphological analyses, several composite raster datasets have been generated by combining the GMLs (Figure 48).

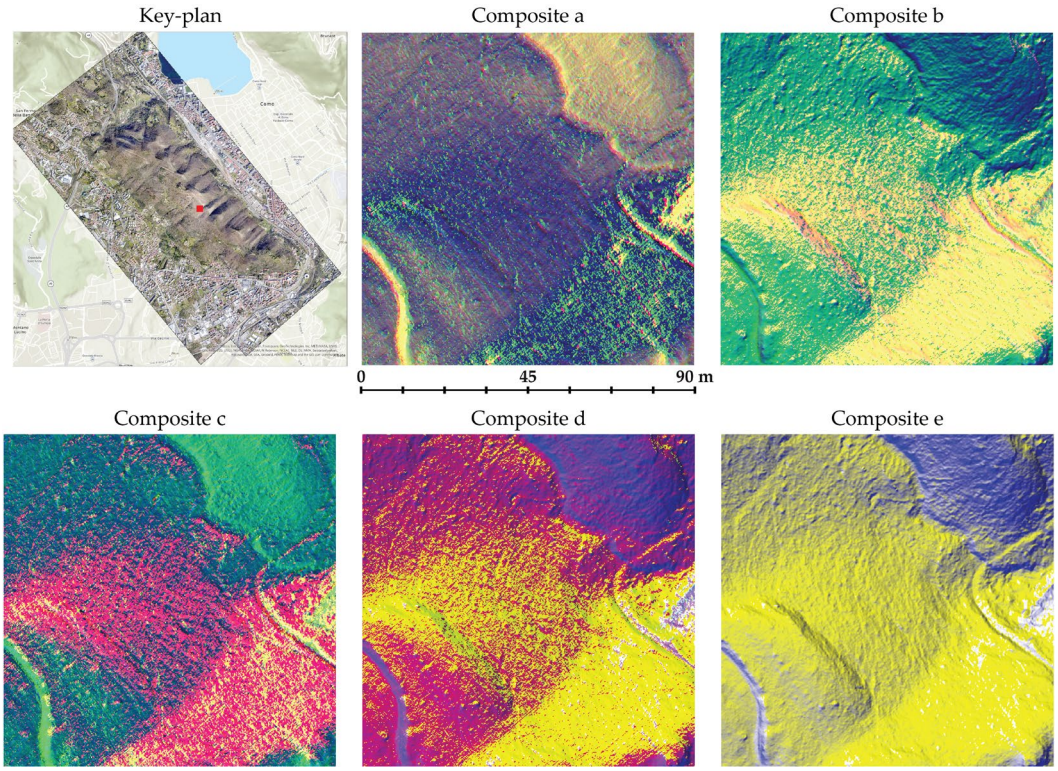

Figure 48. Comparison of the chosen composite geomorphological raster. In Table 4, it is possible to observe the RGB band disambiguation for each raster – credits (Cappellazzo et al., 2024a)

In this case, the aim was to assess whether generating these composite rasters could enhance the classification effectiveness. For this reason, five composite raster data sets were generated. The combination of GMLs in each composite raster is reported in Table 17.

Table 17. RGB bands disambiguation in the composite geomorphological raster, as in Figure 48.

COMPOSITE RASTER	Red band	Green band	Blue band
Composite a	Aspect	Magnetic north direction	Roughness index
Composite b	Flow direction	Shaded visualization	Roughness index
Composite c	Flow direction	Magnetic north direction	Roughness index
Composite d	Shaded visualization	Flow direction	Aspect
Composite e	Shaded visualization	Shaded visualization	Aspect

3.4.2 ML training data preparation strategies focusing on low human-resources consumption

Since it has been established that Machine Learning classifiers (MLCs) are particularly suitable for geospatial imagery (Maxwell et al., 2018), the integration of Machine Learning techniques within the methodological workflow has been tested. However, in contrast to what has been developed so far, some recent studies (Alifu et al., 2020; Maxwell & Warner, 2015; Mazzacca et al., 2022) have investigated ML classification techniques adopting an optical sensor data integration strategy with digital elevation model data. In this step of the pipeline, the goal was to achieve a high level of automation for the macro-scale land-cover mapping task, which was the ultimate objective of the proposed methodology, adopting thus the use of MLCs.

As stated in section 2.1.3 the training samples have a crucial role in the effectiveness of the MLCs, even if there is not a generalized model for the training data preparation. However, it can be assumed that the numerosity and size of training samples must be planned accurately, depending on the classification algorithm, the number of class variables, the quality of the primary data, and the variety within the whole spatial extension (Maxwell et al., 2018). Two approaches in two distinct areas have been employed during the training data preparation (MLC-1 and MLC-1b). In both instances, the predefined dual-class classification scheme was employed to categorize anthropic shapes and ground. The areas and the support vectors that have been used during the training data preparation are displayed in Figure 49 and Figure 50. For this task, a predefined dual-class classification scheme was employed to categorize anthropogenic landforms (namely trails) and ground. The first objective was to minimize human involvement in the labeling process while maximizing label coverage across all regions of the training areas.

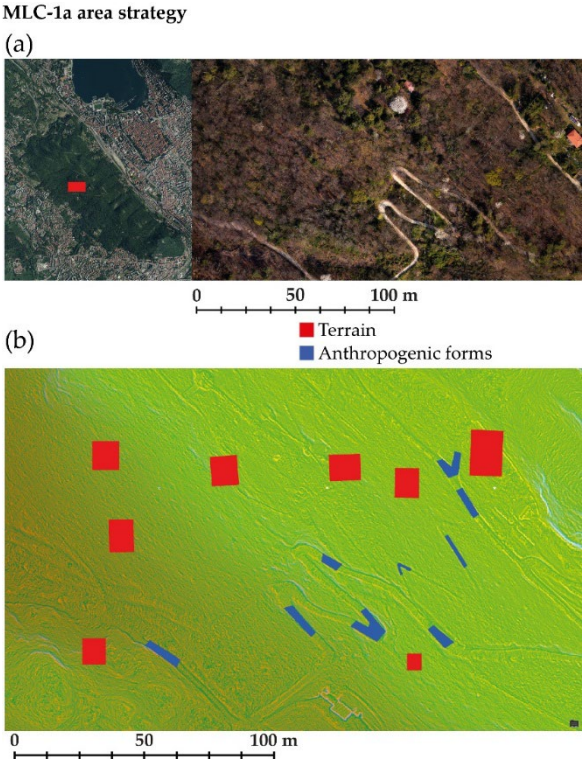

Figure 49. (a) Map of the training area MLC-1a location. (b) Training data label generation strategy. Datum RDN2008, projection UTM zone 32 N (EPSG: 7791) – credits CNR IRPI, author (data); author (elaboration) (Cappellazzo et al., 2024a).

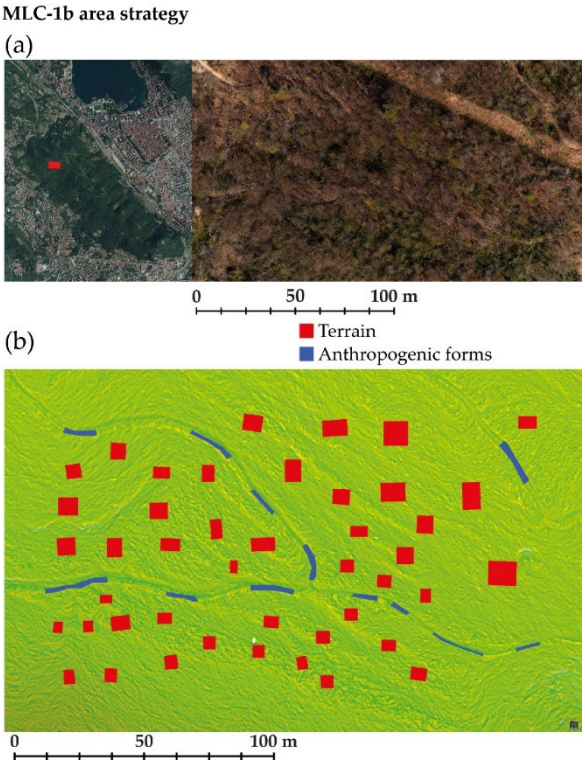

Figure 50. (a) Map of the training area MLC-1b location. (b) Training data label generation strategy. Datum RDN2008, projection UTM zone 32 N (EPSG: 7791) – credits CNR IRPI, author (data); author (elaboration) (Cappellazzo et al., 2024a).

In the first area (MLC-1a), the main aim was the optimization of the labeling procedures by decreasing the number of samples and increasing their average area. Regarding the second area (MLC-1b), the number of labels has been increased up to the recommended minimum (>15) (Maxwell et al., 2018) while reducing the average size of the samples (Table 18). While the SVM classifier succeeded in the classification task even with the few support vectors of MLC-1a, the RF algorithm did not accomplish the classification task due to the low number of labels. For this specific reason, the comparisons between the performance of the two MLCs have been addressed only as concerns MLC-1b. The results of this approach will be discussed in Section 4.3.

Table 18. Traditional ML training data labeling strategy comparison.

	MLC-1a		MLC-1b	
Class	% m^2/total	m^2 average	% m^2/total	m^2 average
Trail class	15.67%	87.92	26.27%	21.89
Terrain class	84.33%	277.54	73.73%	32.11

Chapter 4 – Results and discussions

Results and discussions

This chapter reports the results relative to the integrated methodology presented in the Materials and Methods chapter that has been developed in Chapter 3 to address the data structuring challenges of airborne LiDAR data for extended landscape areas. The classification accuracy of the semantic segmentation and detector DLMs (Section 3.3) and the MLCs (Section 3.4) has been evaluated by comparing the predictions with the ground truth labels. Starting from the data reported in the confusion matrices (true positives, true negatives, false positives, false negatives), the following metrics (Tharwat, 2018) have been estimated to evaluate the achieved results: Accuracy (3), Precision (4), Recall (5), F1 score (6), and mean Average Precision of all classes (C), mAP (7). The metrics have been calculated as follows:

$$\text{Accuracy} = \frac{\text{True positives (TP)} + \text{True negatives (TN)}}{\text{True positives (TP)} + \text{True negatives (TN)} + \text{False negatives (FN)} + \text{False positives (FP)}} \tag{3}$$

$$\text{Precision} = \frac{\text{TP}}{\text{TP} + \text{FP}} \tag{4}$$

$$\text{Recall} = \frac{\text{TP}}{\text{TP} + \text{FN}} \tag{5}$$

$$\text{F1 score} = 2 \times \frac{\text{Precision} \times \text{Recall}}{\text{Precision} + \text{Recall}} \tag{6}$$

$$\text{mAP} = \frac{1}{|C|} \sum_{c \in C} \text{AP}_c \tag{7}$$

4.1 Unsupervised filter approaches: a semi-automatic pipeline for training data preparation

4.1.1 Spina Verde Park: validation of the method

Concerning the application of the integrated filtering approach based on the SMRF filter (ground) and geometric feature-based filter (off-ground) for deriving the three classes (Section 3.2.1), the following results can be analyzed and discussed.

Considering the unsupervised approach (Figure 51), positive outcomes have been experienced for terrain and vegetation classes. In contrast, the building class is the one characterized by the worst results in terms of metrics (Table 19).

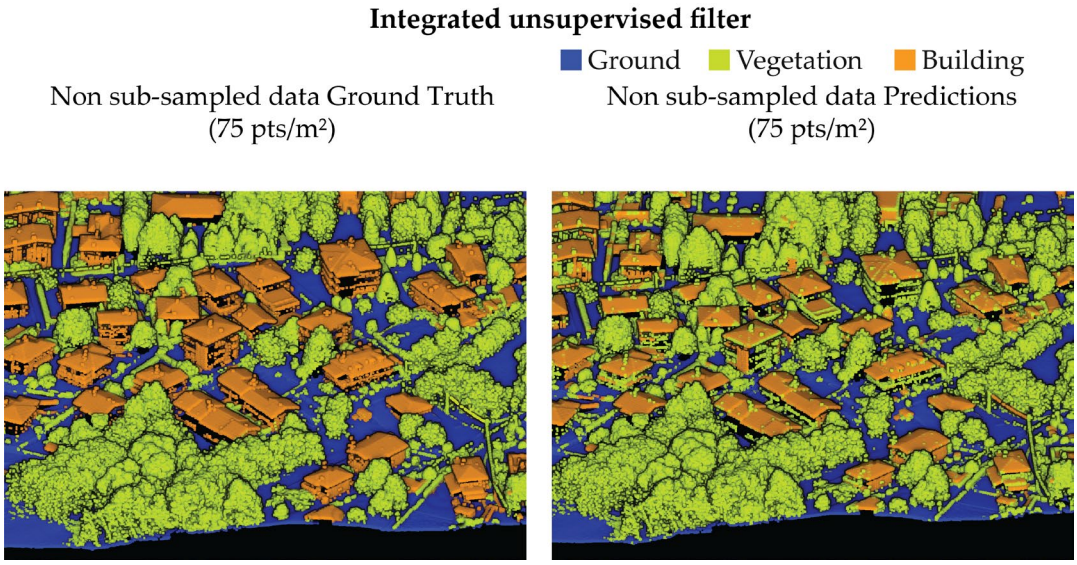

Figure 51. Unsupervised filter results: ground truth comparison with prediction results on the T-V-a validation dataset – credits (Cappellazzo et al., 2024a).

Table 19. Accuracy metric assessment of the unsupervised geometric filters carried out on the T-V-a validation dataset

Class	Accuracy	Precision	Recall	F1 score	Elapsed Time [hh:mm:ss]
Macro Average	0.93	0.79	0.86	0.82	00:14:33
2 – Ground	0.90	0.76	0.99	0.86	
5 – High Vegetation	0.90	0.99	0.86	0.92	
6 – Building	0.99	0.62	0.73	0.67	

The high Accuracy metric achieved (≈99%) is due to the heavy numerical imbalance of points belonging to this class. For this reason, the very high number of true negatives (10776575 out of 10990089, ca. 98% of total points) significantly affects the Accuracy of this class. However, considering also the Precision, Recall, and F1 score, it can be observed that the building class is the one characterized by the lowest performance. This highlights the difficulties of the employed unsupervised algorithm in unambiguously recognizing the considered class. Overall, the results can be considered adequate for the accurate generation of a digital model of the terrain. Specifically, a sensitive evaluation of the results for individual classes demonstrates how the SMRF filter (Pingel et al., 2013) manages to apply good generalization in ground points. However, cases of under-prediction are observed in some areas (Precision ≈76%). Integrating a geometric features filter algorithm allows disambiguation between building classes using only the eigenvalue of normal (λ_3) and the geometric value of sphericity, which was then evaluated. In this case, the significant imbalance between the two classes does not lead to easily interpretable results, especially regarding points related to buildings. However, it is evident from Table 16 that the vegetation class does not demonstrate an optimal sensitivity (Recall ≈86%) if compared to the one achieved for the Ground class (Recall ≈99%). As shown in Figure 52, a high percentage of over-prediction can be observed, particularly localized on building roof areas with higher noise and

characterized by architectural objects deviating from the average surface (e.g., chimneys).

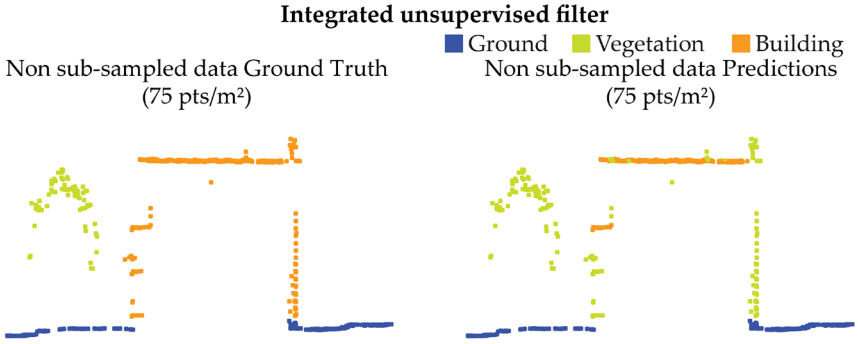

Figure 52. Example of filter results ambiguities. Comparison of Ground truth with prediction results of the unsupervised filter adopting a section in a reduced point cloud sample – credits (Cappellazzo et al., 2024a).

Similar behavior occurs in the case of the vertical elements related to facades, which are generally less dense and noisier than the horizontal ones. Due to this topological difference, the points pertaining to these surfaces are less assimilable as belonging to a plane and thus associated with the vegetation class.

However, considering that the main objective was to segment ALS data in order to evaluate the effectiveness of the unsupervised integrated filter, this objective is not precluded or influenced by the results obtained. As observable by the evaluation metrics related to the ground class and reported in Table 16, this step of the proposed methodology represents a valuable solution for generating accurate DTMs. The classification results of the unsupervised filter have been thus evaluated with a visual inspection of a human operator and, where necessary, refined in order to be used as the primary dataset to train a DL classification model.

4.1.2 Sardinia Military Landscapes: testing data fusion approaches for method implementation

Although the predictive model results represent the final stage of the methodology, it is equally important to discuss the outcomes achieved during the data preparation stage. As introduced in Section 3.1.2, the echo information embedded in the airborne LiDAR data was either absent or incomplete. To address this, the present research analyzed and compared return information, reflectance intensity, and newly calculated fields (see Figure 53). From both visual and statistical inspections, the echo return information (Figure 53a) and intensity (Figure 53b) were found to be incomplete and noisy, making them unsuitable for accurately distinguishing between classes. Moreover, it is possible to observe that the presented NIR data fusion approach (Figure 53c) is particularly suitable for segmentation where water bodies correspond to equation 8 (Drusch et al., 2012).

$$\text{NIR reflectance} \leq 0.09 \tag{8}$$

Furthermore, λ3 (normals) eigenvalue (Figure 53d) is considered suitable for a preliminary building class exclusion compared to LiDAR intensity and return information. The threshold value is, in this case, given by the statistical distribution analysis and is relative to the topology of this specific LiDAR dataset (9).

$$\lambda_3 \geq 0.1 \tag{9}$$

In this specific case study, the integration of the NIR band and the employment of a reduced number of geometric features for the unsupervised filter have allowed effective results for the generation of a reference dataset.

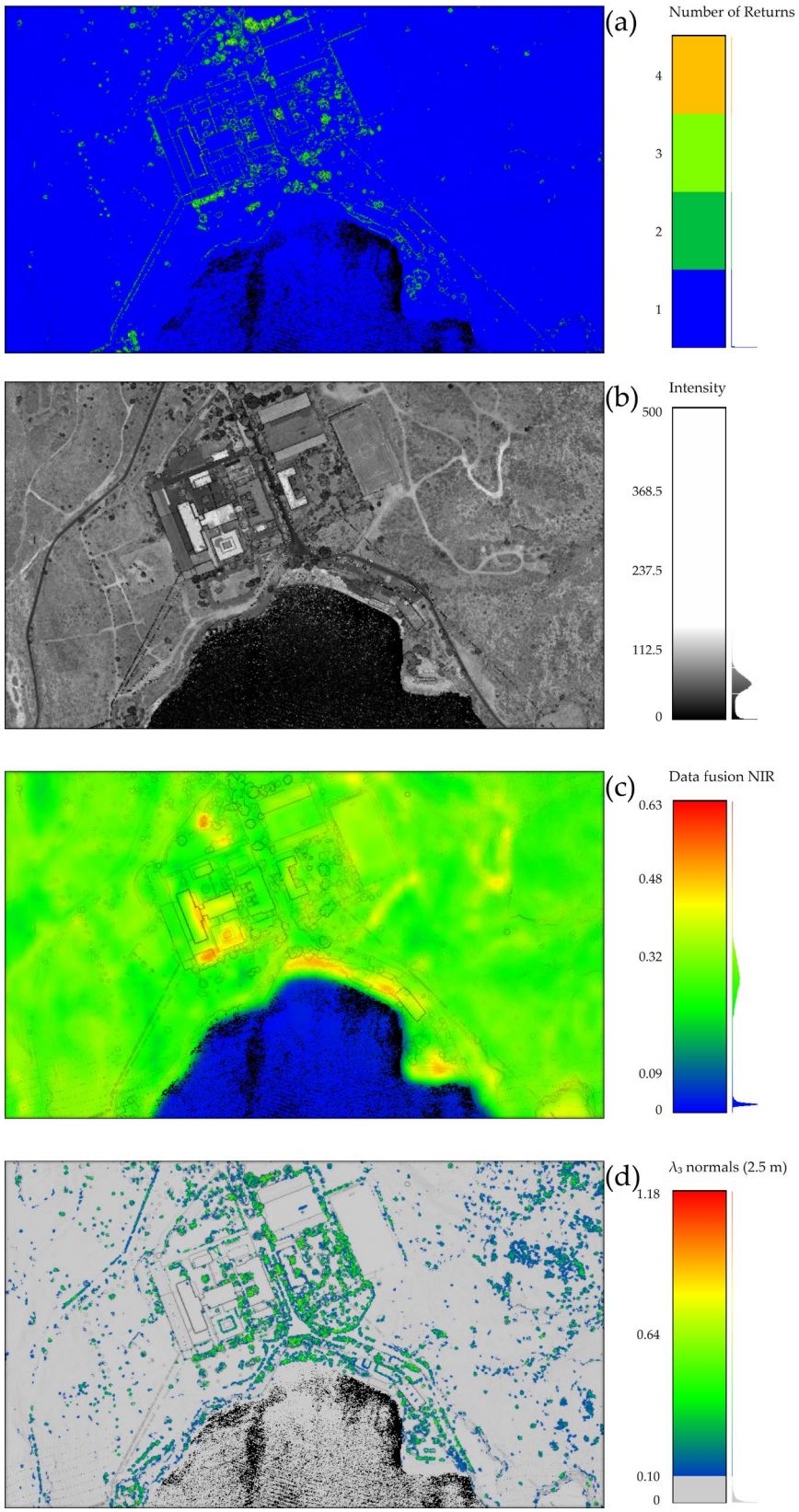

Figure 53. Point cloud echo information, reflectance intensity, and newly calculated scalar field comparison for geometrical and digital number filtering unsupervised segmentation. Number of Returns (a). Intensity (b). Data fusion Near Infrared from Sentinel 2 band 8, 784 nm-899.5nm (c). λ3 eigenvalue (normals) calculated on 2.5 m radius (d) – credits (Cappellazzo et al., 2024b).

4.2 Deep Learning Models for semantic segmentation and object detection results

4.2.1 Spina Verde Park

As stated in Section 3.3.1, two DLMs were trained from the finally selected TV-1C training dataset: Model 1 and Model 2. While Model 1 was trained using the original resolution dataset, Model 2 is derived instead from a subsampled dataset.

The DLM 1, trained with the RandLA-Net architecture, stopped on the 25th epoch after approximately seven hours, resulting in an overall accuracy of 92% (Table 20). Considering the comparisons between ground truth and predictions of each area and the results of individual classes, the sensitivity (Recall) of the ground class appears lower than that of the vegetation class. At the same time, the specificity (Precision) is higher, contrary to what happened with the use of unsupervised filters (Table 19, see section 4.1.1). The visual results can also be observed on the classified Validation dataset (Figure 54).

Table 20. Accuracy metric assessment of the DLM 1 with the RandLA-Net architecture. The analyses are performed using the validation reference dataset.

Class	Accuracy	Precision	Recall	F1 score	Elapsed Time [hh:mm:ss]
Macro average	0.92	0.75	0.86	0.79	06:59:36
2 – Ground	0.91	0.77	0.91	0.83	
5 – High Vegetation	0.91	0.98	0.88	0.93	
6 – Building	0.95	0.50	0.79	0.61	

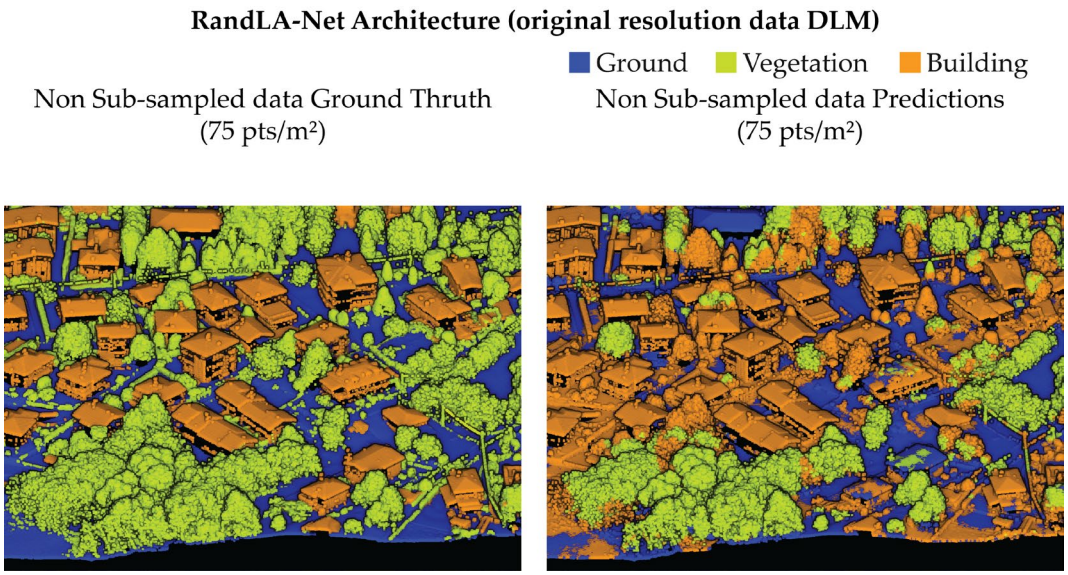

Figure 54. Ground truth comparison with prediction results on validation dataset of the trained Model 1 with the RandLA-Net architecture – credits (Cappellazzo et al., 2024a).

Also, in class 6 (buildings), the results did not meet the desired expectations. This is probably due to the limited number of points belonging to this class, and although part of the training dataset is related to an urban area, this led to an imbalance in the training data.

The DLM 2 (derived from the PointCNN architecture) finished the training in approximately 27 hours at the end of the 25th epoch. As well as for Model 1, Model 2 was then evaluated on the validation dataset (Figure 55). From the evaluation metrics reported in Table 21, the ground class is more sensitive to over-predictions, unlike class 5 (vegetation), which is generally under-predicted.

Table 21. Accuracy metric assessment of the trained DLM 2 with the PointCNN architecture. The analyses are performed using the validation reference dataset.

Class	Accuracy	Precision	Recall	F1 score	Elapsed Time [hh:mm:ss]
Macro average	0.92	0.87	0.80	0.83	26:39:36
2 – Ground	0.92	0.94	0.95	0.95	
5 – High Vegetation	0.96	0.53	0.62	0.57	
6 – Building	0.92	0.87	0.80	0.83	

The metrics observed for the 'building' class are consistent with the results obtained with model 1, highlighting that this class is generally not predicted adequately in both cases. This is evident from the evaluation metrics – the lowest among the considered classes in the case of both models predictions.

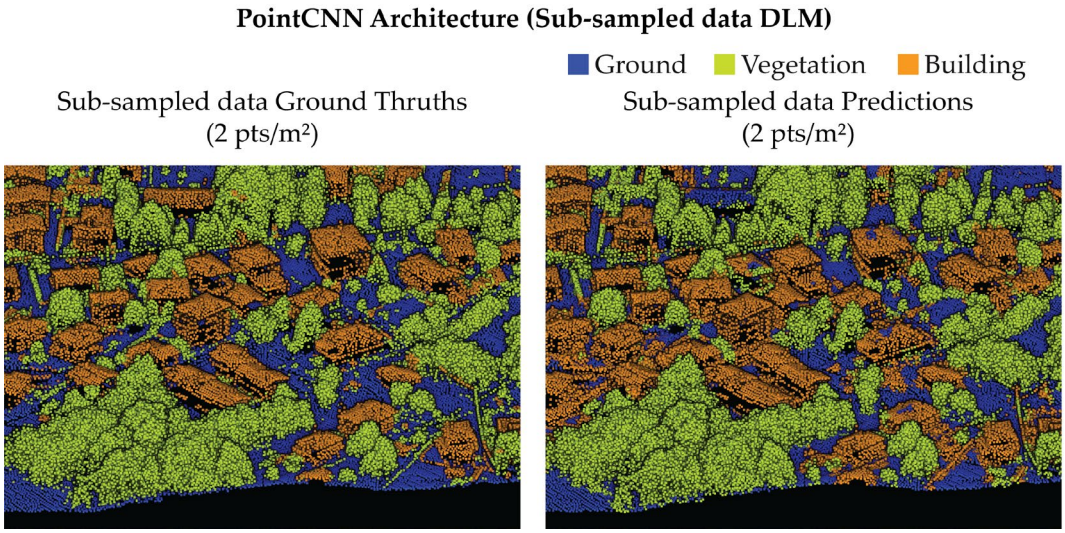

Figure 55. Ground truth comparison from prediction results on the trained DLM 2 validation dataset with the PointCNN architecture – credits (Cappellazzo et al., 2024a).

An overall comparison of the results derived from the adopted approaches (Unsupervised geometric filter vs. Deep Learning) (Table 22) shows that the unsupervised filter method slightly outperformed the two DLMs in terms of Accuracy and F1 score. This corresponds to the preliminary expectations, as the state-of-the-art has shown that the effectiveness of geometric-based methods is currently more efficient for this type of task than DL-based methods (Poux & Billen, 2019). Moreover, the computational cost of the unsupervised filtering is more effective in terms of elapsed time, as well as human and machine resources.

Furthermore, all the classification approaches have been tested using both original resolution and subsampled datasets. The aim was to assess how differences in terms of spatial resolution could affect the final classification results and, additionally, evaluate the effectiveness of a DLM on a less dense point cloud. In fact, open LiDAR datasets, such as those from Case Study 2, available from public administration's landscape-scale survey campaigns are generally less dense than the

point clouds pertaining to Case Study 1. For this reason, it is thus necessary to conduct further evaluations on sparser datasets to validate this method's suitability and adaptability on a different case study where it is not possible to acquire ad hoc datasets (as for the current dataset). The doctoral thesis thus underlines that the significant results achieved using both original resolution and subsampled data are characterized by the same order of magnitude, confirming how this methodology is suitable for classifying point clouds with different densities.

Table 22. Comparison of point cloud classification approaches result on the validation dataset from Case Study 1 (TV-1c).

Unsupervised geometric filter (Original resolution data)		RandLA-Net (Original resolution data)		PointCNN (Subsample data)	
Accuracy	F1 score	Accuracy	F1 score	Accuracy	F1 score
0.93	0.82	0.92	0.79	0.93	0.78

Although the state-of-the-art typically employs more eigenvalues for defining class thresholds, the authors decided to use only the λ3 eigenvalue (normal) and the curvature geometric values. This approach has been followed to evaluate the effectiveness of a classification based on the proposed method while simultaneously reducing computational effort, considering the significant extent of the study area. From the evaluation metrics, it is possible to observe the effectiveness of this type of approach and witness the correct behavior of the predictive algorithm. However, it should be underlined that the DL-based approach also led to adequate results. In particular, the model derived from RandLA-Net outperformed the one trained from PointCNN architecture, as seen in Table 20, Table 21, and Table 22.

Still, the model was also evaluated on the four test areas (Figure 42, see section 3.3.1) using both original resolution and sub-sampled data in order to evaluate the classification in different morphological and urban contexts. In this case, the aim was to evaluate both the generalization capability of the model and the performance in classifying data characterized by different resolutions and densities compared to the training data.

From Table 23 and Table 24, it becomes evident that the classification results are more uniform in dense urban areas characterized by a balanced class distribution (test area 1). In contrast, the classification model has not performed a valuable generalization in areas with a more non-balanced class distribution. Of course, better performance is correlated to the majority class. Moreover, these considerations have been presented by the comparison of metrics analytics supported by the visual inspection of Figure 57 and Figure 58. The analysis demonstrates that the methodology, besides the improvement capability, is suitable for application with sparser ALS datasets. In fact, open-access low-resolution LiDAR datasets provided by Regional and National administrations could benefit from the scalability of the presented approach, despite these not being acquired for specific semantic classification purposes.

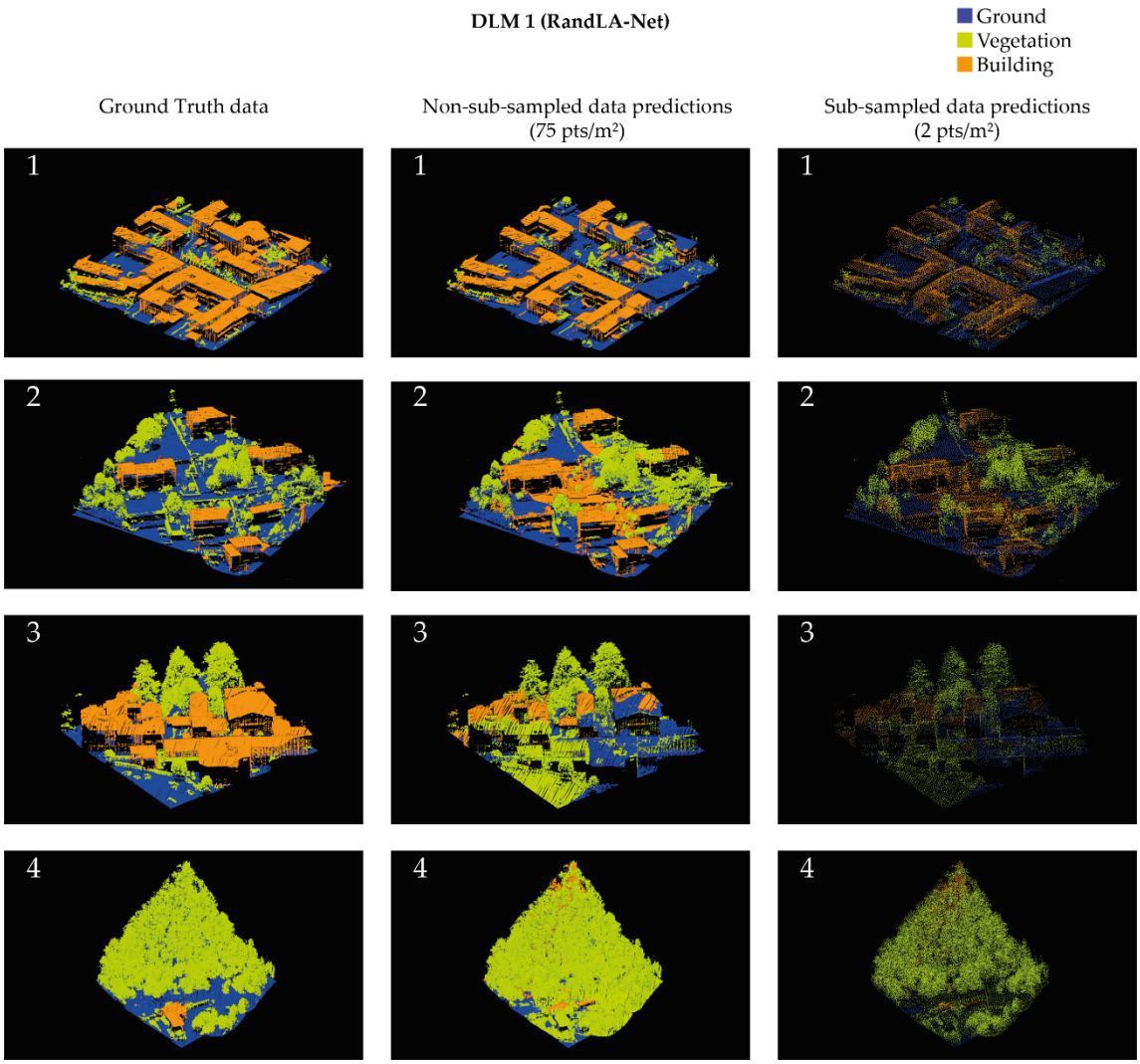

Figure 56. Prediction results of Model 1 on 4 test datasets with RandLA-Net architecture – credits (Cappellazzo et al., 2024a).

Table 23. Accuracy metric assessment of the trained Model 1 with the RandLA-Net architecture, applied to four test areas. The metrics have been analyzed by comparing the adopted strategy for both original resolution and sub-sampled data.

		Original resolution data				Sub-sampled data			
		Accuracy	Precision	Recall	F1 score	Accuracy	Precision	Recall	F1 score
1	Ground		0.69	0.98	0.81		0.65	0.97	0.78
	High Vegetation		0.48	0.47	0.47		0.49	0.48	0.48
	Building		0.96	0.68	0.80		0.94	0.68	0.79
	Macro average	0.78	0.71	0.71	0.69	0.75	0.69	0.71	0.68
2	Ground		0.95	0.57	0.71		0.88	0.54	0.67
	High Vegetation		0.57	0.76	0.65		0.74	0.78	0.76
	Building		0.37	0.76	0.50		0.39	0.75	0.51
	Macro average	0.64	0.63	0.70	0.62	0.67	0.67	0.69	0.65
3	Ground		0.46	0.54	0.50		0.48	0.56	0.52
	High Vegetation		0.47	0.93	0.63		0.58	0.92	0.72
	Building		0.86	0.31	0.45		0.84	0.31	0.46
	Macro average	0.53	0.60	0.59	0.53	0.59	0.64	0.60	0.56
4	Ground		0.48	0.56	0.52		0.90	0.15	0.25
	High Vegetation		0.58	0.92	0.72		0.85	0.94	0.89
	Building		0.84	0.31	0.46		0.03	0.24	0.05
	Macro average	0.59	0.64	0.60	0.56	0.78	0.59	0.44	0.40

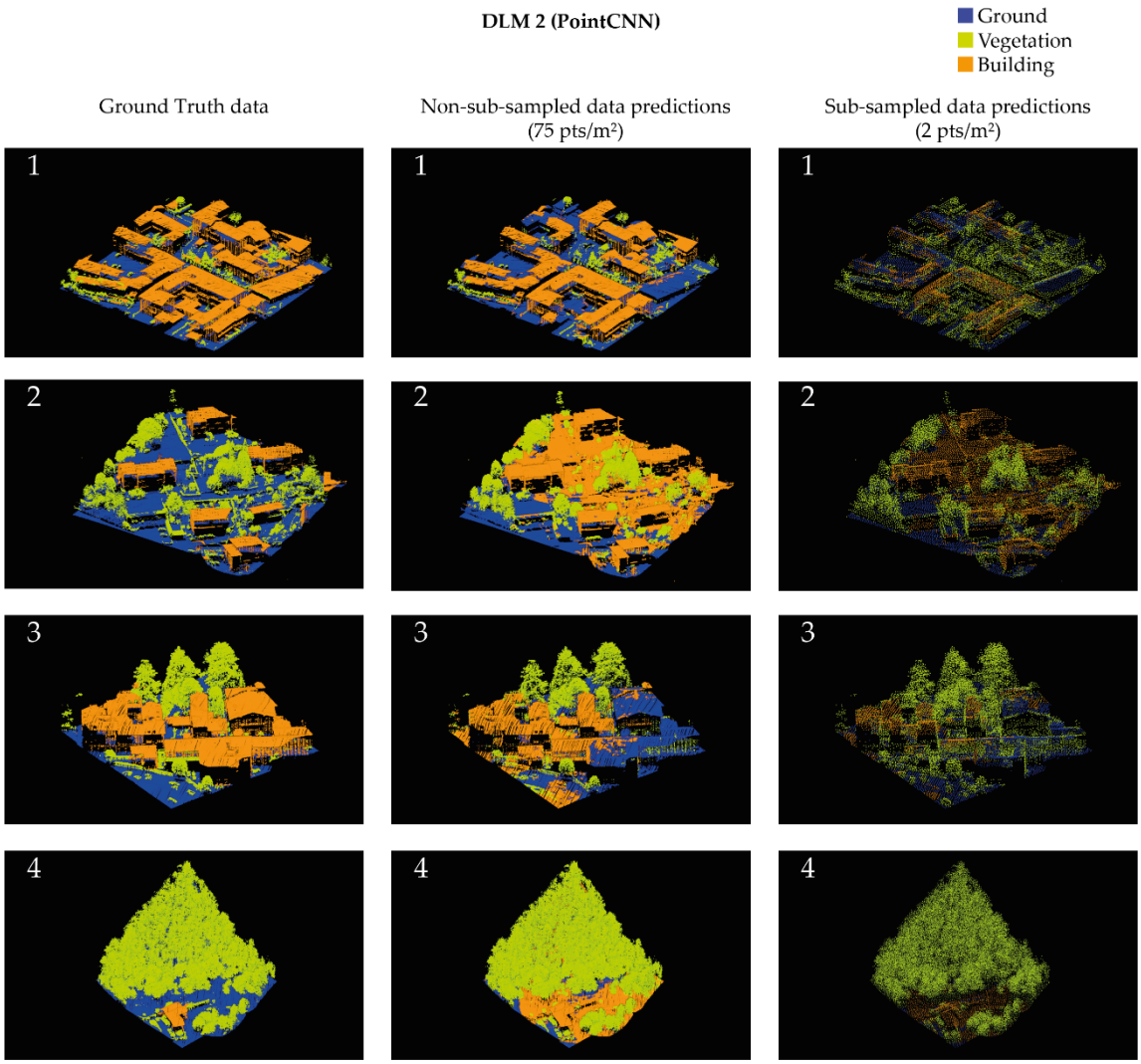

Figure 57. Prediction results of Model 2 on 4 test datasets with PointCNN architecture – credits (Cappellazzo et al., 2024a).

Table 24. Accuracy metric assessment of the trained Model 2 with the PointCNN architecture, applied to four test areas. The metrics have been analyzed by comparing the adopted strategy for both original resolution and sub-sampled data.

		Original resolution data				Sub-sampled data			
		Accuracy	Precision	Recall	F1 score	Accuracy	Precision	Recall	F1 score
1	Ground		0.73	0.98	0.84		0.69	0.60	0.64
	High Vegetation		0.55	0.52	0.54		0.19	0.90	0.32
	Building		0.98	0.75	0.85		0.97	0.33	0.49
	Macro average	0.83	0.75	0.75	0.74	0.48	0.62	0.61	0.48
2	Ground		0.91	0.35	0.51		0.96	0.31	0.47
	High Vegetation		0.96	0.60	0.74		0.79	0.86	0.82
	Building		0.25	0.99	0.40		0.32	0.85	0.46
	Macro average	0.51	0.71	0.65	0.55	0.62	0.69	0.67	0.58
3	Ground		0.50	0.65	0.56		0.64	0.57	0.60
	High Vegetation		0.86	0.86	0.86		0.53	0.97	0.69
	Building		0.67	0.54	0.60		0.85	0.26	0.39
	Macro average	0.65	0.68	0.68	0.67	0.59	0.67	0.60	0.56
4	Ground		0.99	0.23	0.37		0.99	0.04	0.07
	High Vegetation		0.85	0.98	0.91		0.84	1.00	0.91
	Building		0.09	1.00	0.17		0.18	0.84	0.29
	Macro average	0.68	0.64	0.73	0.49	0.81	0.67	0.63	0.43

4.2.2 Sardinia Defensive Landscapes

Semantic segmentation predictive models

As described in Section 3.3.2, a DL predictive model (DLM 3) for the semantic segmentation of low-scale ALS point clouds has been trained, and it was completed in 46 hours after 38 epochs. The model was trained and validated with reference data pertaining to Area 1 (Figure 43). As shown in Table 25, the model achieved excellent results in terms of Accuracy and Precision, while slightly lower and improvable results have been observed for the Recall and F1 score metrics.

Table 25. DLM 3 predictive model validation results. The metrics of the table have been calculated using the validation data from the training dataset (Area 1).

Class	Accuracy	Precision	Recall	F1 score
0 - Unclassified	0.95	0.78	0.29	0.42
2 - Ground	0.92	0.93	0.94	0.94
5 - High Vegetation	0.97	0.81	0.90	0.85
6 - Building	0.94	0.78	0.89	0.84
9 - Water	0.99	0.71	0.64	0.67
Macro Average	0.95	0.80	0.73	0.74

The lower overall metrics results are attributable to classes 0 and 9, which are under-represented in the training dataset. In fact, the segmentation results on the validation dataset for the most represented objects (ground, high vegetation, and building) are slightly better than those for the remaining classes, as observed in Figure 58. Nevertheless, despite the overall good results, some limitations can be observed. These include the over-prediction of the building class in flat ground areas and its under-prediction on oblique or occluded surfaces. A general misprediction of small wall objects pertaining to building class interests the unclassified points, while small Mediterranean evergreen shrubs, which are difficult to distinguish from the ground, are often under-predicted. Additionally, the water class also shows instances of under-

prediction. In fact, the low values pertaining to the water are imputable to the low representativity of the class in the training dataset.

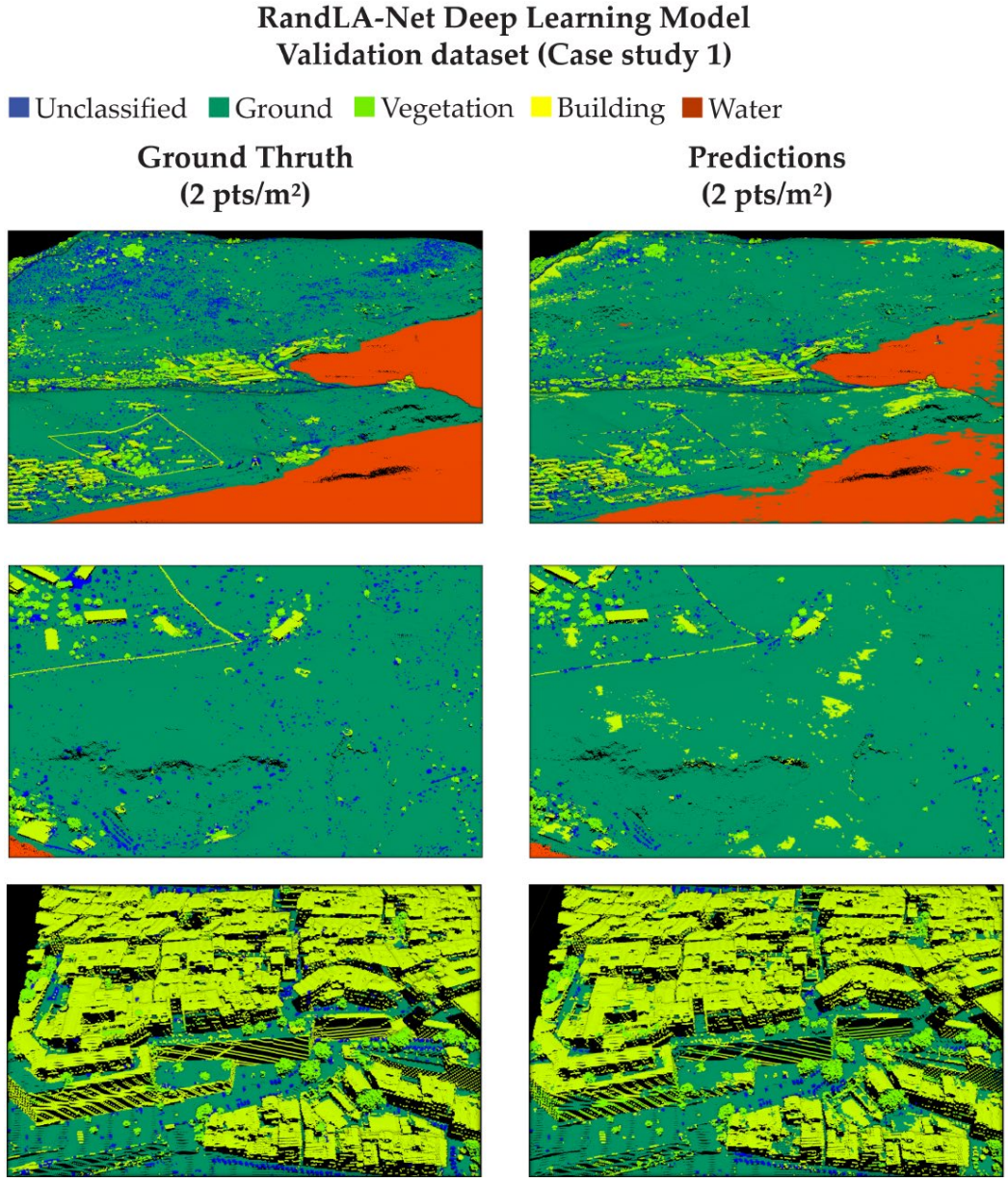

Figure 58. Predictive model training results. The model performance is evaluated using the validation data from the Training dataset of Area 1 (Cagliari) – credits (Cappellazzo et al., 2024b).

Since the focus of the application of DL semantic segmentation methodologies is on historical defensive contexts, it should be underlined that specific artifact recognition is considered a challenging issue. In fact, the accuracy evaluation has indicated that while the model is highly precise, there is a trade-off in its ability to classify correctly relevant structures, particularly those that are partially eroded or

obscured. In fact, the identification of fortification walls and bastions represents a true limit where there is a lack of reference training data.

In order to analyze accurately the model behavior, four supplementary data blocks from Case Study 2 (Figure 45) were selected to test the DLM performances. The aim was to understand the model generalization capabilities with higher-scale ALS point cloud datasets, describing areas with different urban and territorial morphology.

The results of applying the semantic segmentation DLM on the test dataset areas (5,6,7,8) have been analyzed and summarized in Table 26 (following page). The metrics statistics successfully demonstrate the generalization capabilities of the predictive model, although further improvements are still to be estimated.

Moreover, Figure 59 confirms, from a visual perspective, the excellent generalization capability of the trained model in classifying higher-resolution datasets from Area 2 (10 pts/m^2). In the test areas, cases of under-prediction and over-prediction are observable, similar to the validation dataset areas.

In this scenario, Deep Learning approaches for point cloud semantic segmentation are thus confirmed as a valuable tool for the Heritage context, despite the accurate identification issue of specific elements (e.g., bastions) should be adequately addressed for future perspectives.

Table 26. Predictive model test results. The metrics of the table have been calculated using the test data 5, 6, 7, and 8 in Area 2 (Alghero).

Area	Class	Accuracy	Precision	Recall	F1-Score
5	0 - Unclassified	0.99	0.71	0.58	0.64
	2 - Ground	0.84	0.80	0.93	0.86
	5 - High Vegetation	0.98	0.57	0.66	0.61
	6 - Building	0.89	0.89	0.81	0.85
	9 - Water	0.95	0.97	0.21	0.35
	Macro Average	0.93	0.79	0.64	0.66
6	0 - Unclassified	0.97	0.78	0.53	0.64
	2 - Ground	0.94	0.87	1.00	0.93
	5 - High Vegetation	0.97	0.86	0.80	0.83
	6 - Building	0.89	0.92	0.83	0.87
	Macro Average	0.96	0.86	0.79	0.82
7	0 - Unclassified	0.99	0.98	0.30	0.46
	2 - Ground	0.99	0.94	1.00	0.97
	5 - High Vegetation	1.00	0.87	0.92	0.89
	6 - Building	0.98	0.99	0.99	0.99
	Macro Average	0.99	0.95	0.80	0.83
8	0 - Unclassified	0.99	0.97	0.58	0.73
	2 - Ground	0.96	0.91	1.00	0.96
	5 - High Vegetation	0.99	0.99	0.98	0.99
	6 - Building	0.96	0.95	0.83	0.89
	Macro Average	0.97	0.96	0.85	0.89

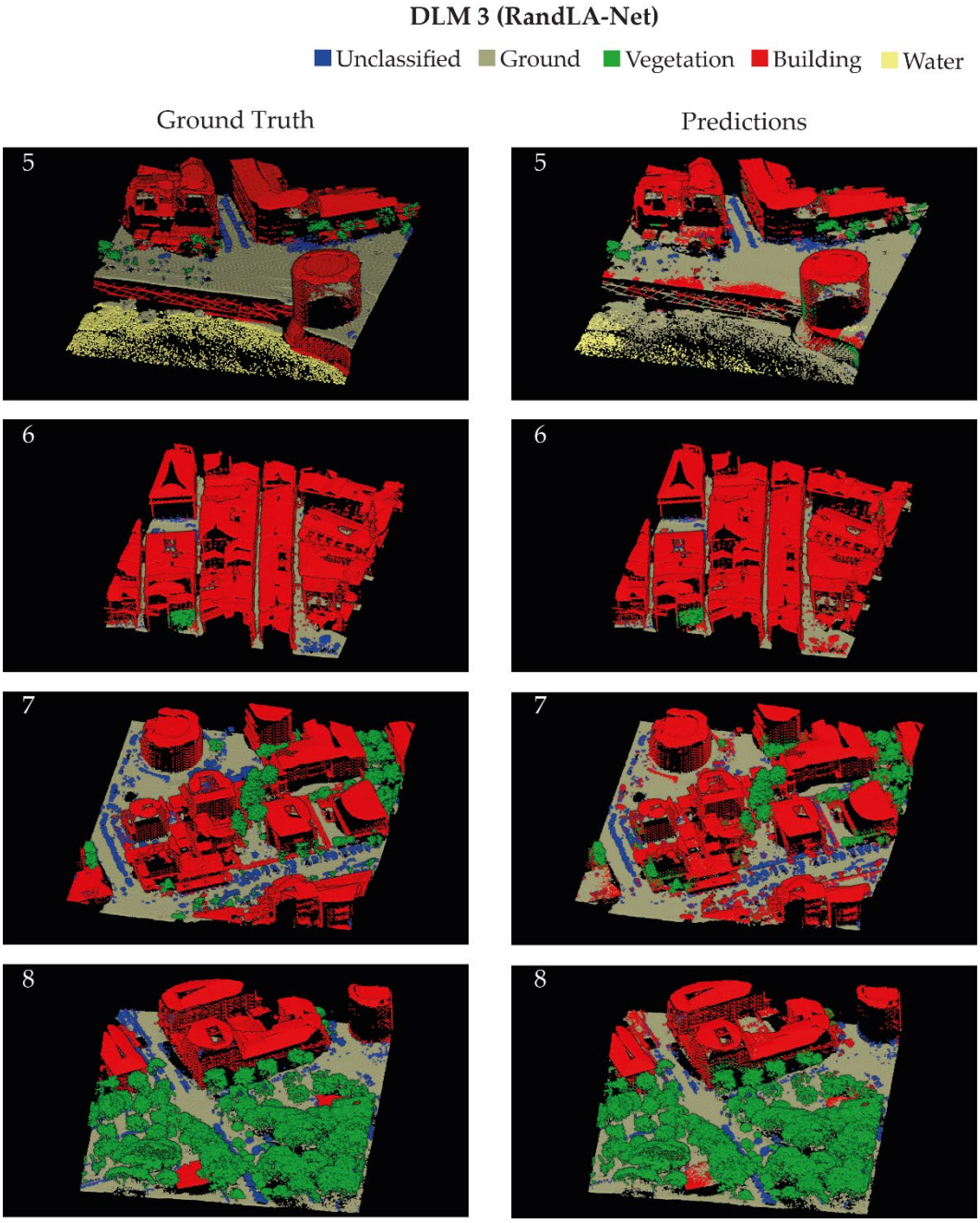

Figure 59. Predictive model testing results. The model performance is evaluated using the test datasets 5, 6, 7, and 8 of Area 2 (Alghero) – credits (Cappellazzo et al., 2024b).

Deep neural detector for preliminary defensive artifact mapping

Concerning the object detection approach of historical defense architectures, the semi-automatic labeling task effectiveness has been demonstrated, where 66 3D bounding boxes have been generated (Figure 60).

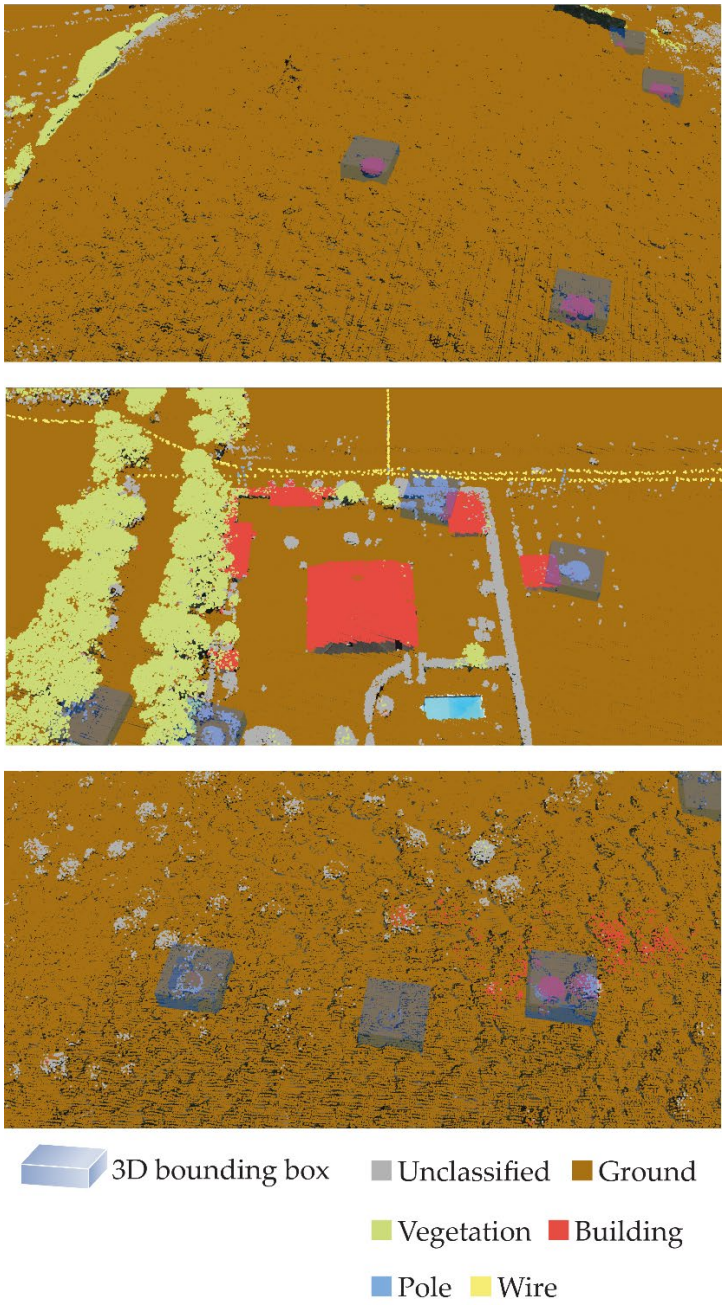

Figure 60. Bounding box generation processing for reference data generation. The aim is to apply 3D Deep Learning for defensive heritage mapping. In this case, the three areas are focused on bunker class objects – credits (Cappellazzo et al., 2024b).

The object detection model has been trained by employing an entropy loss function for training and validation datasets (10) (Good, 1952):

$$\text{Loss} = -\frac{1}{N}\sum_{i}^{N}(y_{true} \cdot \log(p_i) + (1 - y_{true})\log(1 - p_i)) \quad (10)$$

where N is the total number of observations, y_{true} is the binary indicator for the correctness prediction for observation i, and p_i is the probability of the observation being in the correct class. Since a 3D detector should be evaluated by taking into consideration classification and localization accuracy, the performance of the model has been analyzed with the mean Average Precision (mAP) metric, as described in (Wu et al., 2021).

However, from the training graph in Figure 61, it can be observed that the calculation of the validation loss function was unconcluded throughout the batch processing, demonstrating the difficulties of the model in effectively learning the given task. Moreover, the localization and classification accuracies given by the mAP metric were not applicable. The experimental result was yet predictable because the number of bunker architectures—and thus of reference training data—was not sufficient to train and validate any object-detection model.

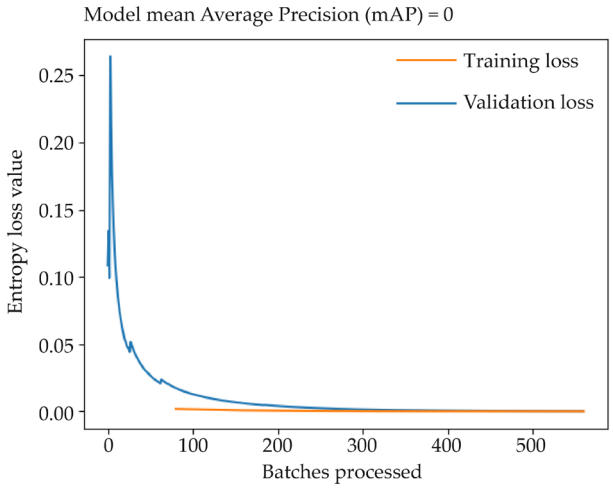

Figure 61. Model validation graph, showing training and validation logarithmic loss functions during epochs. While the training loss function decreases, validation loss is constantly flat – credits (Cappellazzo et al., 2024b).

4.3 Machine Learning Classifiers for anthropogenic shapes classification

In order to assess the most effective classification technique for detecting the anthropic shapes of the terrain, the MLCs outcomes have been analyzed for each prepared geomorphological layer. According to the error-test pipeline, this step was crucial to assess the suitability of the GMLs and to determine which one was the most effective as primary data for classification. Moreover, another significant aim was to evaluate the effectiveness of combining various geomorphological analyses as an alternative to the use of individual bands.

4.3.1 Single geomorphological layers (GMLs) evaluation

An initial assessment of the evaluation metrics has been carried out for the RF classifier in MLC-1b from Case Study 1, and the results are presented in Table 27, where it is possible to observe that Hillshade GML is the best-performing one yet the only one reaching sufficient metrics (all the observed values are approximately ≥50%). As mentioned in the methodology section, the RF algorithm trained from the approach in MLC-1a failed to adequately segment the processed data according to the considered classes. This may be attributed to the lower number of labels manually generated by the human operator according to the labeling strategy followed in MLC-1a (Table 18).

The reduced number of training samples was thus insufficient to predict the correct classes. In fact, following this strategy, all the pixels have been assigned to a single class (terrain) without producing appreciable results regarding the classification of the trails class. In this case, the second labeling strategy was the only one that – balancing the number and the area of samples – enabled us to apply the RF classification method successfully. However, as observable from the comparison between the evaluation metrics reported in Table 27 and Table 28, the

SVM classifier outperformed the RF approach. In fact, SVM results are characterized by an average F1 score higher (+15%) than the one achieved with RF. In particular, while Recall performance is comparable, an increase in overall Accuracy (+19%) and Precision (+13%) has been observed.

Table 27. RF classifier: accuracy metric assessment for each GLM, tested on the training area MLC-1b (Case Study 1).

Area	Analysis	Class	Accuracy	Precision	Recall	F1 score
1b	Aspect	Terrain	0.75	0.98	0.75	0.85
		Anthropogenic forms	0.75	0.12	0.75	0.21
	Flow Direction	Terrain	0.95	0.97	0.97	0.97
		Anthropogenic forms	0.95	0.41	0.40	0.40
	Hillshade	Terrain	0.97	0.98	0.99	0.98
		Anthropogenic forms	0.97	0.65	0.48	0.55
	Magnetic North	Terrain	0.80	0.98	0.80	0.88
		Anthropogenic forms	0.80	0.14	0.71	0.23
	Roughness	Terrain	0.56	0.97	0.56	0.71
		Anthropogenic forms	0.56	0.06	0.64	0.11
	Slope	Terrain	0.58	0.98	0.57	0.72
		Anthropogenic forms	0.58	0.07	0.71	0.13

Table 28. SVM classifier: accuracy metric assessment for each GLM, tested on the training areas MLC-1a and MLC-1b (Case Study 1). Continues on the following page.

Analysis	Area	Class	Accuracy	Precision	Recall	F1 score
Aspect	1a	Terrain	0.90	0.98	0.90	0.92
		Anthropogenic forms	0.90	0.27	0.59	0.37
	1b	Terrain	0.97	0.98	0.99	0.98
		Anthropogenic forms	0.97	0.65	0.48	0.55
Flow Direction	1a	Terrain	0.92	0.97	0.95	0.96
		Anthropogenic forms	0.92	0.30	0.44	0.36
	1b	Terrain	0.97	0.98	0.99	0.99
		Anthropogenic forms	0.97	0.74	0.56	0.64
Hillshade	1a	Terrain	0.94	0.97	0.97	0.97
		Anthropogenic forms	0.94	0.35	0.33	0.34
	1b	Terrain	0.97	0.98	0.99	0.98
		Anthropogenic forms	0.97	0.70	0.49	0.58
Magnetic North	1a	Terrain	0.89	0.97	0.92	0.94
		Anthropogenic forms	0.89	0.20	0.39	0.26
	1b	Terrain	0.95	0.97	0.98	0.98
		Anthropogenic forms	0.95	0.46	0.45	0.46
Roughness	1a	Terrain	0.91	0.95	0.95	0.95
		Anthropogenic forms	0.91	0.10	0.10	0.10
	1b	Terrain	0.95	0.96	0.99	0.97
		Anthropogenic forms	0.95	0.30	0.14	0.19
Slope	1a	Terrain	0.91	0.97	0.94	0.95
		Anthropogenic forms	0.91	0.27	0.46	0.34
	1b	Terrain	0.93	0.97	0.96	0.96
		Anthropogenic forms	0.93	0.23	0.28	0.25

Since the superior effectiveness of the SVM over the RF classifier has been confirmed according to the approach adopted in MLC-1b, further analyses were addressed. In particular, the performance of the two labeling strategies – applied to the SVM method – have been compared. As expected, the training dataset preparation strategy adopted for Area 2 slightly improves the classification results in terms of performance. In this case, an improvement has been quantified in terms of Accuracy (+5%), Precision (+14%), Recall (+3%), and F1 score (+9%). Contrarily to the RF classifier, from the SVM results, it can be noted that several GMLs reached sufficient metrics and, therefore, considered suitable for this kind of classification, but again, only following the MLC-1b labeling strategy (Aspect, Flow Direction, Hillshade).

4.3.2 Composite geomorphologic raster evaluation

Similarly to the analyses carried out in the previous section, the evaluation metrics have also been compared to evaluate the employed classifiers and, specifically, which composite raster performs better for the aimed classification task. Considering the evaluation metrics reported in Table 29 and Table 30, it is evident that the SVM classification results outperformed again the RF results. In fact, while the Recall results are comparable, a significant improvement in terms of Accuracy (+16%), Precision (+17%), and F1 score (+19%) has been observed following the approach adopted in MLC-1b (Figure 49). From the evaluation metrics reported in Table 29 – and from a visual inspection, as observable in Figure 62 – it is evident that the RF classifier applied on the composite raster datasets has been slightly less effective than SVM for detecting the pixels belonging to the anthropogenic shapes class.

Table 29. Accuracy metric assessment of RF classifier executed on each composite geomorphological raster.

Area	Analysis	Class	Accuracy	Precision	Recall	F1 score
1b	Composite a	Terrain	0.87	0.98	0.87	0.93
		Anthropogenic forms	0.87	0.20	0.67	0.31
	Composite b	Terrain	0.72	0.99	0.72	0.83
		Anthropogenic forms	0.72	0.12	0.83	0.21
	Composite c	Terrain	0.85	0.99	0.85	0.91
		Anthropogenic forms	0.85	0.19	0.76	0.31
	Composite d	Terrain	0.68	0.99	0.67	0.80
		Anthropogenic forms	0.68	0.11	0.85	0.19
	Composite e	Terrain	0.83	0.99	0.84	0.91
		Anthropogenic forms	0.83	0.18	0.78	0.29

Table 30. Accuracy metric assessment of SVM classifier executed on each composite geomorphological raster.

Analysis	Area	Class	Accuracy	Precision	Recall	F1 score
Composite a	1a	Terrain	0.85	0.98	0.86	0.92
		Anthropogenic forms	0.85	0.21	0.74	0.32
	1b	Terrain	0.95	0.98	0.96	0.97
		Anthropogenic forms	0.95	0.44	0.61	0.51
Composite b	1a	Terrain	0.90	0.98	0.91	0.94
		Anthropogenic forms	0.90	0.28	0.68	0.39
	1b	Terrain	0.95	0.98	0.96	0.97
		Anthropogenic forms	0.95	0.45	0.65	0.53
Composite c	1a	Terrain	0.88	0.98	0.89	0.94
		Anthropogenic forms	0.88	0.25	0.69	0.36
	1b	Terrain	0.95	0.98	0.97	0.97
		Anthropogenic forms	0.95	0.46	0.61	0.52
Composite d	1a	Terrain	0.93	0.98	0.95	0.96
		Anthropogenic forms	0.93	0.34	0.54	0.42
	1b	Terrain	0.96	0.98	0.98	0.98
		Anthropogenic forms	0.96	0.58	0.60	0.59
Composite e	1a	Terrain	0.92	0.98	0.93	0.95
		Anthropogenic forms	0.92	0.30	0.55	0.39
	1b	Terrain	0.96	0.98	0.98	0.98
		Anthropogenic forms	0.96	0.58	0.62	0.60

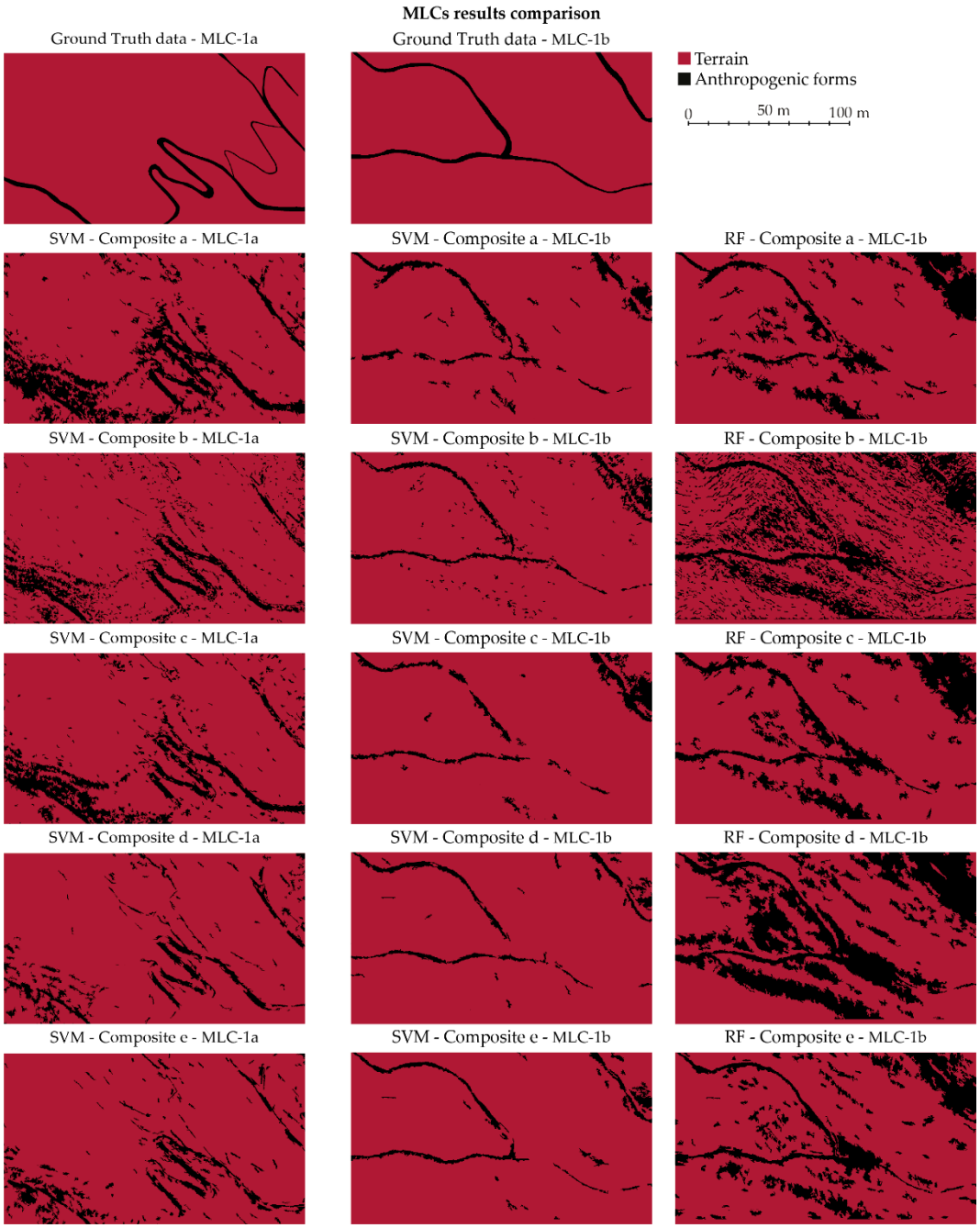

Figure 62. Qualitative comparison of the MLCs on composite geomorphological raster – credits (Cappellazzo et al., 2024a).

Specifically, RF results in the classification of composite images achieved approximately comparable results, but overall insufficient, and lower than the single layer classification (see Hillshade results in Table 27). In particular, the Anthropogenic forms class is generally over-predicted, resulting in a high level of noise after the classification task.

Regarding the SVM approach, the labeling used in MLC-1a led to results characterized by higher metrics. This is further supported by the visual inspection of Figure 62, where it is evident that among the two approaches, this strategy produced predictions with the lowest level of noise. However, a slight under-prediction can be observed, as indicated by the relatively low Precision value, which is always the lowest metric across all the other values. Generally, the data that led to the best results adopting the SVM approach is the Composite e (Hillshade, Hillshade, Aspect). This result is consistent with what was observed while analyzing the classification task on the individual GMLs, where the bands that enabled the achievement of better generalization were Hillshade and Aspect.

Contrarily, this does not apply regarding the RF approach, as the classification carried out on the Hillshade GML produced only adequate results, effectively outperforming the strategy based on the use of composite images.

4.3.3 Trained machine learning classification models validation

Considering what has been analyzed so far and the achieved results, as illustrated in the above section, two final models have been trained:

- Model RF: Random Forest algorithm. This model has been applied to Hillshade GML
- Model SVM: Support Vector Machines algorithm. This model has been applied to Composite e raster (Hillshade, Hillshade, Aspect).

This section aimed to evaluate the effectiveness of the MLCs trained models in three test areas (A, B, C) (Figure 63) that differ from the area where the training labels were extracted. Moreover, in each area, manual labels have been generated by a human operator to provide ground truth data for assessing the classification and

calculating the evaluation metrics. Subsequently, the input data have been classified using both SVM and RF classification models.

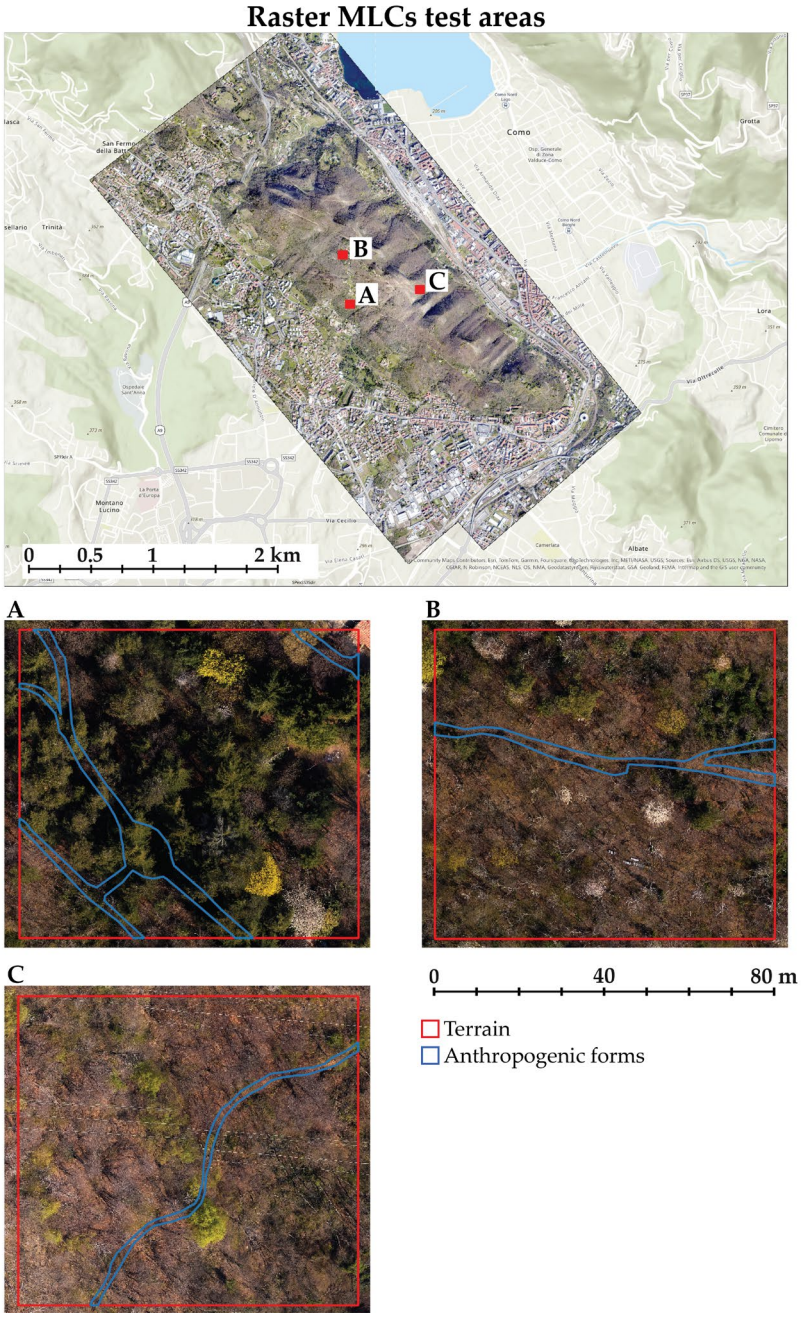

Figure 63. Map of the test areas (A, B, C) location. The presence of heterogeneous features and morphology characterizes the considered areas – credits (Cappellazzo et al., 2024a).

From Figure 64 and the analysis of the evaluation metrics (Table 31), it is evident that the model exhibits a good generalization capability, as the results are coherent with those achieved in the area where the training data were extracted.

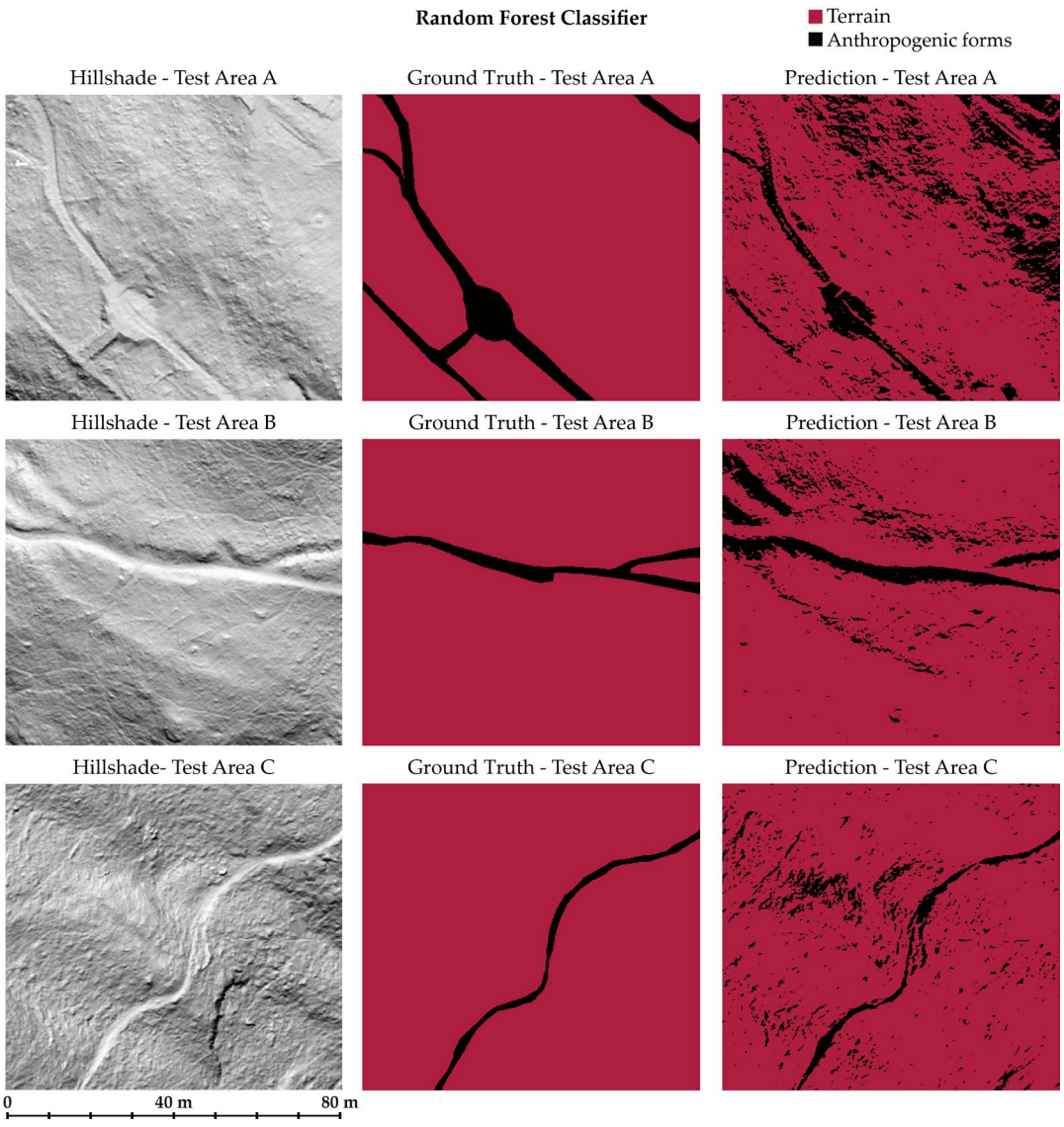

Figure 64. Prediction results of trained Random Forest model for Composite e raster on three test areas – credits (Cappellazzo et al., 2024a).

Table 31. Accuracy metric assessment of the RF classification model executed on three test areas. The low Precision indicates a tendency of the model to mispredict the Trails class and a generally noisy outcome. However, the main anthropogenic elements (Trails) have been adequately predicted.

Analysis	Area	Class	Accuracy	Precision	Recall	F1 score
Hillshade	A	Terrain	0.82	0.96	0.84	0.90
		Anthropogenic forms	0.82	0.26	0.59	0.36
	B	Terrain	0.91	0.99	0.92	0.95
		Anthropogenic forms	0.91	0.27	0.76	0.40
	C	Terrain	0.93	0.99	0.93	0.96
		Anthropogenic forms	0.93	0.21	0.74	0.33

Concerning the model's performance derived from the SVM model, even in this case, the results are comparable to the predictions achieved in the training area (Table 32). Figure 65 reports the classified images related to the three considered areas and, despite a slight under-prediction (in Test Area A) and relatively high nose level – especially in Test Area C, where the interpretation of the anthropogenic forms is more challenging due to the high steepness and roughness of the terrain – the Trails have been detected with an adequate level of accuracy.

Table 32. Accuracy metric assessment of the SVM classification model executed on three test areas

Analysis	Area	Class	Accuracy	Precision	Recall	F1 score
Composite e	A	Terrain	0.91	0.93	0.97	0.95
		Anthropogenic forms	0.91	0.40	0.19	0.32
	B	Terrain	0.96	0.99	0.97	0.98
		Anthropogenic forms	0.96	0.47	0.68	0.55
	C	Terrain	0.90	0.99	0.90	0.95
		Anthropogenic forms	0.90	0.15	0.68	0.24

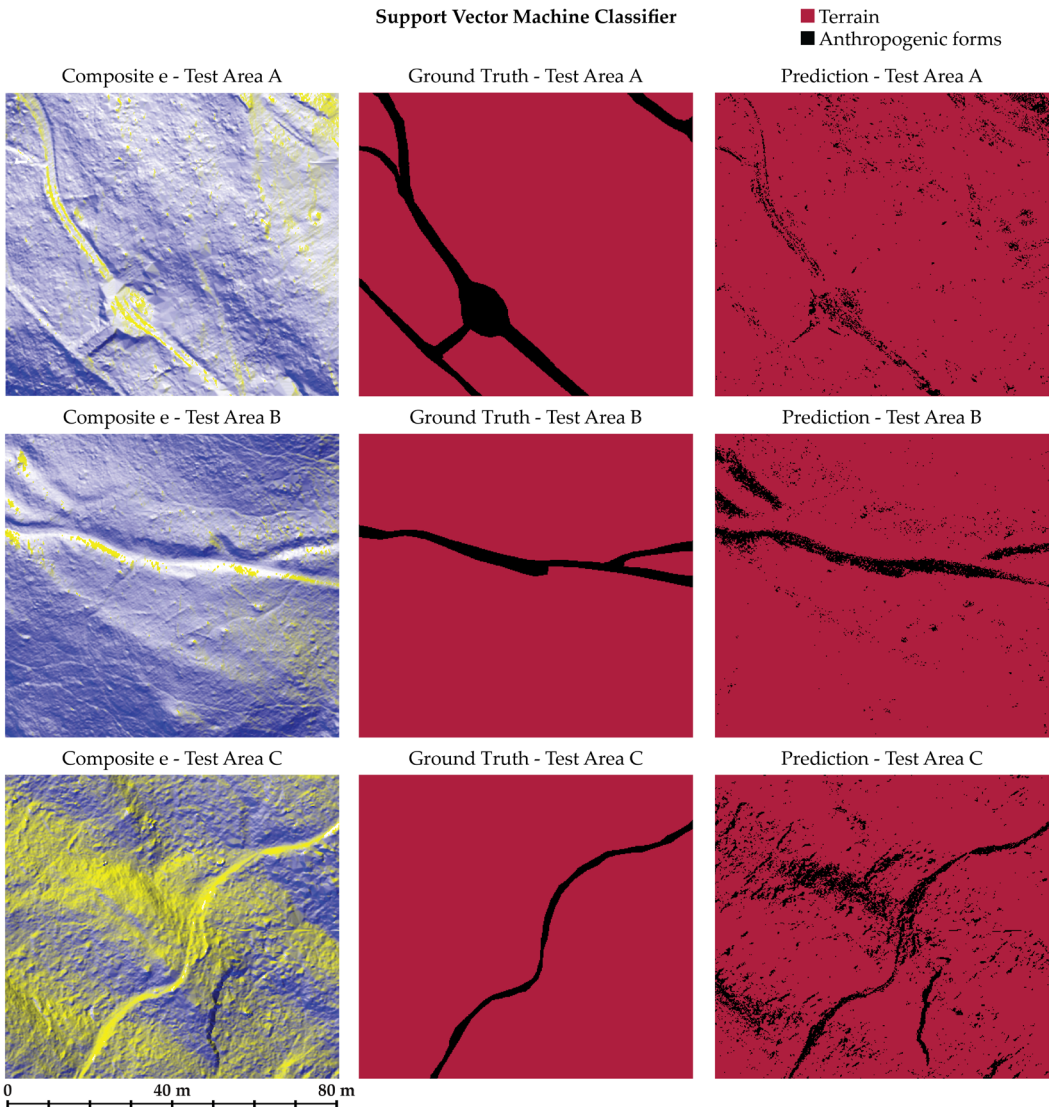

Figure 65. Prediction results of trained Support Vector Machine model for Composite e raster on the three test areas – credits (Cappellazzo et al., 2024a).

Throughout the pipeline observed previously, particularly regarding the two steps preceding the training of Models SVM/RF, the evaluation metrics underlined a general superiority of the SVM approach over the RF method. While evaluating the performance of the Trail class in each step of the pipeline, it can be noted from Table 33 that all the observed F1 score values are generally superior in the case of the SVM classification.

Table 33. MLC models comparison. Despite the SVM method outperforming RF in the first two steps, the results of the final predictive models are substantially comparable.

	F1 score Average		F1 score Max		F1 score Min	
	SVM	RF	SVM	RF	SVM	RF
Single geomorphologic analyses*	0.45	0.27	0.64	0.55	0.19	0.11
Geomorphologic composite*	0.54	0.26	0.59	0.31	0.51	0.19
Classification Models**	0.37	0.36	0.55	0.40	0.24	0.33

* F1 score comparisons are calculated only from MLCs results from the Trail class

** The classification models are trained using the best resultant raster for each classifier. SVM: Composite e; RF: Shaded visualization DTM.

Chapter 5

Conclusions and future perspectives

Considering the discussion that has emerged from the results of the methodologies presented in the previous section, it should be underlined that the integration of various proposed methodologies for CH knowledge and preservation strategies provided valuable lessons and opportunities. The doctoral research underlines the importance of combining diverse approaches, as well as critically evaluating and analyzing the method from a multi-scale perspective. In fact, the resulting insights pertaining to automating data structuring significantly contribute to advancements for automation in RS data analysis and structuring and thus support CH site conservation. Moreover, the topic of semantic classification and detection discussed in the thesis also addressed the topic of user-oriented approaches, demonstrating how graphical user interface software could represent a valuable solution for heritage domain experts.

The Conclusion and future perspective chapter thus tries to summarize the challenges and issues that this doctoral research aimed to overcome by specifically analyzing four crucial different topics.

- The first topic is related to 3D primary data employment, where the suitability of full-waveform high and low-scale LiDAR data for semantic segmentation and DTM generation is evaluated.
- The second topic, which is also linked to the primary data evaluation, provides an overview and future perspectives for the integrated unsupervised and supervised DL methodologies for ALS data macro-classification.
- The third topic focuses on the outcomes and challenges in the application of ML OBIA methodologies, which have been used for the classification and, thus, mapping of anthropogenic landforms through DTM analysis.
- The fourth topic considers some critical concerns about the issues that have been encountered in the LiDAR object-detection approach are presented, focusing on possible future development strategies for this research.

Finally, an overall consideration sub-section is necessary to summarize the main advancements and shortcomings of this doctoral thesis.

5.1 Primary data evaluation

Regarding airborne LiDAR technology, it should be clear that previous research works have underlined the suitability of full-waveform LiDAR sensors for archaeological, heritage investigations, and semantic classification (Mallet et al., 2011; Mazzacca et al., 2022). Specifically, this doctoral research demonstrates how airborne LiDAR represents the most suitable technology to provide a better description of the terrain morphology in the analyzed areas. In fact, while passive image-based approaches are traditionally cost-effective for environmental surveys,

they are limited in capturing areas with dense vegetation, thus preventing the digital reconstruction of an accurate Digital Terrain Model. In fact, using a full waveform ALS solution enables the penetration of the sparse vegetation and, consequently, is more suitable in areas similar to the Spina Verde. However, it should be underlined that the high costs of this type of sensor represent a significant issue when using this technology in the framework of landscape heritage documentation. Nevertheless, as introduced, this limitation can be overcome by the recent development of low-cost UAS-based LiDAR technologies. These systems have been increasingly used in recent years and can guarantee greater accessibility to this type of sensor, ensuring sustainable data acquisition for geomorphological analysis purposes. However, the penetration capabilities of these more compact solutions are still being evaluated and validated in the literature (Kalacska et al., 2021; Wieser et al., 2016).

While from Case Study 1 it has been demonstrated the suitability of full-waveform LiDAR in heritage contexts, and despite recent advancements in remote sensing technologies (Kölle et al., 2021), lower-density ALS data such as point clouds from Case Study 2 has proven to be still effective for landscape heritage monitoring. In fact, although those have been acquired for cartographic production purposes, the application of DL methodologies for semantic segmentation enhanced the automation for data structuring and accurate DHM generation.

5.2 Point cloud data structuring methodologies for extended Landscape contexts

Starting from the outcomes of Case Study 1, the semantic enrichment of 3D unstructured data represents a valuable opportunity to enhance automation in the processes related to landscape and terrain morphology knowledge. Here, the results

obtained from the DL approach highlight how neural networks represent a valid and powerful alternative to the more consolidated geometric unsupervised filter. While the geometric-based filters are effective compared to the DL approach, they are strictly dependent on the topography and the vegetation of each considered site, as well as the urban and architectural morphology. Supervised methods, such as NN-based methods, can achieve higher levels of abstraction and, consequently, higher generalization capability, highlighting the significant perspectives associated with using this technology.

Moreover, the supervised methods allow less generalized semantic classes to be assigned, leading to more effective segmentation. However, it should be underlined that artificial NNs require significant structured data for the training. Thus, generating an adequately structured training dataset can be a time-consuming and demanding bottleneck. Recently, this issue has been addressed, and several solutions have been proposed to overcome the criticality represented by the generation of the training dataset, for example, generating an artificial training dataset (Patrucco & Setragno, 2023; Pellis et al., 2023), using open-source benchmark datasets (Kölle et al., 2021; Varney et al., 2020) or exploiting pre-trained NN for fine-tuning purposes (Han et al., 2021; Iman et al., 2023). Generally, this research direction represents one of the main perspectives for future application development.

Furthermore, the application of DL methodologies for Case Study 2 highlighted that integrating point clouds with satellite multispectral imagery data is a valuable strategy to overcome the lack of information provided by point clouds consisting only of coordinates. Still, it should be noted that enhancing the spatial and radiometric resolution of free, open-source satellite data (Drusch et al., 2012) remains a crucial issue where the necessity is to match the resolution of point cloud data. In this research framework, the employment of high-resolution satellite datasets can be considered, although the DL super-resolution approaches could

represent a more innovative and valid further implementation, e.g. (Collins et al., 2017).

Since this research aimed to test DL approaches for data structuring, it should be clear that NNs are widely explored but not yet fully established tools for heritage domain applications (Matrone et al., 2020a; S. Yang et al., 2023). Thus, in Case Study 2, the application of ML methodologies demonstrated how segmentation predictive DLMs are a valuable approach for semantic structuring of ALS point cloud data in a landscape heritage context. Moreover, despite the DLM being suitable for extended applications, the model has been tested in areas that were representative of the morphological and urban conformation of the case studies, assessing its accuracy in these heritage contexts. In fact, the topic of transferability represents a specific and considered issue that represents a concrete possibility of further development as well. Specifically, it is crucial to investigate the implementation of the most updated NNs in the semantic segmentation domain. Specifically, neural networks such as SPT (Robert et al., 2023) leveraging transformers architectures integration allow embedding segment-level descriptors extracted from 3D point clouds, aiming to achieve efficient and accurate 3D semantic segmentation. Moreover, since data structuring and labeling applications are strictly dependent on primary data, methodologies such as transfer learning and continuous learning are key insights to provide further advancements in the 3D semantic data structuring domain. This is especially crucial for the CH domain, where the lack of real-world data is not comparable to other application fields. In this sense, the generation of synthetic data could certainly represent promising further developments, at least considering the consistency of data. Still, the variability of reference data will surely represent the main issue in semantic structuring for built, archaeological, and landscape heritage domains.

Finally, starting from these considerations, the application of DL pipelines should also be addressed by including the generation of shared and consolidated

semantic ontologies by correlating point cloud geometries, as also suggested by (Colucci et al., 2021).

5.3 ML OBIA methodologies for DTM grid

Concerning the traditional ML approach for the classification of anthropogenic earthworks from the DTMs, instead of considering the raster-based classification approach and evaluating the performances of the two MLC algorithms, as expected (Maxwell et al., 2018), the methodology developed in this thesis addressed the overall superiority of the SVM classifier compared to the RF classifier. However, it is worth mentioning that both the employed MLCs represent an adequate approach for developing automation solutions for the classification aims.

Moreover, it is worth emphasizing that the recognition of anthropogenic forms characterized by a high level of granularity represents a challenging task not only for supervised or unsupervised methods but also for traditional manual classification operations performed by a domain expert image analyst. In the framework of this type of landscape and urban-scale analysis, when a classification and detection task is required, a significant imbalance between classes is not uncommon due to the granularity of the features, as in the case presented in this thesis. In this regard, it should be underlined that the effectiveness of unsupervised geometric filtering methods is not affected by class imbalance, contrary to what happens in supervised methods such as ML and DL. Balanced classes are preferable for supervised approaches to obtain optimal results (Vargas et al., 2018). However, an imbalanced distribution of class population can lead to difficulties in the interpretation of metrics, as for classes composed of a limited number of samples, a few incorrect predictions can heavily influence the values of evaluation metrics. In fact, despite relatively low metric values (≤ 60%), upon visually inspecting the classified images,

it is worth underlining that the classification models adequately detected and classified the anthropogenic forms in the raster datasets.

Moreover, a reflection is crucial in training data preparation to generate the minimum number of support vectors (Maxwell et al., 2018). Since the aim of the tested OBIA approach was to minimize operator manual activities, the proposed methodology could represent a significant contribution to advancements in enhancing automation for classification processes.

Finally, some considerations can also be addressed regarding the application of OBIA methodologies to DSMs raster, aiming at the classification of specific defensive heritage artifacts. In this sense, it can be said that this approach could also be transferred to built heritage object classification, but in this case, there is the necessity to enhance the time of human activity. Firstly, it is crucial to employ high-resolution DSM data (GSD>50 cm) that can overcome difficult disambiguation issues emerging from the classification of vertical structures. Subsequently, there is the necessity to produce more training samples while enhancing human involvement without training a transferable model. Thus, the preliminary test for object-detection methodologies has been addressed to overcome this sensitively crucial bottleneck.

5.4 NN detectors for LiDAR point clouds

Finally, concerning the preliminary tests addressed in Case Study 2 aiming at the automatic detection of defensive and military artifacts, some considerations can be made. Since it is crucial to establish a minimum threshold for data density and accuracy, several issues have been overcome when investigating point cloud object-detection approaches. In this research context, the employment of low-scale ALS point clouds from Area 1 in Case Study 2 (2 pts/m^2) has been declared not

compatible due to the difficulty of recognizing specific elements from point clouds. Moreover, due to the original defensive specific functions, most of these architectural objects are not easily detectable using spaceborne or airborne imagery products due to the designed camouflage characteristics. For this reason, further developments of a DL object detection methodology exploiting existing LiDAR point clouds are considered a crucial future challenge.

Yet, it has already been stated in Section 2.1.3 that most DL methodologies related to point cloud processing are mostly pertaining to robotics, autonomous driving, and indoor modeling (Guo et al., 2021). Therefore, in CH and landscape contexts, it is hard to address the most relevant issues of these approaches without significant adaptations.

Specifically, the number of annotations required for training NN detectors is considerably high, with a minimum of 70k bounding boxes (Huang et al., 2018), as shown in Section 3.3.2. The limitations of the results from the first training experiment conducted in Section 4.2.2 are particularly evident, as shown by the loss functions and the non-calculable metrics (Figure 50). Due to the number of available annotations (Table 3, see Chapter 3), this predictable result nonetheless represents a starting point for overcoming the challenges inherent in 3D detection. In this sense, preparing functions algorithms that allow the generation of synthetic point cloud data and 3D bounding box labels by copying and transforming (e.g., translation, rotation) the original data is considered to be a valuable future development. Therefore, it is thus crucial to integrate data augmentation strategies (Hahner et al., 2020; Zhu et al., 2024) that will be investigated in future research works.

5.5 Final considerations

Lastly, it is necessary to overview the doctoral thesis by providing some final evaluations regarding the advancements and shortcomings of this research.

Firstly, it should be underlined that already available data can assist heritage conservation professionals and researchers in the preliminary investigation stage by allowing the enhancement of the knowledge about sites before planning more substantial and high-resolution data acquisitions. In particular, the employment of open-access LiDAR low-scale data can help in the identification of areas of interest and the refinement of spatial analysis, thus improving the efficiency of conservation efforts. Yet, while leveraging available data from public administrations, it is crucial to underline that this approach has some limitations. In fact, effectively checking the availability and working with open-access datasets still requires theoretical and technical expertise, as incompleteness or uncertainties in the available data can cause difficulties in processing. In this sense, given the complexity of CH context and sites, access to specialized knowledge and high-quality reference data is necessary to maintain control of the automated processing.

In this framework, automation in spatial data processing has become a game-changer in cultural heritage studies, especially for the complexities of big and heterogeneous datasets. The present research explicitly focused on the integration of machine learning and deep learning methods, significantly accelerating the analysis and structuring of RS data. In fact, these tools improve the efficiency of documentation and, thus, conservation plans by reducing the time and labor for several tasks, including semantic classification, segmentation, and feature detection. A critical advantage of automated systems that this thesis has confirmed is their transferability among various heritage scenarios. Starting by applying standardized and consolidated methodologies, the lessons learned from one case study can be transferred to the other/s, fostering scalability in heritage data management.

However, the reliability of these automated approaches depends heavily on the availability of high-quality reference datasets. Training ML algorithms or deep NNs requires consistent and precise data inputs to ensure accuracy, especially given the unique complexities of the described cultural landscape contexts. In this framework, this doctoral research has extensively clarified that the numerosity of heritage artifacts or features and reference datasets is usually not compatible with DL methodologies. In this sense, the study identifies these challenges and highlights synthetic data generation as one of the possible solutions (Figure 66).

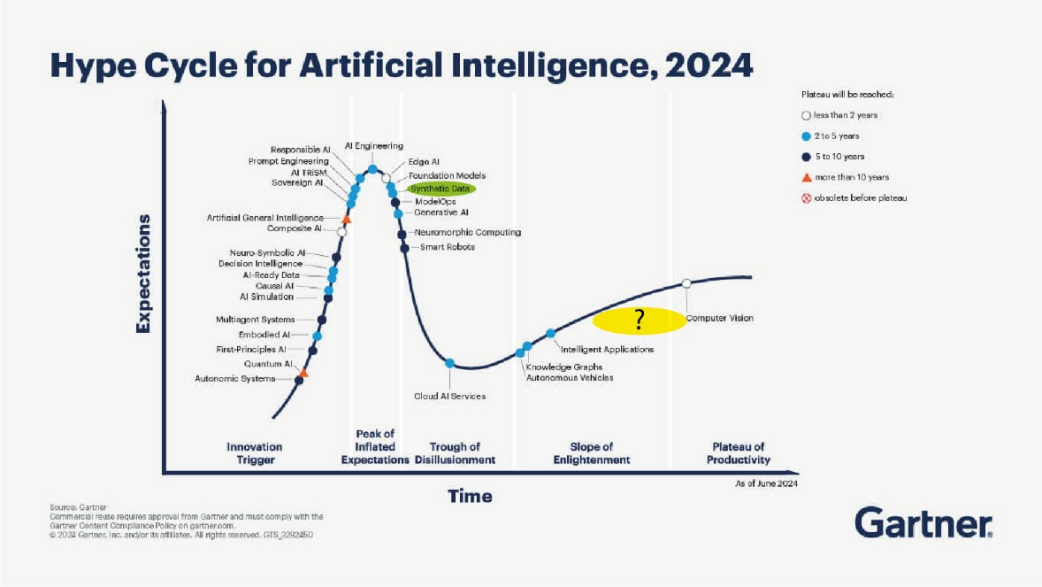

Figure 66. Gartner Hype Cycle graph for Artificial Intelligence (2024) – credits Gartner (www.gartner.com)

In fact, synthetic data could complement real data or even replace it, allowing generalization models that might be trained to complete and succeed in several time-consuming tasks.

Moreover, a key advantage of this study was the leveraging of GUI GIS software, which has simplified the management of both spatial data and predictive models within a single software environment, enabling non-expert users to access such tools. Specifically, user-friendly GIS and coding and library management platforms (e.g., ArcGIS Pro, MATLAB, Anaconda) embed GeoAI toolboxes, enabling both traditional machine learning and deep neural networks. These

platforms support complete workflow within a single software environment, also by the leverage of codes from open digital repositories such as GitHub. Nonetheless, theoretical and methodological knowledge is again crucial for the development of meaningful applications. In fact, such systems do not fully exploit the more actual and contemporary research advancements for remote sensing data, thus requiring deeper technical expertise.

Finally, it is clear that the integration of machine learning and remote-sensing data has great potential for improving management and conservation at heritage sites. However, as this research has pointed out, while GIS platforms with graphical interfaces make these tools more accessible, they also limit the ability to exploit state-of-the-art advances in the field. It is then still important that further developments continue in the perspective of optimizing both the theoretical frameworks and the practical methodologies. In fact, continuous research will surely allow these technologies to be coherently and effectively applied, supporting thus the conservation of cultural heritage.

References

Abate, N., Frisetti, A., Marazzi, F., Masini, N., & Lasaponara, R. (2021). Multitemporal–Multispectral UAS Surveys for Archaeological Research: The Case Study of San Vincenzo Al Volturno (Molise, Italy). Remote Sensing 2021, Vol. 13, Page 2719, 13(14), 2719. https://doi.org/10.3390/RS13142719

Adamopoulos, E., & Rinaudo, F. (2019). 3D INTERPRETATION and FUSION of MULTIDISCIPLINARY DATA for HERITAGE SCIENCE: A REVIEW. International Archives of the Photogrammetry, Remote Sensing and Spatial Information Sciences - ISPRS Archives, 42(2/W15), 17–24. https://doi.org/10.5194/isprs-archives-XLII-2-W15-17-2019

Adamopoulos, E., & Rinaudo, F. (2020). Enhancing image-based multiscale heritage recording with near-infrared data. ISPRS International Journal of Geo-Information, 9(4). https://doi.org/10.3390/ijgi9040269

Adedapo, S. M., & Zurqani, H. A. (2024). Evaluating the performance of various interpolation techniques on digital elevation models in highly dense forest vegetation environment. Ecological Informatics, 81, 102646. https://doi.org/10.1016/j.ecoinf.2024.102646

Agapiou, A., & Skarlatos, D. (2023). Geomatic Sensors for Heritage Documentation: A Meta-Analysis of the Scientific Literature. Heritage, 6(10), 6843–6861. https://doi.org/10.3390/heritage6100357

Aicardi, I., Chiabrando, F., Maria Lingua, A., & Noardo, F. (2018). Recent trends in cultural heritage 3D survey: The photogrammetric computer vision

approach. Journal of Cultural Heritage, 32, 257 – 266. https://doi.org/10.1016/j.culher.2017.11.006

Albrecht, C. M., Fisher, C., Freitag, M., Hamann, H. F., Pankanti, S., Pezzutti, F., & Rossi, F. (2020). Learning and Recognizing Archeological Features from LiDAR Data. Proceedings - 2019 IEEE International Conference on Big Data, Big Data 2019, 5630–5636. https://doi.org/10.1109/BigData47090.2019.9005548

Alifu, H., Vuillaume, J. F., Johnson, B. A., & Hirabayashi, Y. (2020). Machine-learning classification of debris-covered glaciers using a combination of Sentinel-1/-2 (SAR/optical), Landsat 8 (thermal), and digital elevation data. Geomorphology, 369, 107365. https://doi.org/10.1016/j.geomorph.2020.107365

Alivernini, S., & Roncoroni, F. (2016). Le tracce carraie nell'area dell'abitato protostorico della Spina Verde a Como. Vecchi e nuovi ritrovamenti e analisi interpretativa. In D. Daudry (Ed.), Numéro spécial consacré aux Actes du XIVe Colloque sur les Alpes dans l'Antiquité Evolène / Valais, Suisse 2-4 octobre 2015 (pp. 223–234). Société Valdôtaine de Préhistoire et d'Archéologie. http://www.archeosvapa.eu/news-posts/bepa-xxvii/

Argyrou, A., & Agapiou, A. (2022). A Review of Artificial Intelligence and Remote Sensing for Archaeological Research. Volume 14, Issue 23, 14(23). https://doi.org/10.3390/rs14236000

Ballouch, Z., Hajji, R., Poux, F., Kharroubi, A., & Billen, R. (2022). A Prior Level Fusion Approach for the Semantic Segmentation of 3D Point Clouds Using Deep Learning. Remote Sensing, 14(14), 3415. https://doi.org/10.3390/rs14143415

Barazzetti, L., Previtali, M., Cantini, L., & Oteri, A. M. (2023). Digital Recording of Historical Defensive Structures in Mountainous Areas Using Drones:

Considerations and Comparisons. Drones, 7(8).https://doi.org/10.3390/drones7080512

Barreca, G., Bruno, V., Dardanelli, G., Guglielmino, F., Lo Brutto, M., Mattia, M., Pipitone, C., & Rossi, M. (2020). An integrated geodetic and InSAR technique for the monitoring and detection of active faulting in southwestern Sicily. Annals of Geophysics, 63(1), SE101. https://doi.org/10.4401/ag-8327

Bassier, M., Vergauwen, M., & Van Genechten, B. (2017). Automated classification of Heritage buildings for as-built BIM using Machine Learning techniques. ISPRS Annals of the Photogrammetry, Remote Sensing and Spatial Information Sciences, 4(2W2), 25–30. https://doi.org/10.5194/isprs-annals-IV-2-W2-25-2017

Bassier, M., Vincke, S., Hernandez, R. de L., & Vergauwen, M. (2018). An overview of innovative heritage deliverables based on remote sensing techniques. Remote Sensing, 10(10), 1607. https://doi.org/10.3390/rs10101607

Batar, A. K., Watanabe, T., & Kumar, A. (2017). Assessment of land-use/land-cover change and forest fragmentation in the Garhwal Himalayan region of India. Environments - MDPI, 4(2), 1–16. https://doi.org/10.3390/environments4020034

Bendea, H., Boccardo, P., Dequal, S., Giulio Tonolo, F., Marenchino, D., & Piras, M. (2008). Low cost UAV for post-disaster assessment. International Archives of the Photogrammetry, Remote Sensing and Spatial Information Sciences - ISPRS Archives, 37, 1373–1380.

Bhushan, S., Shean, D., Alexandrov, O., & Henderson, S. (2021). Automated digital elevation model (DEM) generation from very-high-resolution Planet SkySat triplet stereo and video imagery. ISPRS Journal of Photogrammetry and Remote Sensing, 173, 151–165. https://doi.org/10.1016/j.isprsjprs.2020.12.012

Bitelli, G., Girelli, V. A., Remondino, F., & Vittuari, L. (2007). The potential of 3D techniques for cultural heritage object documentation. Videometrics IX, 6491, 64910S. https://doi.org/10.1117/12.705012

Boccardo, P., & Giulio Tonolo, F. (2012a). Haiti earthquake damage assessment: Review of the remote sensing role. International Archives of the Photogrammetry, Remote Sensing and Spatial Information Sciences - ISPRS Archives, 39, 529–532.

Boccardo, P., & Giulio Tonolo, F. (2012b). Remote-sensing techniques for natural disaster impact assessment. In Advances in Mapping from Remote Sensor Imagery: Techniques and Applications. https://doi.org/10.1201/b13770

Boehler W., Marbs A. (2004) 3D scanning and photogrammetry for heritage recording: a comparison. Proceedings of the 12th International Conference on Geoinformatics, University of Gavle, Sweden, 291–298.

Borgogno Mondino, E., Giulio Tonolo, F., Boccardo, P., & Bellone, T. (2004). DTMs generation from satellite stereo images: accuracy tests in mountain region. In M. Ehlers, F. Posa, H. J. Kaufmann, U. Michel, & G. De Carolis (Eds.), SPIE 5574 Remote Sensing for Environmental Monitoring, GIS Applications, and Geology IV (p. 341). Remote Sensing for Environmental Monitoring, GIS Applications, and Geology. https://doi.org/10.1117/12.565564

Bouhenaki, M. (2003). The interdependency of the tangible and intangible cultural heritage. 14th ICOMOS General Assembly and International Symposium: 'Place, Memory, Meaning: Preserving Intangible Values in Monuments and Sites', 27 – 31 Oct 2003, Victoria Falls, Zimbabwe. [Conference or Workshop Item]. https://openarchive.icomos.org/id/eprint/468/

Breiman, L. (2001). Random forests. Machine Learning, 45(1), 5–32. https://doi.org/10.1023/A:1010933404324/METRICS

Brovelli, M. A., Cina, A., Crespi, M., Lingua, A., Manzino, A., & Garretti, L. (2009). Ortoimmagini e modelli altimetrici a grande scala-Linee guida.

Brusco, D., Belcore, E., & Piras, M. (2023). Popillia Japonica Newman Detection Through Remote Sensing and AI Computer Vision. 2023 IEEE Conference on AgriFood Electronics, CAFE 2023 - Proceedings, 50–54. https://doi.org/10.1109/CAFE58535.2023.10291926

Bundzel, M., Jaščur, M., Kováč, M., Lieskovský, T., Sinčák, P., & Tkáčik, T. (2020). Semantic Segmentation of Airborne LiDAR Data in Maya Archaeology. Remote Sensing 2020, Vol. 12, Page 3685, 12(22), 3685. https://doi.org/10.3390/RS12223685

Caesar, H., Bankiti, V., Lang, A. H., Vora, S., Liong, V. E., Xu, Q., Krishnan, A., Pan, Y., Baldan, G., & Beijbom, O. (2019). nuScenes: A multimodal dataset for autonomous driving. Proceedings of the IEEE Computer Society Conference on Computer Vision and Pattern Recognition, 11618–11628. https://doi.org/10.1109/CVPR42600.2020.01164

Candiago, S., Remondino, F., De Giglio, M., Dubbini, M., & Gattelli, M. (2015). Evaluating multispectral images and vegetation indices for precision farming applications from UAV images. Remote Sensing, 7(4), 4026–4047. https://doi.org/10.3390/rs70404026

Cappellazzo, M. (2019). Layered landscape and Archeology of military heritage. Valorization strategies for Porto Conte Park territories (Alghero, SS) with GIS technologies and low-cost survey contributions. [Master's Degree]. Politecnico di Torino.

Cappellazzo, M., Baldo, M., Sammartano, G., & Spanò, A. (2023). Integrated airborne LiDAR-UAV methods for archaeological mapping in vegetation-covered areas. The International Archives of the Photogrammetry, Remote Sensing and

Spatial Information Sciences, XLVIII-M-2–2023(M-2–2023), 357–364. https://doi.org/10.5194/ISPRS-ARCHIVES-XLVIII-M-2-2023-357-2023

Cappellazzo, M., Patrucco, G., Sammartano, G., Baldo, M., & Spanò, A. (2024a). Semantic Mapping of Landscape Morphologies: Tuning ML/DL Classification Approaches for Airborne LiDAR Data. Remote Sensing 2024, Vol. 16, Page 3572, 16(19), 3572. https://doi.org/10.3390/RS16193572

Cappellazzo, M., Patrucco, G., & Spanò, A. (2024b). ML Approaches for the Study of Significant Heritage Contexts: An Application on Coastal Landscapes in Sardinia. Heritage 2024, Vol. 7, Pages 5521-5546, 7(10), 5521–5546. https://doi.org/10.3390/HERITAGE7100261

Carbonneau, P. E., & Dietrich, J. T. (2017). Cost-effective non-metric photogrammetry from consumer-grade sUAS: implications for direct georeferencing of structure from motion photogrammetry. Earth Surface Processes and Landforms, 42(3), 473–486. https://doi.org/10.1002/esp.4012

Catacchio, N. N., Metta, C., & Guerra, V. (2019). Le strutture produttive del sito di Pianvalle (Como). Fornaci, focolari e strutture in connessione a punti di fuoco. IpoTESI Di Preistoria, 12, 251–264. https://doi.org/10.6092/ISSN.1974-7985/10310

Chane, C. S., Mansouri, A., Marzani, F. S., & Boochs, F. (2013). Integration of 3D and multispectral data for cultural heritage applications: Survey and perspectives. Image and Vision Computing, 31(1), 91–102. https://doi.org/10.1016/j.imavis.2012.10.006

Charter for the Protection and Management of the Archaeological Heritage, ICOMOS, ICAHM (1990).

Chen, X., Ma, H., Wan, J., Li, B., & Xia, T. (2016). Multi-View 3D Object Detection Network for Autonomous Driving. Proceedings - 30th IEEE

Conference on Computer Vision and Pattern Recognition, CVPR 2017, 2017-January, 6526–6534. https://doi.org/10.1109/CVPR.2017.691

Chen, Z., Gao, B., & Devereux, B. (2017). State-of-the-Art: DTM Generation Using Airborne LIDAR Data. Sensors 2017, Vol. 17, Page 150, 17(1), 150. https://doi.org/10.3390/S17010150

Cherchi, G., Fiorino, D. R., Pais, M. R., & Pirisino, M. S. (2023). Bunker landscapes : from traces of a traumatic past to key elements in the citizen identity. Defensive Architecture of the Mediterranean : Vol. XV, 1195–1201. https://doi.org/10.12871/9788833397948150

Choay, F. (2012). Patrimonio e globalizzazione. Alinea.

Codice Dei Beni Culturali e Del Paesaggio, Pub. L. No. DL 42/2004, Gazzetta Ufficiale della Repubblica Italiana (2004).

Collins, C. B., Beck, J. M., Bridges, S. M., Rushing, J. A., & Graves, S. J. (2017). Deep learning for multisensor image resolution enhancement. Proceedings of the 1st Workshop on GeoAI: AI and Deep Learning for Geographic Knowledge Discovery, GeoAI 2017, 37–44. https://doi.org/10.1145/3149808.3149815

Colomina, I., & Molina, P. (2014). Unmanned aerial systems for photogrammetry and remote sensing: A review. ISPRS Journal of Photogrammetry and Remote Sensing, 92, 79–97. https://doi.org/10.1016/J.ISPRSJPRS.2014.02.013

Colucci, E., Xing, X., Kokla, M., Mostafavi, M. A., Noardo, F., & Spanò, A. (2021). Ontology-based semantic conceptualisation of historical built heritage to generate parametric structured models from point clouds. Applied Sciences (Switzerland), 11(6). https://doi.org/10.3390/APP11062813

Convention Concerning the Protection of the World Cultural and Natural Heritage (1972).

Corte, E., Ajmar, A., Camporeale, C., Cina, A., Coviello, V., Giulio Tonolo, F., Godio, A., Macelloni, M. M., Tamea, S., & Vergnano, A. (2023). Multitemporal characterisation of a proglacial system: a multidisciplinary approach. Earth Syst. Sci. Data Discuss. https://doi.org/https://doi.org/10.5194/essd-2023-94

Cortes, C., Vapnik, V., & Saitta, L. (1995). Support-vector networks. Machine Learning 1995 20:3, 20(3), 273–297. https://doi.org/10.1007/BF00994018

Council Directive 92/43/EEC of 21 May 1992 on the Conservation of Natural Habitats and of Wild Fauna and Flora, Pub. L. No. EEC 1973/1992, Official Journal of European Communities (1992).

Council of Europe Landscape Convention, Pub. L. No. ETS No. 176, Council of Europe Landscape Convention (2000).

Davis, D. S., Caspari, G., Lipo, C. P., & Sanger, M. C. (2021). Deep learning reveals extent of Archaic Native American shell-ring building practices. Journal of Archaeological Science, 132, 105433. https://doi.org/10.1016/J.JAS.2021.105433

De Marinis, R. C. (1986). L'abitato protostorico di Como. In Como fra Etruschi e Celti (pp. 25–37).

De Marinis, R. C., Casini, S., & Rapi, M. (2001). L'abitato protostorico dei dintorni di Como. In La protostoria in Lombardia : 3. convegno archeologico regionale ; atti del convegno, Como - Villa Olmo 22-23-24 ottobre 1999. Societa Archeologica comense.

Deidda, M., Musa, C., & Vacca, G. (2015). A GIS of Sardinia's coastal defence system (XVI – XVIII century). The International Archives of the Photogrammetry,

Remote Sensing and Spatial Information Sciences, XL-4/W7, 17–22. https://doi.org/10.5194/isprsarchives-XL-4-W7-17-2015

Della Torre, S. Della. (2022). Conservazione programmata: la visione, le politiche, le pratiche. IL CAPITALE CULTURALE, Supplementi, 12, 93–104. https://doi.org/10.2/JQUERY.MIN.JS

Della Torre, S. (2003). La conservazione programmata del patrimonio storico architettonico. Linee guida per il piano di manutenzione e il consuntivo scientifico. Guerini e associati.

Diara, F., & Roggero, M. (2022). Quality Assessment of DJI Zenmuse L1 and P1 LiDAR and Photogrammetric Systems: Metric and Statistics Analysis with the Integration of Trimble SX10 Data. Geomatics, 2(3), 254–281. https://doi.org/10.3390/geomatics2030015

Directive 2009/147/EC of the European Parliament and of the Council of 30 November 2009 on the Conservation of Wild Birds, Pub. L. No. EC 147/2009, Official Journal of the European Union (2009).

Disposizioni Urgenti per La Tutela Delle Zone Di Particolare Interesse Ambientale, Pub. L. No. Legge 431/1985, Gazzetta Ufficiale della Repubblica Italiana (1985).

Drusch, M., Del Bello, U., Carlier, S., Colin, O., Fernandez, V., Gascon, F., Hoersch, B., Isola, C., Laberinti, P., Martimort, P., Marchese, F., & Bargellini, P. (2012). Sentinel-2: ESA's Optical High-Resolution Mission for GMES Operational Services. Remote Sensing of Environment, 120, 25–36. https://doi.org/10.1016/j.rse.2011.11.026

Eppich, R., Leblanc, F., Chabbi, A., & Letellier, R. (2007). Guiding principles and illustrated examples recording, documenting and information management for

the conservation of Cultural Heritage places. 21st CIPA Symposium - AntiCIPAting the Future of the Cultural Past. http://gcibibs.getty.edu/asp

Estes, J. E., Sailer, C., & Tinney, L. R. (1986). APPLICATIONS OF ARTIFICIAL INTELLIGENCE TECHNIQUES TO REMOTE SENSING. The Professional Geographer, 38(2), 133–141. https://doi.org/10.1111/J.0033-0124.1986.00133.X

Felicetti, A., Paolanti, M., Zingarettia, P., Pierdicca, R., & Malinverni, E. S. (2021). Mo.Se.: Mosaic image segmentation based on deep cascading learning. Virtual Archaeology Review, 12(24), 25–38. https://doi.org/10.4995/VAR.2021.14179

Fiorino, D. R. (2017). Military Landscapes. A future for Military Heritage. In D. R. Fiorino (Ed.), Proceedings of the International Conference, La Maddalena, Italia, 21-24 giugno 2017. Skirà.

Fiorino, D. R. (2021). Sinergies. Interinstitutional experiences for the rehabilitation of military areas (Vol. 1). UNICApress.

Fiorino, D. R., Grillo, S. M., Pilia, E., & Quaquero, E. (2017a). Methods and processes of critic assessment for the historical military heritage: integrated use of raumbuch and HBIM for the reuse of the Cascino barrack in Cagliari. In Military Landscapes. A future for military heritage (pp. 1285–1301). Skirà.

Fiorino, D. R., Pintus, V., & Vacca, G. (2017b). Un WebGIS per conoscenza e tutela delle tecniche murarie tradizionali in Sardegna. ANANKE, Numero Speciale GeoRES, 129–134.

Fiorucci, M., Khoroshiltseva, M., Pontil, M., Traviglia, A., Del Bue, A., & James, S. (2020). Machine Learning for Cultural Heritage: A Survey. Pattern Recognition Letters, 133, 102–108. https://doi.org/10.1016/j.patrec.2020.02.017

Folk, M., Heber, G., Koziol, Q., Pourmal, E., & Robinson, D. (2011). An overview of the HDF5 technology suite and its applications. ACM International Conference Proceeding Series, 36–47. https://doi.org/10.1145/1966895.1966900

Forte, M., & Campana, S. (Eds.). (2016). Digital Methods and Remote Sensing in Archaeology. Springer International Publishing. https://doi.org/10.1007/978-3-319-40658-9

Franceschetti, G., & Lanari, R. (2018). Synthetic aperture radar processing. Synthetic Aperture Radar Processing, 1–307. https://doi.org/10.1201/9780203737484/SYNTHETIC-APERTURE-

Freeland, T., Heung, B., Burley, D. V., Clark, G., & Knudby, A. (2016). Automated feature extraction for prospection and analysis of monumental earthworks from aerial LiDAR in the Kingdom of Tonga. Journal of Archaeological Science, 69, 64–74. https://doi.org/10.1016/J.JAS.2016.04.011

Gawior, D., Rutkiewicz, P., Malik, I., & Wistuba, M. (2017). Contribution to understanding the post-mining landscape - Application of airborn LiDAR and historical maps at the example from Silesian Upland (Poland). AIP Conference Proceedings, 1906. https://doi.org/10.1063/1.5012452

Geiger, A., Lenz, P., & Urtasun, R. (2012). Are we ready for autonomous driving? the KITTI vision benchmark suite. Proceedings of the IEEE Computer Society Conference on Computer Vision and Pattern Recognition, 3354–3361. https://doi.org/10.1109/CVPR.2012.6248074

Giannattasio, C., Bartolomucci, C., & Pretelli, M. (2020). Arte muraria tradizionale in Sardegna : conoscenza conservazione miglioramento. Gangemi.

Golden, C., Scherer, A. K., Schroder, W., Murtha, T., Morell-Hart, S., Fernandez Diaz, J. C., Del Pilar Jiménez Álvarez, S., Firpi, O. A., Agostini, M., Bazarsky, A., Clark, M., Van Kollias, G., Matsumoto, M., Recinos, A. R., Schnell,

J., & Whitlock, B. (2021). Airborne Lidar Survey, Density-Based Clustering, and Ancient Maya Settlement in the Upper Usumacinta River Region of Mexico and Guatemala. Remote Sensing 2021, Vol. 13, Page 4109, 13(20), 4109. https://doi.org/10.3390/RS13204109

Gomarasca, M. A. (2009). Basics of Geomatics. Springer Netherlands. https://doi.org/10.1007/978-1-4020-9014-1

Good, I. J. (1952). Rational Decisions. Journal of the Royal Statistical Society. Series B (Methodological), 14(1), 107–114. http://www.jstor.org/stable/2984087

Goodfellow, I., Bengio, Y., Courville, A., 2006. Deep learning, Deep learning. MIT Press.

Graham, L. (2012). LAS 1.4 Specification. PHOTOGRAMMETRIC ENGINEERING AND REMOTE SENSING, 93–102.

Granshaw, S. I. (2020). Photogrammetric terminology: fourth edition. The Photogrammetric Record, 35(170), 143–288. https://doi.org/10.1111/phor.12314

Grilli, E., Dininno, D., Petrucci, G., & Remondino, F. (2018). From 2D to 3D supervised segmentation and classification for cultural heritage applications. International Archives of the Photogrammetry, Remote Sensing and Spatial Information Sciences - ISPRS Archives, 42(2), 399–406. https://doi.org/10.5194/ISPRS-ARCHIVES-XLII-2-399-2018

Grilli, E., Farella, E. M., Torresani, A., & Remondino, F. (2019). GEOMETRIC FEATURES ANALYSIS for the CLASSIFICATION of CULTURAL HERITAGE POINT CLOUDS. International Archives of the Photogrammetry, Remote Sensing and Spatial Information Sciences - ISPRS Archives, 42(2/W15), 541–548. https://doi.org/10.5194/isprs-archives-XLII-2-W15-541-2019

Guo, Y., Wang, H., Hu, Q., Liu, H., Liu, L., & Bennamoun, M. (2019). Deep Learning for 3D Point Clouds: A Survey. IEEE Transactions on Pattern Analysis and Machine Intelligence, 43(12), 4338–4364. https://doi.org/10.1109/TPAMI.2020.3005434

Guo, Y., Wang, H., Hu, Q., Liu, H., Liu, L., & Bennamoun, M. (2021). Deep Learning for 3D Point Clouds: A Survey. IEEE Transactions on Pattern Analysis and Machine Intelligence, 43(12), 4338–4364. https://doi.org/10.1109/TPAMI.2020.3005434

Guyot, A., Hubert-Moy, L., & Lorho, T. (2018). Detecting Neolithic Burial Mounds from LiDAR-Derived Elevation Data Using a Multi-Scale Approach and Machine Learning Techniques. Remote Sensing 2018, Vol. 10, Page 225, 10(2), 225. https://doi.org/10.3390/RS10020225

Hackel, T., Wegner, J. D., & Schindler, K. (2016). Contour detection in unstructured 3D point clouds. Proceedings of the IEEE Computer Society Conference on Computer Vision and Pattern Recognition, 2016-December, 1610–1618. https://doi.org/10.1109/CVPR.2016.178

Hahner, M., Dai, D., Liniger, A., & Van Gool, L. (2020). Quantifying Data Augmentation for LiDAR based 3D Object Detection. https://arxiv.org/abs/2004.01643v2

Han, X., Zhang, Z., Ding, N., Gu, Y., Liu, X., Huo, Y., Qiu, J., Yao, Y., Zhang, A., Zhang, L., Han, W., Huang, M., Jin, Q., Lan, Y., Liu, Y., Liu, Z., Lu, Z., Qiu, X., Song, R., … Zhu, J. (2021). Pre-trained models: Past, present and future. AI Open, 2, 225–250. https://doi.org/10.1016/j.aiopen.2021.08.002

Hemingway, H., & Opalach, D. (2024). Integrating Lidar Canopy Height Models with Satellite-Assisted Inventory Methods: A Comparison of Inventory

Estimates. Forest Science, 70(1), 2–13. https://doi.org/10.1093/FORSCI/FXAD047

Holtorf, C., & Högberg, A. (2020). Cultural Heritage and the Future. In Cultural Heritage and the Future. Routledge. https://doi.org/10.4324/9781315644615/CULTURAL-HERITAGE-FUTURE-CORNELIUS-HOLTORF-ANDERS-H

Hsu, S.-Y. (1979). AUTOMATION IN CARTOGRAPHY WITH REMOTE SENSING METHODOLOGIES AND TECHNOLOGIES. Cartographica: The International Journal for Geographic Information and Geovisualization, 16(2), 183–194. https://doi.org/10.3138/84P7-4T06-63UK-NR81

Hu, Q., Yang, B., Xie, L., Rosa, S., Guo, Y., Wang, Z., Trigoni, N., & Markham, A. (2019). RandLA-Net: Efficient Semantic Segmentation of Large-Scale Point Clouds. Proceedings of the IEEE Computer Society Conference on Computer Vision and Pattern Recognition, 11105–11114. https://doi.org/10.1109/CVPR42600.2020.01112

Hu, Q., Yang, B., Xie, L., Rosa, S., Guo, Y., Wang, Z., Trigoni, N., & Markham, A. (2021). Learning Semantic Segmentation of Large-Scale Point Clouds with Random Sampling. IEEE Transactions on Pattern Analysis and Machine Intelligence, 44(11), 8338–8354. https://doi.org/10.1109/TPAMI.2021.3083288

Huang, X., Wang, P., Cheng, X., Zhou, D., Geng, Q., & Yang, R. (2018). The ApolloScape Open Dataset for Autonomous Driving and its Application. IEEE Transactions on Pattern Analysis and Machine Intelligence, 42(10), 2702–2719. https://doi.org/10.1109/tpami.2019.2926463

ICOMOS Ethical Principles, Ethical Principles adopted by the 18th General Assembly (Florence, 2014) to replace the Ethical Commitment Statement adopted by the 13th General Assembly (Madrid, 2002), and amended by the 20th General Assembly (Online, 2020). (2020).

ICOMOS Guidelines on Fortifications and Military Heritage, Pub. L. No. GA 2021 6-1 (2021).

Iglhaut, J., Cabo, C., Puliti, S., Piermattei, L., O'Connor, J., & Rosette, J. (2019). Structure from Motion Photogrammetry in Forestry: a Review. Current Forestry Reports, 5(3), 155–168. https://doi.org/10.1007/s40725-019-00094-3

Iman, M., Arabnia, H. R., & Rasheed, K. (2023). A Review of Deep Transfer Learning and Recent Advancements. Technologies, 11(2), 40. https://doi.org/10.3390/technologies11020040

Jacobsen, K. (2003). DEM generation from satellite data. Remote Sensing in Transition, EARSeL Ghent, 273–276.

James, M. R., & Robson, S. (2012). Straightforward reconstruction of 3D surfaces and topography with a camera: Accuracy and geoscience application. Journal of Geophysical Research: Earth Surface, 117(F3). https://doi.org/10.1029/2011JF002289

Jenson, S. K., & Domingue, J. O. (1988). Extracting Topographic Structure from Digital Elevation Data for Geographic Information System Analysis. PHOTOGRAMMETRIC ENGINEERING & REMOTE SENSING, 54(11), 1593–1600.

Johnson, K., Nissen, E., Saripalli, S., Arrowsmith, J. R., McGarey, P., Scharer, K., Williams, P., & Blisniuk, K. (2014). Rapid mapping of ultrafine fault zone topography with structure from motion. Geosphere, 10(5), 969–986. https://doi.org/10.1130/GES01017.1

Jokilehto, J. (2018). A history of architectural conservation. In A history of architectural conservation (2nd ed.). Routledge.

Kalacska, M., Arroyo-Mora, J. P., & Lucanus, O. (2021). Comparing UAS LiDAR and Structure-from-Motion Photogrammetry for Peatland Mapping and Virtual Reality (VR) Visualization. Drones 2021, Vol. 5, Page 36, 5(2), 36. https://doi.org/10.3390/DRONES5020036

Kerr, J. T., & Ostrovsky, M. (2003). From space to species: ecological applications for remote sensing. Trends in Ecology & Evolution, 18(6), 299–305. https://doi.org/10.1016/S0169-5347(03)00071-5

Kersten, T., Wolf, J., & Lindstaedt, M. (2022). INVESTIGATIONS INTO THE ACCURACY OF THE UAV SYSTEM DJI MATRICE 300 RTK WITH THE SENSORS ZENMUSE P1 AND L1 IN THE HAMBURG TEST FIELD. The International Archives of the Photogrammetry, Remote Sensing and Spatial Information Sciences, XLIII-B1-2022(B1-2022), 339–346. https://doi.org/10.5194/ISPRS-ARCHIVES-XLIII-B1-2022-339-2022

Kioussi, A., Karoglou, M., Labropoulos, K., Bakolas, A., & Moropoulou, A. (2013). Integrated documentation protocols enabling decision making in cultural heritage protection. Journal of Cultural Heritage, 14(3), e141–e146. https://doi.org/10.1016/J.CULHER.2013.01.007

Kirillov, A., Mintun, E., Ravi, N., Mao, H., Rolland, C., Gustafson, L., Xiao, T., Whitehead, S., Berg, A. C., Lo, W. Y., Dollár, P., & Girshick, R. (2023). Segment Anything. Proceedings of the IEEE International Conference on Computer Vision, 3992–4003. https://doi.org/10.1109/ICCV51070.2023.00371

Knapp, A. B., & Ashmore, W. (2000). Archaeological Landscapes: Constructed, Conceptualized, Ideational. In W. Ashmore & A. B. Knapp (Eds.), Archaeologies of Landscape (pp. 1–30). Blackwell.

Kölle, M., Laupheimer, D., Schmohl, S., Haala, N., Rottensteiner, F., Wegner, J. D., & Ledoux, H. (2021). The Hessigheim 3D (H3D) benchmark on semantic segmentation of high-resolution 3D point clouds and textured meshes from UAV LiDAR and Multi-View-Stereo. ISPRS Open Journal of Photogrammetry and Remote Sensing, 1, 100001. https://doi.org/10.1016/j.ophoto.2021.100001

Lanaras, C., Bioucas-Dias, J., Galliani, S., Baltsavias, E., & Schindler, K. (2018). Super-resolution of Sentinel-2 images: Learning a globally applicable deep neural network. ISPRS Journal of Photogrammetry and Remote Sensing, 146, 305–319. https://doi.org/10.1016/j.isprsjprs.2018.09.018

Lang, A. H., Vora, S., Caesar, H., Zhou, L., Yang, J., & Beijbom, O. (2019). Pointpillars: Fast encoders for object detection from point clouds. Proceedings of the IEEE Computer Society Conference on Computer Vision and Pattern Recognition, 2019-June, 12689–12697. https://doi.org/10.1109/CVPR.2019.01298

Laupheimer, D., & Haala, N. (2022). MULTI-MODAL SEMANTIC MESH SEGMENTATION IN URBAN SCENES. ISPRS Annals of the Photogrammetry, Remote Sensing and Spatial Information Sciences, 5(2), 267–274. https://doi.org/10.5194/isprs-annals-V-2-2022-267-2022

Li, Y., Bu, R., Sun, M., Wu, W., Di, X., & Chen, B. (2018). PointCNN: Convolution On X-Transformed Points. ArXiv, 1–11. https://arxiv.org/abs/1801.07791v5

Li, Y., Ma, L., Zhong, Z., Liu, F., Chapman, M. A., Cao, D., & Li, J. (2021). Deep Learning for LiDAR Point Clouds in Autonomous Driving: A Review. IEEE Transactions on Neural Networks and Learning Systems, 32(8), 3412–3432. https://doi.org/10.1109/TNNLS.2020.3015992

Logothetis, S., Delinasiou, A., & Stylianidis, E. (2015). Building information modelling for cultural heritage: A review. ISPRS Annals of the Photogrammetry, Remote Sensing and Spatial Information Sciences, 2(5W3), 177 – 183. https://doi.org/10.5194/isprsannals-II-5-W3-177-2015

Lovitt, J., Rahman, M. M., & McDermid, G. J. (2017). Assessing the Value of UAV Photogrammetry for Characterizing Terrain in Complex Peatlands. Remote Sensing 2017, Vol. 9, Page 715, 9(7), 715. https://doi.org/10.3390/RS9070715

Lu, D., & Weng, Q. (2007). A survey of image classification methods and techniques for improving classification performance. International Journal of Remote Sensing, 28(5), 823–870. https://doi.org/10.1080/01431160600746456

Lu, H., Chen, X., Zhang, G., Zhou, Q., Ma, Y., & Zhao, Y. (2019). Scanet: Spatial-channel Attention Network for 3D Object Detection. ICASSP, IEEE International Conference on Acoustics, Speech and Signal Processing - Proceedings, 2019-May, 1992–1996. https://doi.org/10.1109/ICASSP.2019.8682746

Luo, L., Wang, X., Guo, H., Lasaponara, R., Zong, X., Masini, N., Wang, G., Shi, P., Khatteli, H., Chen, F., Tariq, S., Shao, J., Bachagha, N., Yang, R., & Yao, Y. (2019). Airborne and spaceborne remote sensing for archaeological and cultural heritage applications: A review of the century (1907–2017). Remote Sensing of Environment, 232, 111280. https://doi.org/10.1016/j.rse.2019.111280

Maas, H.-G., & Vosselman, G. (2010). Airborne and Terrestrial Laser Scanning. Whittles Publishing. https://www.whittlespublishing.com/Airborne_and_Terrestrial_Laser_Scanning

Maity, A. (2016). Supervised Classification of RADARSAT-2 Polarimetric Data for Different Land Features. https://arxiv.org/abs/1608.00501v1

Mallet, C., & Bretar, F. (2009). Full-waveform topographic lidar: State-of-the-art. ISPRS Journal of Photogrammetry and Remote Sensing, 64(1), 1–16. https://doi.org/10.1016/j.isprsjprs.2008.09.007

Mallet, C., Bretar, F., Roux, M., Soergel, U., & Heipke, C. (2011). Relevance assessment of full-waveform lidar data for urban area classification. ISPRS Journal of Photogrammetry and Remote Sensing, 66(6), S71–S84. https://doi.org/10.1016/J.ISPRSJPRS.2011.09.008

Mameli, M., & Sanjust, P. (2015). The coastal military architecture of World War II in Sardinia. FORTMED2015 - International Conference on Modern Age Fortifications of the Western Mediterranean Coast. http://ocs.editorial.upv.es/index.php/FORTMED/FORTMED2015/paper/view/1784

Mancini, F., Dubbini, M., Gattelli, M., Stecchi, F., Fabbri, S., & Gabbianelli, G. (2013). Using Unmanned Aerial Vehicles (UAV) for High-Resolution Reconstruction of Topography: The Structure from Motion Approach on Coastal Environments. Remote Sensing 2013, Vol. 5, Pages 6880-6898, 5(12), 6880–6898. https://doi.org/10.3390/RS5126880

Marotta, A. (2018). Military Landscapes. A Future for Military Heritage. Diségno, 2018(2), 183–186. https://doi.org/10.26375/DISEGNO.2.2018.20

Martino, A., Gerla, F., & Balletti, C. (2023). Multi-scale and multi-sensor approaches for the protection of cultural natural heritage: The island of santo spirito in venice. International Archives of the Photogrammetry, Remote Sensing and Spatial Information Sciences - ISPRS Archives, 48(M), 1027–1034. https://doi.org/10.5194/isprs-Archives-XLVIII-M-2-2023-1027-2023

Masini, N., Coluzzi, R., Lasaponara, R., Masini, N., Coluzzi, R., & Lasaponara, R. (2011). On the Airborne Lidar Contribution in Archaeology: from

Site Identification to Landscape Investigation. Laser Scanning, Theory and Applications. https://doi.org/10.5772/14655

Massonnet, D., & Rabaute, T. (1993). Radar Interferometry: Limits and Potential. IEEE Transactions on Geoscience and Remote Sensing, 31(2), 455–464. https://doi.org/10.1109/36.214922

Maté-González, M. Á., Di Pietra, V., & Piras, M. (2022). Evaluation of Different LiDAR Technologies for the Documentation of Forgotten Cultural Heritage under Forest Environments. Sensors, 22(16), 6314. https://doi.org/10.3390/s22166314

Matrone, F., Grilli, E., Martini, M., Paolanti, M., Pierdicca, R., & Remondino, F. (2020). Comparing Machine and Deep Learning Methods for Large 3D Heritage Semantic Segmentation. ISPRS International Journal of Geo-Information 2020, Vol. 9, Page 535, 9(9), 535. https://doi.org/10.3390/IJGI9090535

Matrone, F., Lingua, A., Pierdicca, R., Malinverni, E. S., Paolanti, M., Grilli, E., Remondino, F., Murtiyoso, A., & Landes, T. (2020). A benchmark for large-scale Heritage point cloud semantic segmentation. The International Archives of the Photogrammetry, Remote Sensing and Spatial Information Sciences, XLIII-B2-2020, 1419–1426. https://doi.org/10.5194/isprs-archives-XLIII-B2-2020-1419-2020

Mattausch, O., Panozzo, D., Mura, C., Sorkine-Hornung, O., & Pajarola, R. (2014). Object detection and classification from large-scale cluttered indoor scans. Computer Graphics Forum, 33(2), 11–21. https://doi.org/10.1111/cgf.12286

Maxwell, A. E., & Warner, T. A. (2015). Differentiating mine-reclaimed grasslands from spectrally similar land cover using terrain variables and object-based

machine learning classification. International Journal of Remote Sensing, 36(17), 4384–4410. https://doi.org/10.1080/01431161.2015.1083632

Maxwell, A. E., Warner, T. A., & Fang, F. (2018). Implementation of machine-learning classification in remote sensing: An applied review. International Journal of Remote Sensing, 39(9), 2784–2817. https://doi.org/10.1080/01431161.2018.1433343

Mazzacca, G., Grilli, E., Cirigliano, G. P., Remondino, F., & Campana, S. (2022). Seeing among foliage with LiDaR and Machine Learning: towards a transferable archaeological pipeline. The International Archives of the Photogrammetry, Remote Sensing and Spatial Information Sciences, XLVI-2-W1-2022(2/W1-2022), 365–372. https://doi.org/10.5194/ISPRS-ARCHIVES-XLVI-2-W1-2022-365-2022

McFeeters, S. K. (1996). The use of the Normalized Difference Water Index (NDWI) in the delineation of open water features. International Journal of Remote Sensing, 17(7), 1425–1432. https://doi.org/10.1080/01431169608948714

Merlo, R., & Frigerio, G. (1986). L'abitato: tecnologie edilizie. In Como fra Etruschi e Celti (pp. 41–61).

Moullou, D., Vital, R., Sylaiou, S., & Ragia, L. (2024). Digital Tools for Data Acquisition and Heritage Management in Archaeology and Their Impact on Archaeological Practices. Heritage, 7(1), 107–121. https://doi.org/10.3390/heritage7010005

Mukherjee, I., & Singh, U. K. (2020). Delineation of groundwater potential zones in a drought-prone semi-arid region of east India using GIS and analytical hierarchical process techniques. CATENA, 194, 104681. https://doi.org/10.1016/J.CATENA.2020.104681

Murru, S. (2015). Le torri costiere della Sardegna nel Mediterraneo: cronotipologie delle strutture murarie. [PhD thesis]. Università degli Studi di Cagliari.

Nex, F., & Rinaudo, F. (2011). LiDAR or photogrammetry? Integration is the answer. Italian Journal of Remote Sensing / Rivista Italiana Di Telerilevamento, 43(2), 107–121. https://doi.org/10.5721/ItJRS20114328

Niculiță, M. (2020). Geomorphometric Methods for Burial Mound Recognition and Extraction from High-Resolution LiDAR DEMs. Sensors 2020, Vol. 20, Page 1192, 20(4), 1192. https://doi.org/10.3390/S20041192

Nishanbaev, I., Champion, E., & McMeekin, D. A. (2019). A Survey of Geospatial Semantic Web for Cultural Heritage. Heritage 2019, Vol. 2, Pages 1471-1498, 2(2), 1471–1498. https://doi.org/10.3390/HERITAGE2020093

Nong, X., Bai, W., & Liu, G. (2023). Airborne LiDAR point cloud classification using PointNet++ network with full neighborhood features. PLOS ONE, 18(2), e0280346. https://doi.org/10.1371/JOURNAL.PONE.0280346

Nurunnabi, A., Teferle, N., Balado, J., Chen, M., Poux, F., & Sun, C. (2022). Robust techniques for building footprint extraction in Aerial Laser Scanning 3D point clouds. The International Archives of the Photogrammetry, Remote Sensing and Spatial Information Sciences, XLVIII-3/W2-2022, 43–50. https://doi.org/10.5194/isprs-archives-XLVIII-3-W2-2022-43-2022

Pal, M., & Mather, P. M. (2005). Support vector machines for classification in remote sensing. International Journal of Remote Sensing, 26(5), 1007–1011. https://doi.org/10.1080/01431160512331314083

Patil, A., Malla, S., Gang, H., & Chen, Y. T. (2019). The H3D Dataset for Full-Surround 3D Multi-Object Detection and Tracking in Crowded Urban Scenes. Proceedings - IEEE International Conference on Robotics and

Automation, 2019-May, 9552–9557. https://doi.org/10.1109/ICRA.2019.8793925

Patrucco, G., Bambridge, P., Giulio Tonolo, F., Markey, J., & Spanò, A. (2023). Digital replicas of British Musem artefacts. The International Archives of the Photogrammetry, Remote Sensing and Spatial Information Sciences, XLVIII-M-2–2023(M-2–2023), 1173–1180. https://doi.org/10.5194/ISPRS-ARCHIVES-XLVIII-M-2-2023-1173-2023

Patrucco, G., & Setragno, F. (2021). Multiclass semantic segmentation for digitisation of movable heritage using deep learning techniques. Virtual Archaeology Review, 12(25), 85–98. https://doi.org/10.4995/VAR.2021.15329

Patrucco, G., & Setragno, F. (2023). Enhancing automation of Heritage processes: generation of artificial training datasets from photogrammetric 3D models. The International Archives of the Photogrammetry, Remote Sensing and Spatial Information Sciences, XLVIII-M-2–2023, 1181–1187. https://doi.org/10.5194/isprs-archives-XLVIII-M-2-2023-1181-2023

Pellis, E., Masiero, A., Grussenmeyer, P., Betti, M., & Tucci, G. (2023). Synthetic data generation and testing for the semantic segmentation of Heritage buildings. The International Archives of the Photogrammetry, Remote Sensing and Spatial Information Sciences, XLVIII-M-2–2023, 1189–1196. https://doi.org/10.5194/isprs-archives-XLVIII-M-2-2023-1189-2023

Petschko, H., Bell, R., & Glade, T. (2016). Effectiveness of visually analyzing LiDAR DTM derivatives for earth and debris slide inventory mapping for statistical susceptibility modeling. Landslides, 13(5), 857–872. https://doi.org/10.1007/S10346-015-0622-1/FIGURES/5

Petzet, M. (2008). Genius Loci – The Spirit of Monuments and Sites. 16th ICOMOS General Assembly and International Symposium: 'Finding the Spirit of

Place – between the Tangible and the Intangible', 29 Sept – 4 Oct 2008, Quebec, Canada. [Conference or Workshop Item]

Picollo, M., Cucci, C., Casini, A., & Stefani, L. (2020). Hyper-spectral imaging technique in the cultural heritage field: New possible scenarios. Sensors, 20(10). https://doi.org/10.3390/s20102843

Pingel, T. J., Clarke, K. C., & McBride, W. A. (2013). An improved simple morphological filter for the terrain classification of airborne LIDAR data. ISPRS Journal of Photogrammetry and Remote Sensing, 77, 21–30. https://doi.org/10.1016/J.ISPRSJPRS.2012.12.002

Pomerleau, F., Liu, M., Colas, F., & Siegwart, R. (2012). Challenging data sets for point cloud registration algorithms. Http://Dx.Doi.Org/10.1177/0278364912458814, 31(14), 1705–1711. https://doi.org/10.1177/0278364912458814

Poux, F., & Billen, R. (2019). Voxel-based 3D Point Cloud Semantic Segmentation: Unsupervised geometric and relationship featuring vs deep learning methods. ISPRS International Journal of Geo-Information, 8(5), 213. https://doi.org/10.3390/ijgi8050213

Qi, C. R., Su, H., Mo, K., & Guibas, L. J. (2016). PointNet: Deep Learning on Point Sets for 3D Classification and Segmentation.

Remondino, F. (2011). Heritage recording and 3D modeling with photogrammetry and 3D scanning. Remote Sensing, 3(6), 1104–1138. https://doi.org/10.3390/rs3061104

Riegl, A. (1903). Il culto moderno dei monumenti. Il suo carattere e i suoi inizi. Abscondita.

Rinaudo, F., Chiabrando, F., Lingua, A., & Spanò, A. (2012). Archaeological site monitoring: UAV photogrammetry can be an answer. International Archives of the Photogrammetry, Remote Sensing and Spatial Information Sciences - ISPRS Archives, 39, 583–588.

Robert, D., Raguet, H., & Landrieu, L. (2023). Efficient 3D Semantic Segmentation with Superpoint Transformer. Proceedings of the IEEE International Conference on Computer Vision, 17149–17158. https://doi.org/10.1109/ICCV51070.2023.01577

Robinson, H. (1977). Morphology and Landscape (III edition). University Tutorial Press.

Romano, M., & Trisciuoglio, M. (2008). Casa, città, paesaggio. In La cultura italiana (Vol. 3). UTET.

Rosenblatt, F. (1958). The perceptron: A probabilistic model for information storage and organization in the brain. Psychological Review, 65(6), 386–408. https://doi.org/10.1037/H0042519

Roy, D. P., Li, J., Zhang, H. K., & Yan, L. (2016). Best practices for the reprojection and resampling of Sentinel-2 Multi Spectral Instrument Level 1C data. Remote Sensing Letters, 7(11), 1023–1032. https://doi.org/10.1080/2150704X.2016.1212419

Rumelhart, D. E., Hinton, G. E., & Williams, R. J. (1986). Learning representations by back-propagating errors. Nature, 323(6088), 533–536. https://doi.org/10.1038/323533a0

Sammartano, G., Avena, M., Cappellazzo, M., & Spanò, A. (2021). Hybrid GIS-BIM approach for the torino digital-twin: The implementation of a floor-level 3D city geodatabase. International Archives of the Photogrammetry, Remote

Sensing and Spatial Information Sciences - ISPRS Archives, 43(B4-2021), 423–430. https://doi.org/10.5194/ISPRS-ARCHIVES-XLIII-B4-2021-423-2021

Santoro, V., Patrucco, G., Lingua, A., & Spanò, A. (2023). Multispectral uav data enhancing the knowledge of landscape heritage. International Archives of the Photogrammetry, Remote Sensing and Spatial Information Sciences - ISPRS Archives, 48(M-2–2023), 1419–1426. https://doi.org/10.5194/isprs-archives-XLVIII-M-2-2023-1419-2023

Sardinia Geoportal - Autonomous Region of Sardinia. (2024). https://www.sardegnageoportale.it/index.html

Sarker, S., Sarker, P., Stone, G., Gorman, R., Tavakkoli, A., Bebis, G., & Sattarvand, J. (2024). A comprehensive overview of deep learning techniques for 3D point cloud classification and semantic segmentation. Machine Vision and Applications, 35(4), 67. https://doi.org/10.1007/s00138-024-01543-1

Savino, S., Rumor, M., & Congiu, S. (2011). Automated cartographic generalization in Italy. The International Archives of the Photogrammetry, Remote Sensing and Spatial Information Sciences, XXXVIII-4/C21, 109–114. https://doi.org/10.5194/ISPRSARCHIVES-XXXVIII-4-C21-109-2011

Scaioni, M., Longoni, L., Melillo, V., & Papini, M. (2014). Remote Sensing for Landslide Investigations: An Overview of Recent Achievements and Perspectives. Remote Sensing 2014, Vol. 6, Pages 9600-9652, 6(10), 9600–9652. https://doi.org/10.3390/RS6109600

Schaepman, M. E., Ustin, S. L., Plaza, A. J., Painter, T. H., Verrelst, J., & Liang, S. (2009). Earth system science related imaging spectroscopy—An assessment. Remote Sensing of Environment, 113(SUPPL. 1), S123–S137. https://doi.org/10.1016/J.RSE.2009.03.001

Settis, S. (2010). Paesaggio Costituzione Cemento. La battaglia per l'ambiente contro il degrado civile. In Passaggi Einaudi. Einaudi. http://www.einaudi.it/speciali/Salvatore-Settis-Paesaggio-Costituzione-cemento

Shan, J., & Toth, C. K. (Eds.). (2018). Topographic Laser Ranging and Scanning. CRC Press. https://doi.org/10.1201/9781315154381

Shukla, T., Tang, W., Trettin, C. C., Chen, G., Chen, S., & Allan, C. (2023). Quantification of Microtopography in Natural Ecosystems Using Close-Range Remote Sensing. Remote Sensing 2023, Vol. 15, Page 2387, 15(9), 2387. https://doi.org/10.3390/RS15092387

Società Archeologica Comense. (2013). Le mura di Como - Capitolo 4 - Le difese meridionali. In https://archeologicacomo.com/wp-content/uploads/2018/06/Capitolo_4.pdf (pp. 1–9). Società Archeologica Comense.

Soroush, M., Mehrtash, A., Khazraee, E., & Ur, J. A. (2020). Deep Learning in Archaeological Remote Sensing: Automated Qanat Detection in the Kurdistan Region of Iraq. Remote Sensing 2020, Vol. 12, Page 500, 12(3), 500. https://doi.org/10.3390/RS12030500

Spanò, A., Sammartano, G., Calcagno Tunin, F., Cerise, S., & Possi, G. (2018). GIS-based detection of terraced landscape heritage: comparative tests using regional DEMs and UAV data. Applied Geomatics, 10(2), 77–97. https://doi.org/10.1007/s12518-018-0205-7

Spanò, A. (2022). Tecnologie di mapping 3D aeree e terrestri per la documentazione di siti protostorici nel Parco della Spina Verde di Como. In F. Butti, B. Grassi, & S. Jorio (Eds.), RI-trovamenti. 7000 anni di storia Comense. Catalogo della mostra. Società Archeologica Comense.

Stubbs, J. H. (2009). Time Honored. A global view of architectural conservation. In Time honored : a global view of architectural conservation : parameters, theory & evolution of an ethos. Wiley.

Sun, P., Kretzschmar, H., Dotiwalla, X., Chouard, A., Patnaik, V., Tsui, P., Guo, J., Zhou, Y., Chai, Y., Caine, B., Vasudevan, V., Han, W., Ngiam, J., Zhao, H., Timofeev, A., Ettinger, S., Krivokon, M., Gao, A., Joshi, A., … Anguelov, D. (2019). Scalability in Perception for Autonomous Driving: Waymo Open Dataset. Proceedings of the IEEE Computer Society Conference on Computer Vision and Pattern Recognition, 2443–2451. https://doi.org/10.1109/CVPR42600.2020.00252

Sweeney, C., Sattler, T., Hollerer, T., Turk, M., & Pollefeys, M. (2015). Optimizing the Viewing Graph for Structure-from-Motion. 2015 IEEE International Conference on Computer Vision (ICCV), 801–809. https://doi.org/10.1109/ICCV.2015.98

Takaku, J., Tadono, T., & Tsutsui, K. (2014). Generation of high resolution global DSM from ALOS PRISM. International Archives of the Photogrammetry, Remote Sensing and Spatial Information Sciences - ISPRS Archives, 40(4), 243–248. https://doi.org/10.5194/isprsarchives-XL-4-243-2014

Tharwat, A. (2018). Classification assessment methods. Applied Computing and Informatics, 17(1), 168–192. https://doi.org/10.1016/J.ACI.2018.08.003/FULL/PDF

Tosco, C. (2014). I beni culturali. Storia, tutela e valorizzazione. Il Mulino.

Turitto, O., Baldo, M., Audisio, C., & Lollino, G. (2010). A LiDAR application to assess long-term bed-level changes in a cobble-bed river: the case of the Orco River (North-Western Italy). Geogr. Fis. Dinam. Quat., 33, 61–76.

Tutela Delle Cose d'interesse Artistico e Storico, Pub. L. No. Legge 1089/1939, Gazzetta Ufficiale della Repubblica Italiana (1939).

Vacca, G., Fiorino, D., & Pili, D. (2018). A Spatial Information System (SIS) for the Architectural and Cultural Heritage of Sardinia (Italy). ISPRS International Journal of Geo-Information, 7(2), 49. https://doi.org/10.3390/ijgi7020049

Vargas, R., Mosavi, A., & Ruiz, R. (2018). Deep Learning: A Review. https://doi.org/10.20944/PREPRINTS201810.0218.V1

Varney, N., Asari, V. K., & Graehling, Q. (2020). DALES: A Large-scale Aerial LiDAR Data Set for Semantic Segmentation. IEEE Computer Society Conference on Computer Vision and Pattern Recognition Workshops, 2020-June, 717–726. https://doi.org/10.1109/CVPRW50498.2020.00101

Vavulin, M. V., Chugunov, K. V., Zaitceva, O. V., Vodyasov, E. V., & Pushkarev, A. A. (2021). UAV-based photogrammetry: Assessing the application potential and effectiveness for archaeological monitoring and surveying in the research on the 'valley of the kings' (Tuva, Russia). Digital Applications in Archaeology and Cultural Heritage, 20, e00172. https://doi.org/10.1016/J.DAACH.2021.E00172

Westoby, M. J., Brasington, J., Glasser, N. F., Hambrey, M. J., & Reynolds, J. M. (2012). "Structure-from-Motion" photogrammetry: A low-cost, effective tool for geoscience applications. Geomorphology, 179, 300–314. https://doi.org/10.1016/j.geomorph.2012.08.021

Wieser, M., Hollaus, M., Mandlburger, G., Glira, P., & Pfeifer, N. (2016). ULS LiDAR supported analyses of laser beam penetration from different ALS systems into vegetation. ISPRS Annals of the Photogrammetry, Remote Sensing and Spatial Information Sciences, III–3, 233–239. https://doi.org/10.5194/ISPRS-ANNALS-III-3-233-2016

Wu, Y., Wang, Y., Zhang, S., & Ogai, H. (2021). Deep 3D Object Detection Networks Using LiDAR Data: A Review. IEEE Sensors Journal, 21(2), 1152–1171. https://doi.org/10.1109/JSEN.2020.3020626

Xiong, X., Adan, A., Akinci, B., & Huber, D. (2013). Automatic creation of semantically rich 3D building models from laser scanner data. Automation in Construction, 31, 325–337. https://doi.org/10.1016/j.autcon.2012.10.006

Xu, S., Vosselman, G., & Oude Elberink, S. (2014). Multiple-entity based classification of airborne laser scanning data in urban areas. ISPRS Journal of Photogrammetry and Remote Sensing, 88, 1–15. https://doi.org/10.1016/J.ISPRSJPRS.2013.11.008

Yan, Y., Mao, Y., & Li, B. (2018). SECOND: Sparsely Embedded Convolutional Detection. Sensors 2018, Vol. 18, Page 3337, 18(10), 3337. https://doi.org/10.3390/S18103337

Yang, S., Hou, M., & Li, S. (2023). Three-Dimensional Point Cloud Semantic Segmentation for Cultural Heritage: A Comprehensive Review. Remote Sensing, 15(3), 548. https://doi.org/10.3390/rs15030548

Yang, Z., Sun, Y., Liu, S., & Jia, J. (2020). 3DSSD: Point-based 3D Single Stage Object Detector. Proceedings of the IEEE Computer Society Conference on Computer Vision and Pattern Recognition, 11037–11045. https://doi.org/10.1109/CVPR42600.2020.01105

Yang, Z., Sun, Y., Liu, S., Shen, X., & Jia, J. (2019). STD: Sparse-to-Dense 3D Object Detector for Point Cloud. Proceedings of the IEEE International Conference on Computer Vision, 2019-October, 1951–1960. https://doi.org/10.1109/ICCV.2019.00204

Ye, Z., Xu, Y., Huang, R., Tong, X., Li, X., Liu, X., Luan, K., Hoegner, L., & Stilla, U. (2020). LASDU: A Large-Scale Aerial LiDAR Dataset for Semantic

Labeling in Dense Urban Areas. ISPRS International Journal of Geo-Information 2020, Vol. 9, Page 450, 9(7), 450. https://doi.org/10.3390/IJGI9070450

Zeng, Z., Xu, Y., Xie, Z., Tang, W., Wan, J., & Wu, W. (2024). Large-scale point cloud semantic segmentation via local perception and global descriptor vector. Expert Systems with Applications, 246, 123269. https://doi.org/10.1016/j.eswa.2024.123269

Zhang, W., Qi, J., Wan, P., Wang, H., Xie, D., Wang, X., & Yan, G. (2016). An Easy-to-Use Airborne LiDAR Data Filtering Method Based on Cloth Simulation. Remote Sensing 2016, Vol. 8, Page 501, 8(6), 501. https://doi.org/10.3390/RS8060501

Zhang, X., Xue, R., & Soergel, U. (2022). A TWO-STAGE APPROACH FOR RARE CLASS SEGMENTATION IN LARGE-SCALE URBAN POINT CLOUDS. International Archives of the Photogrammetry, Remote Sensing and Spatial Information Sciences - ISPRS Archives, 43(B2), 329–334. https://doi.org/10.5194/isprs-archives-XLIII-B2-2022-329-2022

Zhang, Y., Zhao, W., Sun, B., Zhang, Y., & Wen, W. (2022). Point Cloud Upsampling Algorithm: A Systematic Review. Algorithms 2022, Vol. 15, Page 124, 15(4), 124. https://doi.org/10.3390/A15040124

Zhou, F., Zou, L., Liu, X., Zhang, Y., Meng, F., Xie, C., & Zhang, S. (2021). Microlandform classification method for grid DEMs based on support vector machine. Arabian Journal of Geosciences, 14(13), 1269. https://doi.org/10.1007/s12517-021-07596-0

Zhu, Q., Fan, L., & Weng, N. (2024). Advancements in point cloud data augmentation for deep learning: A survey. Pattern Recognition, 153, 110532. https://doi.org/10.1016/j.patcog.2024.110532